RING STIFFENED PIPELINES

Nicolaos I. Tselalis

A Dissertation

in

The Faculty

of

Engineering

Presented in Partial Fulfillment of the Requirements
for the degree of Master of Engineering at
Concordia University
Montreal, Québec, Canada

August 1981

ABSTRACT

RING STIFFENED PIPELINES

Nicolaos I. Tselalis

Pipelines are being constructed in ever increasing diameters and at the same time wall thicknesses are reduced as high strenght steels are developed. As a result pipelines are more sensitive to failure due to buckling. In such cases it is often more economic to provide stiffening rings to resist buckling, without being nessecary to increase the pipe's wall thickness.

The purpose of this study is to present in convinient form methods of structural analysis and design, for both belowground and aboveground ring-stiffened pipelines. It collects the essential matter from a vast literature and presents design formulas and other data for pipelines under various loading conditions.

ACKNOWLEDGEMENTS

The work presented in this study was carried under the direct supervision of Dr. M.S. Troitsky, Chairman of the Civil Engineering Departement, to whom the author wishes to express his deepest gratitude for his guidance and encouragement, without which the preparation of this work could not have been possible.

TABLE OF CONTENTS

Table of Contents (cont'd)

Table of Contents (cont'd)

Table of Contents (cont'd)

Table of Contents (cont'd)

LIST OF FIGURES

List of Figures (cont'd.)

List of Figures (cont'd.)

NOTATIONS

A	Cross sectional area of the pipe wall
A_f	Cross sectional area of the ring stiffener
b	Width of the stiffener in contact with the pipe shell
B_d	Effective trench width
D	Mean diameter of the pipe
D_f	Mean diameter of the stiffening ring
D_o	External diameter of the pipe
E	Modulus of Elasticity of the pipe material
E_s	Secant modulus of the pipe material
E_t	Tangent modulus of the pipe material
f_c	Circumferential stress
f_{cr}	Critical buckling stress
f_l	Longitudinal stress
f_y	Yield stress of the pipe material
I	Moment of Inertia of the cross-section of the pipe wall
I_f	Effective moment of Inertia about the centroid of a section comprising one stiffener plus an effective width of the shell
l	The unsupported length of the pipe
L_e	The effective width
L_f	Center to center stiffener spacing
N_x	Normal force in the X direction
N_u	Circumferential Normal force.

Notations (cont'd)

N_{xu}, N_{ux}	Shearing forces
M_x	Bending moment in the X direction
M_u	Circumferential Bending moment
p_e	External pressure
p_i	Internal pressure
p_c	Critical buckling pressure
R	Mean radius of the pipe
R_o	Outside radius of the pipe
t	Thickness of the wall of the pipe
t_f	Thickness of the stiffening ring
w	Unit weight of the filling material
W	Vertical external load
v	Poisson's ratio
γ_i	Unit weight of the ice
γ_L	Unit weight of the liquid
γ_s	Unit weight of the pipe material

CHAPTER I

INTRODUCTION

CHAPTER I

INTRODUCTION

Pipes have been used for many centures for transportation of fluids. The Chinese first used bamboo thousands of years ago, and lead pipes were unearthed at Pompei. In later centuries woodstave pipes were used in England. It was only with the advent of cast iron, however, that pressure pipelines were constructed. Cast iron was used extensively in the 19th century and is still used. Steel pipes were first introduced towards the end of the last century, facilitating construction of small and large bore pipelines. The increasing use of high grade steels and large rolling mills has enabled pipelines with diameters over ten feet and working at high pressures to be manufactured.

Prior to this century water and sewage were practically the only fluids transported by pipelines. The first successful crude oil pipeline was built in 1865 at Pennsylvania. It was a screwed cast iron pipeline only two inches in diameter and six miles long. This pioneer effort had effectively demonstrated the value of pipelines for transporting oil, and a network of pipelines for collecting and delivering crude oil rapidly grew up in and around the Pennsylvania oilfields. By 1900 there were approximately 18,000 miles of crude oil pipelines in the United States alone. The introduction of steel for pipe making in place of cast iron made possible the manufacture of pipes of large

diameters. In consequence the pipeline industry continued to grow and by 1920 there were 53,000 miles of pipelines in use. By 1940 a total of more than 124,000 miles of crude oil and refined product pipelines were used in the United States alone with diameters over 12 inches. The same period saw a great development in pipeline construction outside the United States, especially in the Middle East. The second world war provided a tremendous impetus for pipeline construction either because of the shortage of tankers or to avoid the dangerous voyage to ports, and to ensure continuity supplies to airfields and other important consumers.

Paralel with the development of crude oil and refined product pipelines went the development of natural gas pipelines. At the end of 1956 the total length of crude oil, refined product and natural gas pipelines in the world (excluding the USSR, eastern European countries and China) amounted to some 99,000 miles, 43,000 miles and 160,000 miles respectively.

Nowdays pipelines are the most common means for transporting gases and oils over long distances. Liquid chemicals and solids in slurry form or in containers are also being pumped through pipelines on ever increasing scales.

1.1 Comparison of Pipelines with Other Forms of Transport

1.1.1 Advandages

There are many advantages of pipelines transport compared

with other forms of transport such as road, rail, waterways or air. Some of these advantages are listed below :

1. Pipelines are often the most economic form of transport (considering either capital cost, running cost or overall cost).

2. Pipelines costs are not susceptible to fluctuations in prices, since the major cost is the capital outlay and subsequent operating costs are relatively small.

3. Operations are most susceptible to labour disputes as little attendance is required. Many modern systems operate automatically.

4. Being hidden beneath the ground a pipeline will not influence the natural enviroment.

5. A buried pipeline is reasonably secure against sabotage.

6. A pipeline is independent of external influence such as traffic congestion and the weather.

7. There is normally no problem of returning empty containers to the source.

8. It is relatively easy to increase the capasity of a pipeline by installing a booster pump.

9. A buried pipeline will not disturb surface traffic and services

10. Wayleaves for pipelines are usually easier to obtain than for roads and railways.

11. The accident rate per ton-mile is considerably lower than for other forms of transportation.

12. A pipeline can cross rugged terrain difficult for vehicles to cross.

1.1.2 Disadvantages

Pipeline systems are of course associated with some disadvantages :

1. The initial capital expenditure is often large, so if there is any uncertainty in the demand some degree of speculation may be necessary.

2. There is often a high cost involved in filling a pipeline (especially long fuel lines).

3. Pipelines cannot be used for more than one material at a time (although there are multi-product pipelines operating on batch bases).

4. There are operating problem associated with the pumping of solids, such as blockages or stoppages.

5. It is often difficult to locate leaks or blockages.

1.2 Oil and Gas Pipelines

Pipelines serving the petroleum industry can be divided into three main categories :

a) Gathering lines for moving crude oil from the wells

b) Trunk lines for the long-distance transport of oil from the producing fields to the refineries and transshipping points.

c) Products lines for moving refined products from the refineries to marketing centers and shipping points.

In principle, the same method of stress calculation is applied to all pipe systems, regardless of the fluid or gas to be transported. But there are features characteristic of the individual types of pipeline, depending on the purpose of application.

Gathering lines in the oil field are designed on a provisional basis, because their life is limited by the producing period of the individual wells, and by the highly aggressive nature of crude oil. Therefore, a small size will be selected, regardless of pressure loss. The lines can be laid on the surface by employing simple supports, if they cross traffic routes they can be protected by a covering of earth, capable of withstanding the weight of traffic.

Trunk lines must be designed for long life. Plain-end pipe is used and the girth welds for joining together the individual lengths are made in the field. Because of the large quantities of material employed, accurate design is essential so that the wall thicknes to be precisely calculated to ensure optimum utilization of the material. It is general practice to bury trunk lines, the depth being increased at roads crossings, to prevent the pipes from being subjected to wheel pressure from passing vehicles. Bridging is often considered wherever a stream or small river crossing is encountered. It is only in noncultivated territory, such as desert regions, that long-distance pipelines are surface laid on supports. When pipes are constructed aboveground particular attention must be paid to the stresses through expansion under climatic influences.

Products lines are used for moving the refined products from the refineries to shipping points and marketing centers. The pipe is

similar to that employed for the transportation of fluids in the large scale chemical processing plants. Within the refinery area and along the routes to shipping points, these pipelines are usually laid on the surface or on pipeline bridges, and the connections are welded.

On account of the smaller sizes employed in gathering and product lines, the design of these pipelines and of their supports and suspensions is simpler than that of large pipelines laid on the surface. Thus, it is the design of trunk lines and large size pipe systems for refineries that call for particular attention. When designing pipelines of this kind, a detailed and extensive structural analysis will generally be necessary. It must take account of all local and operating conditions. No more than an outline of the essential design process can be presented in this study, because each particular project requires its own solution.

1.3 Construction Modes

Depending upon the different conditions along the route of a pipeline, there are two basic construction modes, each with a number of variations. These are the belowground and the aboveground construction modes. The belowground construction mode is generally the safest and the most desirable construction mode for a pipeline. In this mode the pipe is placed in a trench, surrounded by select granular material and covered at least with three feet of backfill over the crown. In this way the pipe is essentially restrained from motion. Buried pipe-

lines can only be used where the underlying soil remains stable under static as well as earthquake conditions. Specific consideration should be given to slope stability and liquefaction on a slope. In cases where the pipeline is constructed in frozen soil, the warm fluid flowing in the pipe will thaw nearby soil in a large extent. Therefore, the belowground mode can only be used where the thaw will not have any undesirable consequence, that is the pipe rests on bedrock or thaw stable sand and gravel. In some places, deeper than minimum burial depth is used to reach one of the stable burial conditions, or to go below a potential unstable or liquefiable shallow layer. Deeper burial is also required for scour protection at river crossings.

Aboveground pipeline construction on structural supports is a means to overcome many of the problems of belowground construction mode. Usually the pipeline is unrestrained with thermal expansion accommodated by controlled lateral displacement. In case of extended shut-down during winter the pipe should be insulated. The structural supports may be provided in two basic ways. Either at close spacings with the pipe itself spanning from support to support, or at wider spacing, with a structural system such as a suspension structure provided to span between supports, as shown in Figure (2).

The buried mode has several basic advantages, over the aboveground construction mode. It is the safest, because the pipe is continuously supported in the soil and it cannot be damaged from surface hazards. There is long experience in buried pipeline constru-

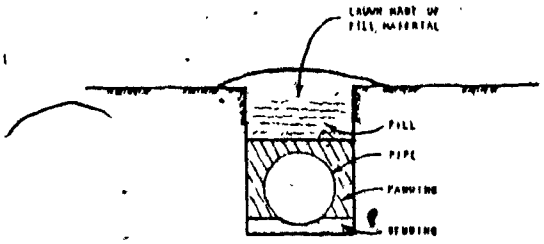

Conventional Burial

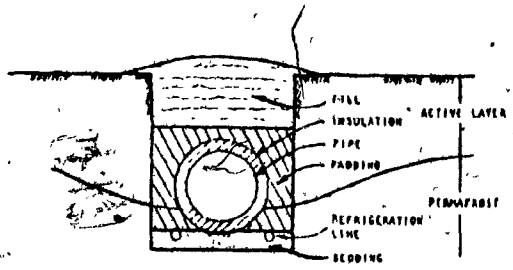

Special Burial

Figure 1. Belowground Construction Modes.

Short-span Support System

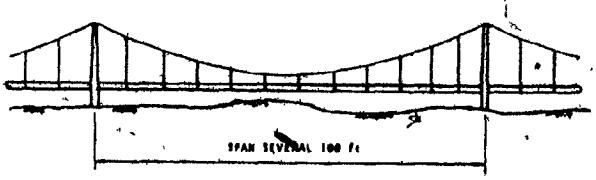

Long-span Support System

Figure 2. Aboveground Construction Modes.

ction. Environmental aspects and esthetic are best provided by buried pipelines. But the most important advantage of buried pipelines is that usually they have the lowest cost.

A very important disadvantage of buried pipelines in permafrost is the large heat transfer to the ground, which after some years of operation cause extensive thaw and consequent potential stability problems wherever the ground is not inherently stable. This problem can be avoided in some extent, by insulated and refrigerated burial construction in such a way so that to keep the soil below the pipeline frozen at all times. But this construction type is associated with high cost and it is therefore unattractive except for short lengths. Another important diadvantage of buried pipelines is that, in cases of ground motions, the pipe is tightly held by the ground and would be forced to distort with the ground. Also in locations where potential scour in a river is deep, the pipe has to be placed below that depth to be safe, causing disturbance of the river regime and high cost.

The main advantages of the aboveground construction system are the reduced dependence of the pipeline support upon the ground stability and the great reduction in permafrost thaw. While the main disadvantages are the increased exposure of the pipeline to surface hazards, such as traffic, avalanches or human influences, and the high cost of structural system, structural supports and if necessary the insulation. In long pipelines both the belowground and aboveground construction modes are usually used, depending on the specific site and environment conditions.

1.4 Ring Stiffened Pipelines.

Stiffening rings are used in pipes for two purposes. The so called tension rings may be used to resist internal pressure. In some cases it is difficult to form pipe walls thick enough to resist the tension produced by some high pressures and it may be advantageous to form the pipe of thinner plate and wind it with tension rings. The second type of rings, the stiffening rings are used to resist buckling both in aboveground and belowground construction modes. Belowground pipelines are being constructed in ever-increasing diameters and at the same time wall thicknesses are reduced as high strengh steels are developed. In such cases the critical load is usually the external pressure which may cause failure due to buckling. It is often economic to provide stiffening rings to resist buckling, and design the pipe wall to resist internal pressure only. Aboveground pipelines are usually constructed as continous over many supports. As a result bending moments are introduced, and compression zones are developed at the top and the bottom of the pipe, at the midspan and over the supports respectively. Stiffening rings may be used to resist buckling at these compression zones without being necessary to increase the pipe wall thickness, and in this way to have a considerable saving in the material.

It must be pointed out that tension rings are not perform the same function as the stiffening rings. As a result the tension rings should be as flat and broad as possible, in order to keep the distance between them to a minimum so that they can resist the tensile stresses

more effectively. Stiffening rings are usually spaced a number of diameters apart and they should be as high as possible to increase the moment of inertia of the longitudinal section throught the pipe. In the following chapters the stiffening rings will only be discussed, and in particular the case of equally spaced rings is considered.

CHAPTER II

BELOWGROUND PIPELINES

CHAPTER II

BELOWGROUND PIPELINES

Buried pipelines is the most widely used type of pipeline construction, because they usually have lower cost than aboveground pipelines. The first problem encountered in the design of belowground pipelines is the evaluation of the imposed loads. This is due to the fact that the loads imposed on a buried pipeline can vary widely depending on the method of installation, the shape of the trench, the properties and the degree of compaction of the fill, etc. While the installation methods are beyond the scope of this project, the estimation of the various loads is essentially a problem of soil mechanics. Therefore in this project we will not present detailed analyses and calculations of the loading conditions. Even so it seems necessary to mention the more general design loads and the required theory to estimate the loads transmitted to a pipeline.

Large steel pipes reinforced with stiffening rings are the main interest of the project. The stresses developed in a buried pipeline are evaluated by methods based on the concept of the pipe-soil interaction. Also some basic concepts for the static design of buried pipelines under seismic loads are mentioned. In pipelines with large diameter to wall thickness ratios the critical pressures are usually not the internal pressures, but the external pressures due to the soil load and live loads, which may cause buckling. In such cases the ring stiffeners are designed to resist bucking and the pipe wall to resist

the introduces stresses. The design considered, is based on the following principles :

1. That the load-carrying capacity of a pipe must be sufficient for the maximum load to be imposed upon it with an adequate factor of safety against fracture or excessive deformation.

2. The design of the pipe wall thickness is based on the yield strenght of the material of the pipe in compression, and in addition on the yield strenght of the wall material in tension for pressure pipes. The advantageous effect of the stiffening rings is not considered at this stage.

3. Since a flexible pipe has little inherent resistance to crushing, because of its small stiffness, permits very large deformations under sustained loading without cracking, and fails by buckling or flattening. The presence of the stiffening rings helps the pipeline to resist bucling by increasing the critical pressure. The required spacing and moment of inertia of the stiffeners are evaluated at this stage.

2.1 THE LOADS IMPOSED ON BELOWGROUND PIPELINES

2.1.1. Classification And Nature Of The Loads

The loads and forces imposed on a buried pipeline can be classified into two categories:

a. Primary loads.

b. Secondary loads and forces.

Secondary loads can be the largely fortitous and frequently undeterminable forces exerted either axially or transversely in any direction, by thermal and moisture changes in the conduit or in the soil, by soil movements, by the relative settlement of any structure to which the conduit is connected, or by bedding of the conduit.

The primary loads are furthermore subdivided in:

a_1. The externally applied, vertically acting, gravitational load caused by the fill and surface surcharges.

a_2. Fluid pressures applied either externally or internally or both.

2.1.1.1 Primary External Loads

The primary external loads comprise:

1. Permanent loads, such as the fill load.
2. Transient load, such as the concentrated surcharges which may be applied at any point on the surface by vehicle wheel loads.
3. Temporary loads, such as uniformly distributed surface surcharges

of large extent, by additional temporary fill, or any similar load which may be placed over.

4. Permanent temporary or transient loads, such as uniformly distributed surcharges of small extent applied at or below the surface, but above the top of the conduit, by tracted construction equipment or any similar load.

5. Permanent or temporary fluid pressures applied to the external perifery of the conduit by the immersion in water or by any possible submergence of the ground surface, like at a river crossing, or by partial vacuum in pressure pipes.

2.1.1.2 Primary Internal Loads

The primary internal fluid pressure loads may be temporary or transient and comprise the maximum pressure to which a pressure pipe may be subjected in service.

2.1.2 Factors Affecting The Various Component Loads

2.1.2.1 The Fill Load

This load is static and permanent and can be assumed to be uniformly distributed over the width of the conduit. Its value depends on the soil properties, the width and shape of the trench, and on the method of instalation.

2.1.2.2 The Contained Liquid Load

This load contributes to the deflection of flexible pipes. It is assumed to be permanent and to depend only on the fraction of the weight of liquid per linear foot .

2.1.2.3 The Self-Weight Of The Pipe

This is a permanent load but its effect on flexible pipe's deflection is rather insignificant in thin-walled pipes.

2.1.2.4 The Uniformly Distributed Surcharges Of Large Extent

These loads are static and usually temporary. They depend upon in almost the same factors as the fill load, namely, the intensity of the surcharge, the width and shape of the trench, the soil properties and the method of installation.

2.1.2.5 The Loads Imposed By Concentrated Surcharges

Usually these loads are dynamic and transient and they caused by vehicle wheels. They depend on the magnitude of the wheel loads and their positions relative to the pipe, and also on the depth and the overall width of the trench.

2.1.2.6 The Loads Imposed By Uniformly Distributed Surcharges Of Small Extent.

These loads are applied at or below the surface but above the pipe and they are of defined and limited area in plan. They may be static or dynamic, and they depend on the same factors as the concen-

trated surcharge loads.

2.1.2.7 External Fluid Pressures

These pressures may be permanent or temporary. They depend only on the height of the water surface above the axis of the pipe. Althought they may reduce the fill load, no such reduction must be considered except if there is not any possibility of subsequent lowering of the water table. In flexure pipes they are of importance since they contribute to the critical buckling pressure when the pipe is not under internal pressure.

2.1.2.8. Internal Fluid Pressures

These pressures may be subjected to large variations caused by surges due to faulty operations or to test pressures which are higher than operating pressures.

2.2. THE THEORY AND DERIVATION OF THE LOAD FORMULAE

Pipelines are usually constructed in relatively narrow trenches and then backfilled with soil up to the ground surface. Therefore the folowing analysis is limited to narrow trench loads only. The derivation of the load formulae for wide trench loads, althought similar, it is not included here.

2.2.1 Trench Fill Loads

The following analysis presented by Spangler (6) is based on the theory of loads, originally proposed by Marston in 1913 and subsequently confirmed experimentally. Marston's theory postulates that the load on the pipe consists of the weight of the prism of earth fill contained within the trench above the top of the pipe, less the sum of the upward shearing forces which are due to the tendency of the backfill to settle downward in relation to the sides of the trench. The cohesion between them is ignored. Therefore the shear forces depend upon the coefficient of sliding friction between the backfill and the sides of the trench and on the ratio, K , which Marston took to be Rankine's value for active pressure :

$$K = \frac{(\mu^2 + 1)^{\frac{1}{2}} - \mu}{(\mu^2 + 1)^{\frac{1}{2}} + \mu} = \frac{1 - \sin\phi}{1 + \sin\phi} = \tan^2(45^\circ - \tfrac{1}{2}\phi) \qquad (1)$$

Where

$\mu = \tan\phi$: coefficient of internal friction of fill material.

ϕ : angle of internal friction of fill material.

Considering a thin horizontal element of the fill material, as shown in Figure (3), and equating the forces acting on it, if V is the effective total load imposed on the top of the element and $K\frac{V}{B_d}$ the lateral unit pressure on each side of it, we obtain :

$$V + dV + 2K\mu\frac{V}{B_d}dh = V + wB_d dh \qquad (2)$$

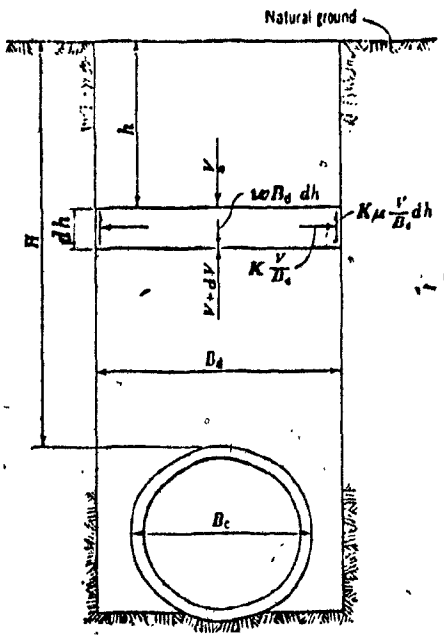

Figure 3. Free body diagram for buried pipelines

The solution of the linear differential Equation (2) provides

$$V = w B_d^2 \frac{(1 - e^{-2K\mu h/B_d})}{2K\mu} \qquad (3)$$

for $h = H$ we obtain

$$W_c = w B_d^2 \left(\frac{1 - e^{-2K\mu H/B_d}}{2K\mu} \right) \qquad (4)$$

The expression in the brackets, is known as the load coefficient, C_d , and in order to evalute it the Figure (5) can be used, in which values of C_d versus H/B_d are plotted for several kinds of filling materials.

Where:

H : the height of the fill above the top of the pipe, in feet.

h : the distance from ground surface down to any horizontal plane in backfill, in feet.

e : the base of the natural logarithms.

w : the unit weight of the filling material, in pounds per ft^3.

B_d : the effective trench width. The effective trench width is depending on the shape of the trench. In Figure (4) the effective trench width for various types of trench, is shown.

Equation (4) may now be written in the following form :

$$W_c = C_d \, w \, B_d^2 \qquad (5)$$

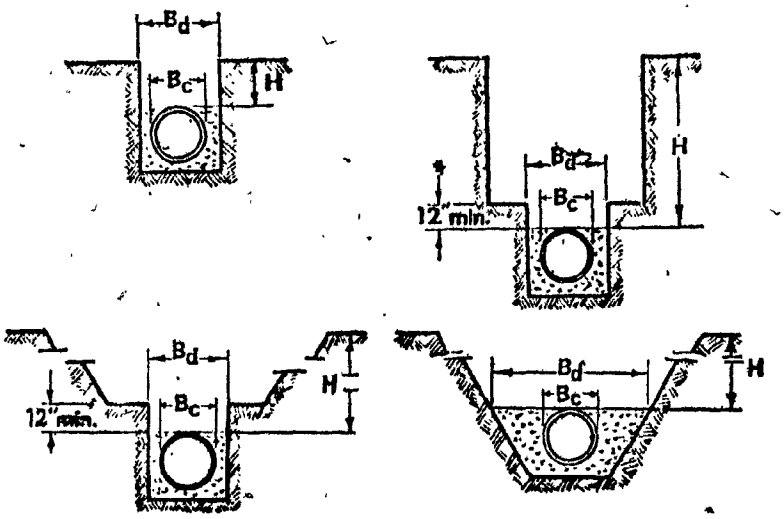

Figure 4. Effective trench width, B_d.

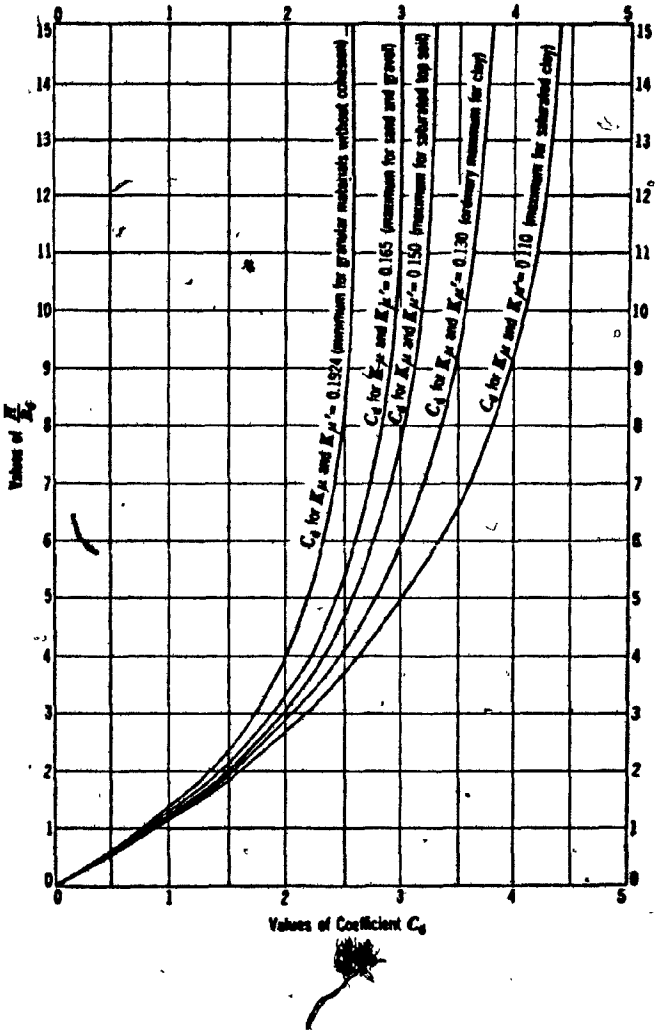

Figure 5. Diagram for coefficient C_d

2.2.2 Loads Imposed By Uniform Surcharges Of Large Extent

If the intensity of the surcharge is denoted by, U_s , in pounds per square foot, there will be a load over the width of the trench at the surface of $B_d U_s$. In this case the differential Equation (2), for $h = 0$ and $V = B_d U_s$ has the following solution :

$$V = w B_d^2 \left(\frac{1 - e^{-2K\mu h/B_d}}{2K\mu}\right) + B_d U_s e^{-2K\mu h/B_d} \qquad (6)$$

For $h = H$

$$V = w B_d^2 \left(\frac{1 - e^{-2K\mu H/B_d}}{2K\mu}\right) + B_d U_s e^{-2K\mu H/B_d} \qquad (7)$$

and if we substruct the fill load, the load imposed by the surcharge is

$$W_{us} = B_d U_s \left(e^{-2K\mu H/B_d} \right) \qquad (8)$$

or

$$W_{us} = C_{us} B_d U_s \qquad (9)$$

Where, the expression in brackets has been replaced by a load coefficient, C_{us} . Values of C_{us} for various values of K and H/B_d are plotted in Figure (6).

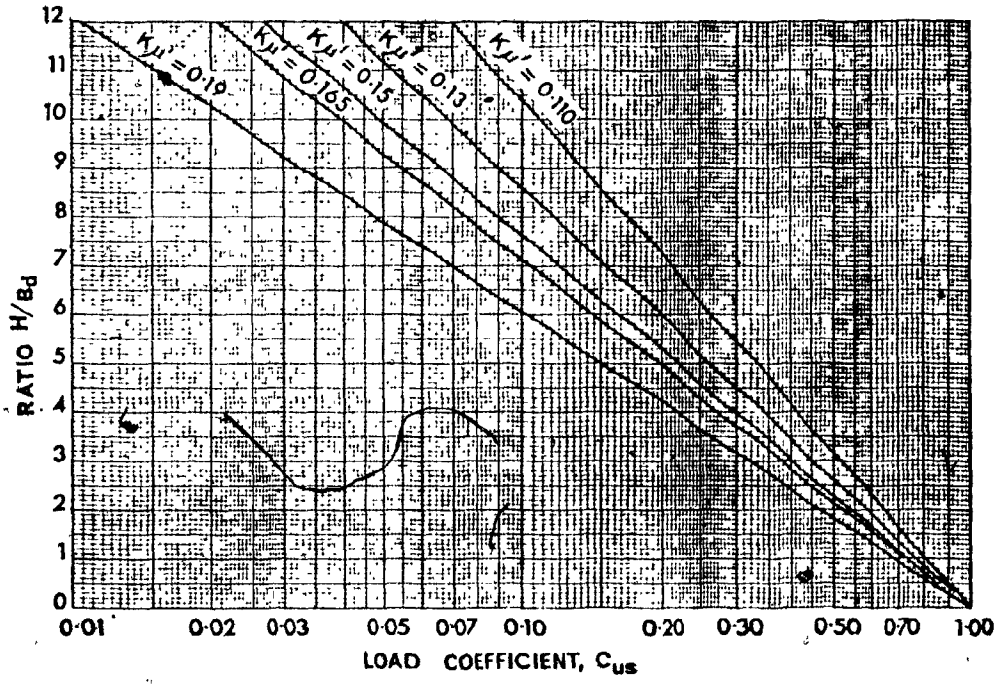

Figure 6. Diagram for coefficient C_{us}

2.2.3 Loads Imposed By Concentrated Surcharges

Marston and latter Spangler proved that the vertical load imposed on a conduit by a point load of P pounds on the surface, vertically above the centre of the pipe, was practically aproximated by the Boussineq's theory of stress distribution in a semi-infinite elastic solid. If the transmitted load is denoted by, W_{cs} ,and the effective lenght of the pipe by l , the formula which Marston introduced can be written as follows :

$$W_{cs} = C_t P F_i / l \qquad \text{(pounds per linear foot)} \qquad (10)$$

In which the load coefficient, C_t, was obtained by summing the Boussinesq stresses at a depth equal to the cover of the pipe, and F_i was an impact factor.

Spangler and Hannesey (29) developed a more advanced method to evaluate the load imposed on a pipe by a point load in any position on the surface or by any number and arrangement of point loads, using Newmark's table of influence values. According to this method the loads which transmitted to the pipe, due to a concentrated surface load is called the transmitted load and it is given by the following modified Marston formula :

$$W_{cs} = \frac{1}{l} (F_{i1} C_{t1} P_1 + F_{i2} C_{t2} P_2 + \ldots + F_{in} C_{in} P_n) \qquad (11)$$

Where W_{cs} is the corrected load per linear foot of pipe.

$F_{i1}, F_{i2}, \ldots$, etc, are the impact factors appropriate to each individual wheel load.

$P_1, P_2, \ldots$ etc, are the actual individual wheel loads, in pounds.

l : the lenght of the pipe or 3 feet, whichever is the less.

$C_{t1}, C_{t2}, \ldots$, etc, are the Load Coefficients. They can be calculated with the help of Newman's table in Fiqure (7), as the algebraical sum of the influence values, I_σ .

The load W_{cs} must be modified for non-uniformity of loads intensity normal to the pipe axis, by multiplying it by a correction factor F_L , to obtain a corrected value W'_{cs} which can be used as a comp-

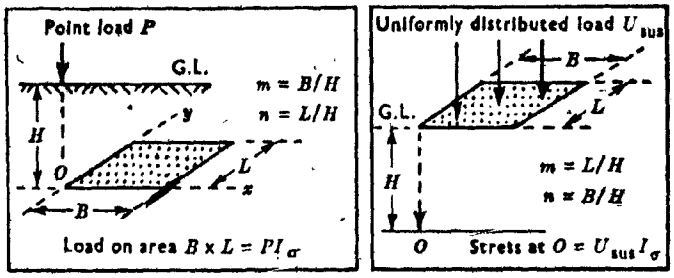

Concentrated surcharge

Uniformly distributed surcharge on a limited area of small extent

N.B. The area $B \times L$ is rectangular in true plan in both cases

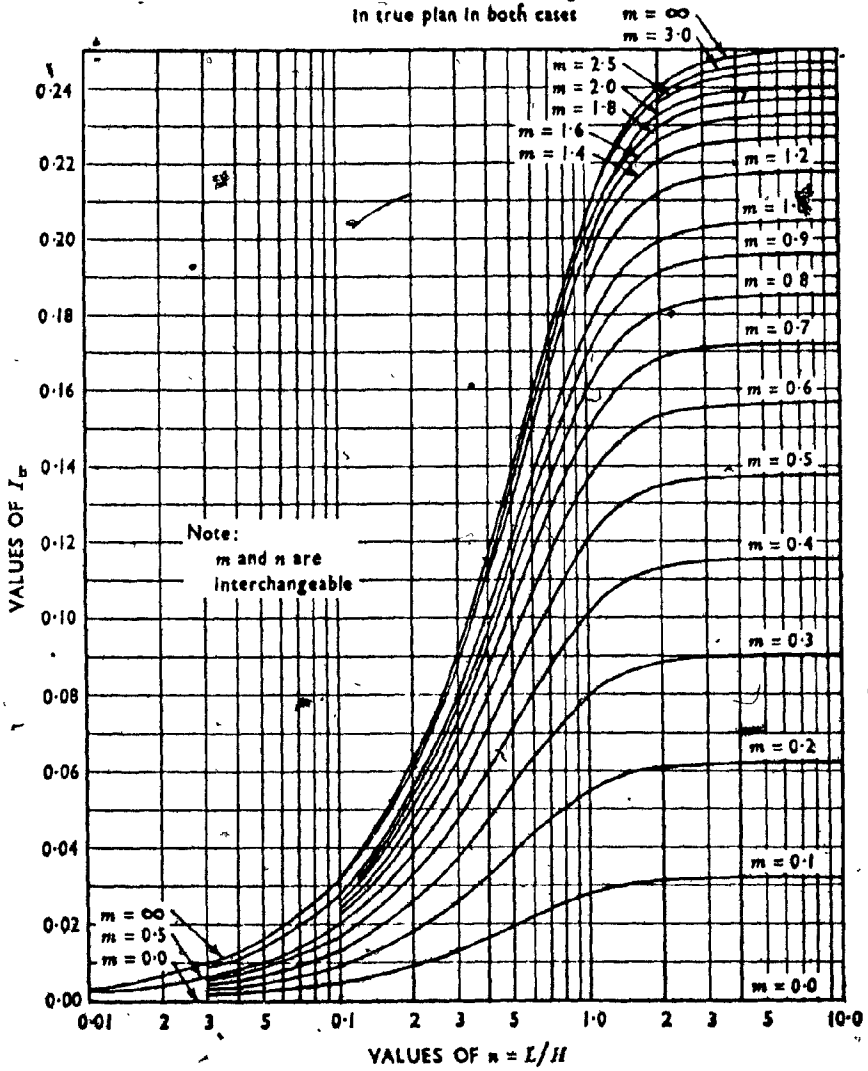

Figure 7. Values of influence value I_σ for concentrated load.

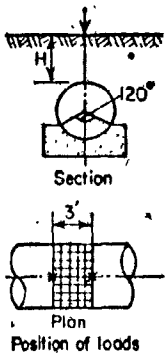

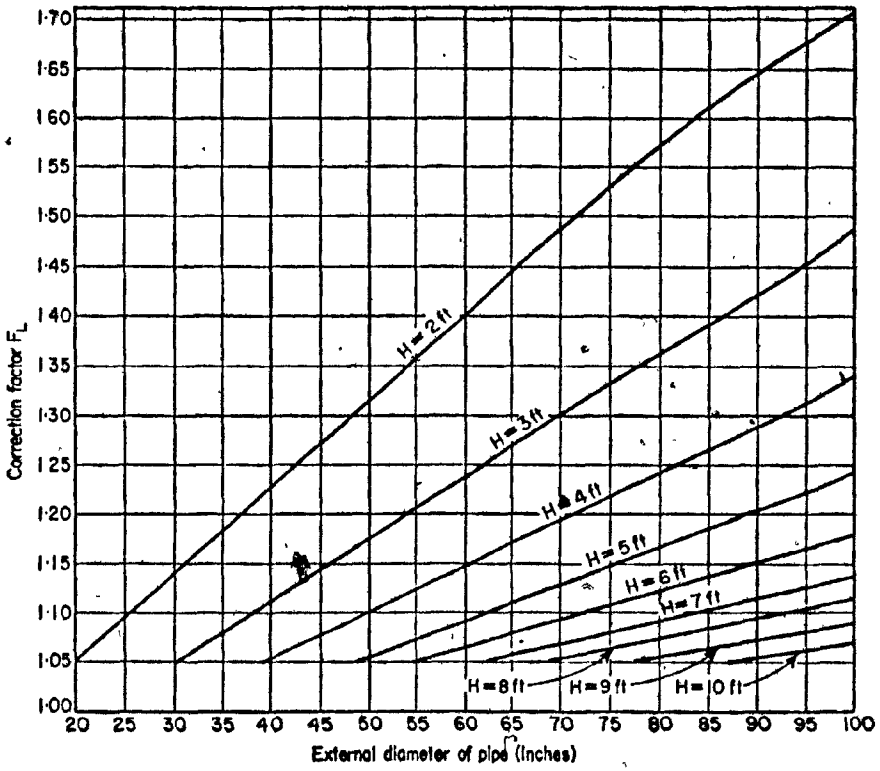

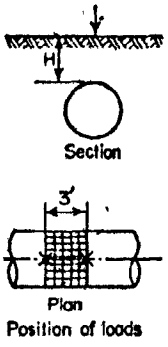

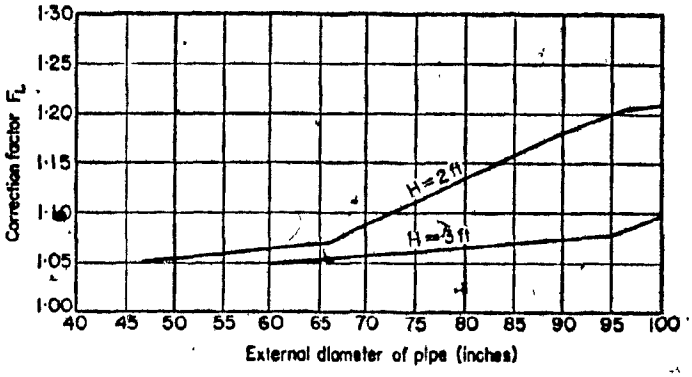

Figure 8. Diagram for correction factor F_L

onent of the total effective external load on the pipe .

$$W'_{cs} = W_{cs} F_L \qquad (12)$$

The correction factor, F_L , can be obtained from Figure (8) presented by Young.

2.2.4 Loads Imposed By Uniformly Distributed Surcharges Of Small Extent

Uniformly distributed load of small extent is considered a surcharge such as a column footing of which the contact area has a largest dimension greater than half the cover depth. The Boussinesq theory of stress in a semi-infinite elastic solid may be used again. For a rectangular, uniformly loaded with a load of intensity U_{su} in pounds per square foot, the following formula can be obtained for the load transmitted to the pipe, W_{su} .

$$W_{su} = C_{su} B_c U_{su} \qquad (\text{lb/Linear foot}) \qquad (12)$$

Where $C_{su} = \sum I_\sigma$, is equal to the algebraic sum of the influence values of the necessary rectangles and can be obtained from Figure (7)

For mobile and transient loads such as tructed construction vehicles, the load transmitted to the pipe is :

$$W'_{su} = W_{su} F_i \qquad (13)$$

Where F_i is an impact factor of which the value estimation is a matter of experience. Usually a value greater than two is adopted.

2.2.5 External Pressure

External pressure usually caused by submergence or vacuum and it can be a major load in cases like pipelines laid under lakes or rivers. These pressures affect the deflection of a circular flexible pipe and they contribute largely to the compressive stress in the pipe wall especially in thin-walled pipes.

If the maximum height of the water level above the top of the pipe is H_s in feet, the external pressure is then :

$$P_g = (H_s + B_c/2)\gamma_w/144 \qquad (\text{lb per inch square}) \qquad (14)$$

If partial vacuum pressures may occur in the pipe, owing to faulty operation, the corresponding pressure P_v must be added, so that the external pressure becomes :

$$P_e = P_g + P_v \qquad (\text{pounds per inch square}) \qquad (15)$$

2.2.6 Internal Pressure

Internal pressure is of major importance in gas pipelines, and it is equal to the pressure of the gas. Also internal pressures may occur where a pipeline is hydraulically surcharged. Its value may be

assumed as the mean static head at zero velocity p_h

$$p_i = p_h \tag{16}$$

In gravity pressure pipelines it must be added any allowance for surge to provide for faulty operations or the maximum test pressure, whichever is the greater.

$$p_i = p_h + p_s \quad \text{or} \quad p_t \tag{17}$$

In pumping mains it must be added the sum of the velocity head plus the friction head.

These pressures cause tensile ring stress in the pipe wall and in flexible pipes they tend to reduce the deflections caused by external loads, to reverse the ring stress and reduce the bending moments in the pipe wall.

2.2.7 Total Design Load

The maximum resultant external load on which the design of the pipe is based, is the sum of the effective component loads which can be imposed simultaneously on the pipeline. In calculating the average vertical external soil pressure acting at the elevation of the top of the pipe, it is usually assumed that any kind of concentrated surcharges will not be imposed simultaneously with distributed surcharges of large extent. The average external soil pressure must be modified by a factor called the pressure transfer coefficient, C_p , which relates

the calculated pressure to the apparent pressure modified by soil pressure reduction (soil arching action) or soil pressure concentration. The coefficient, C_p, can be obtained from Figure (9), for steel pipes. Values of the pressure transfer coefficient are also available for various materials and they can be obtained through the pipe manufacturers.

The ring flexibility which is used in Figure (9) is given by the formula:

$$F = (12/E)(D/t)^2$$

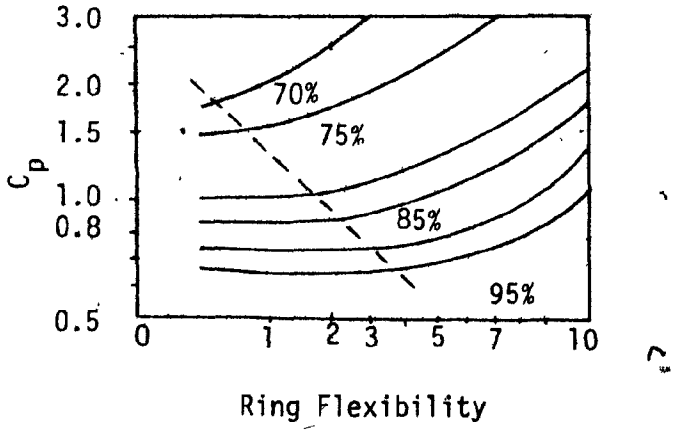

Figure 9. Pressure transfer coefficient for steel pipes as a function of standard soil density and ring flexibility.

2.3 STRESS ANALYSIS OF BELOWGROUND PIPELINES

2.3.1 Pipelines Under External Design Load

A buried pipeline must contain enough strength so that it can resist the forces of handling and the compaction of the earth against it. Once the fill has been placed to the top of the structure, additional fill begins to exercise pressure on the top so as to reduce the requirement for moment strength. At some point above the structure, this fill reaches an amount which exactly overcomes the active lateral pressure on the structure and the pipe then becomes completely a compression ring. Analysis of the normal components on the active pressures on a structure performed by White and Layer (11), shows this point of height of cover to be approximately one-quarter the diameter of a pipe. The composite performance of both the pipe and the soil in which it is buried, must be considered in the design of buried pipelines. The structural phenomenon is usually referred to as soil-structure interaction. The soil exerts pressure on the pipe and at the same time if the pipe compresses or deforms under the soil load, soil pressure on the structure may be relieved by the protective strength of the soil. The soil actually arches over the structure like a masonry arch. Arching action depends on the soil strength and on the relative compression of the soil and pipe. The phenomenon is statically indeterminate to a high degree, so performance data and simplified analyses are necessary.

Based on the elastic theory of the rings an analysis to obtain

stresses and deflections in the pipe wall can be performed. Althought, it would appear that a pipeline more exactly conforms to the condition of plain strain, initial longitudinal stresses in the pipe due to slack laying and uneveness in the bottom of the ditch may modify this condition to the extent that it is impossible to say definitely whether a condition of plain strain or plane stress is to be assumed. Spangler in his classical analysis employed the condition of plane stress, in which it is assumed that the pipe metal is free to deform in the direction normal to a cross section and, consequently, no stresses, due to Poisson's ratio act upon either end of a short segment of the pipe.

Moments and deflections in a loaded thin ring can be determined in the following manner, When external loads on the ring are symmetrical about the vertical axis the tangents to the circle at the top and the bottom will remain horizontal, and the normal cross-sections at these points remain vertical regardless of the direction and magnitude of the angular displacements of tangent and normal sections at indermediate points. Therefore the sum of all the elementary angular displacements will be zero, and this condition leads to the following equation for the determination of the bending moment, M , at any point on the ring

$$\int_0^{\pi} M \, d\phi = 0 \qquad (18)$$

Where ϕ is the central angle between the vertical axis and the radius to the point whose bending moment is considered.

From Equation (18) the moment and thrust may be obtained for either the

top or bottom point on a ring, by substituting a general expression for moment of the actual loads for M. From the moment and thrust at either the top or the bottom point, the moment, tangential thrust, and radial shear may be obtained at any point of the ring from the equations of equilibrium. In Figure (10) the variation of moment around a pipe ring resulting from loads at diametrically opposite points, is shown.

The compressive ring stress in the pipe wall can easily obtained if the compression ring theory of White and Layer (11) is adopted. This theory postulates that the compressive ring stress is uniform around the periphery. The free body diagram of half the circular cylinder is considered, as shown in Figure (11) . The vertical component of the external pressure at the top of the pipe will cause a force on the half structure. This must be carried by the pipe wall, half on each side. The resulting ring compression stress in the wall is in this case given by :

$$f_c = \frac{p_e D_o}{2t}$$

Where

t : the pipe wall thickness.

D_o: the outside diameter of the pipe.

The deflections of the ring, both vertical and horizontal, may be derived by the displacement theory of the arches. According to this theory the origin is taken at a point on the ring that is assumed to be free to move with respect to any other point. If A, in Figure (10) is the fixed point and C the free point, the displacement of any

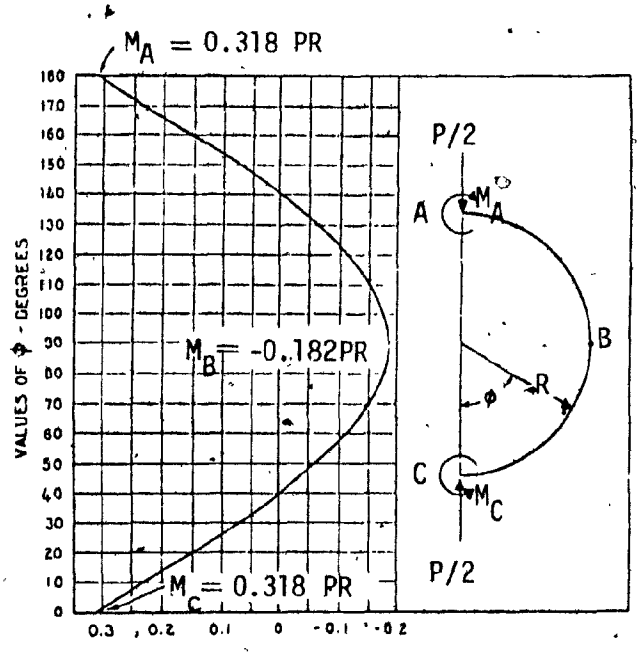

Figure 10. Variation of moment around a pipe due to diametrically opposite points.

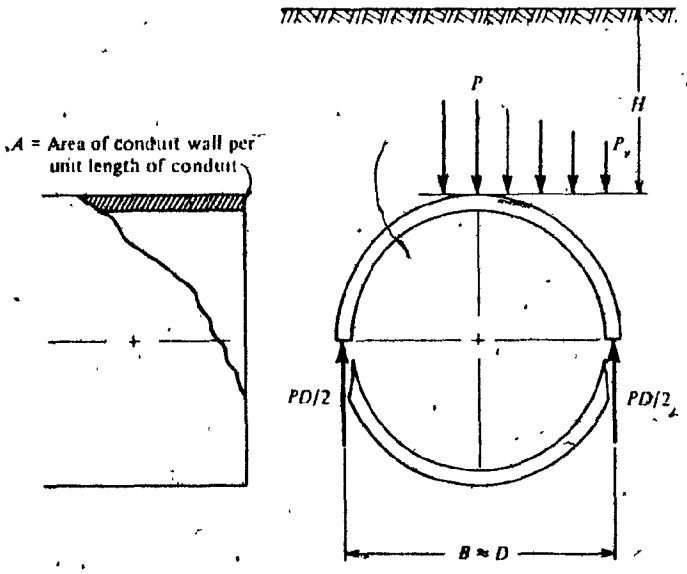

Figure 11. Free body diagram of a buried pipe, showing the ring compression force due to vertical pressure.

intermediate point is the product of the moment at that point multiplied by its ordinate measured perpendicularly to the supposed displacement. Thus the ordinate in the case of horizontal movement of any intermediate point is the vertical distance from C to this point. When the ring is symmetrically loaded about the vertical axis the horizontal displacement of the point B at midway between A and C, relative to A is one half the horizontal deflection. If the loads are also symmetrical about the horizontal axis, the normal cross-sections at the ends of the horizontal diameter will not rotate in relation to their unloaded position and the tangents at the sides of the ring will remain vertical. In such a case it can be shown that:

$$D_x = \frac{2R^2}{EI}\int_0^{\frac{1}{2}\pi} M \cos\phi \, d\phi \qquad (20)$$

Similarly the vertical displacement of the point C relative to A will be:

$$D_y = \frac{R^2}{EI}\int_0^{\pi} M \sin\phi \, d\phi \qquad (21)$$

For vertical loads and reactions on an elastic ring, the above procedure leads to the following equations for moments and deflections, recommended by Spangler (6).

If W is the vertical external load

R is the radius of the pipe

E is the modulus of elasticity of ring material

I is the moment of inertia of cross-section of the ring

$$M = K W R \tag{22}$$

$$D'_x = K_x \frac{W R^3}{E I} \tag{23}$$

$$D_y = K_y \frac{W R^3}{E I} \tag{24}$$

The values of the parameter K can be obtained from Table (13). K_b, K_t, and K_s, are the parameters for the moment at the bottom, top and sides respectively. K_x and K_y are for the horizontal and vertical deflections. The angles α and β are defined at Figure (12).

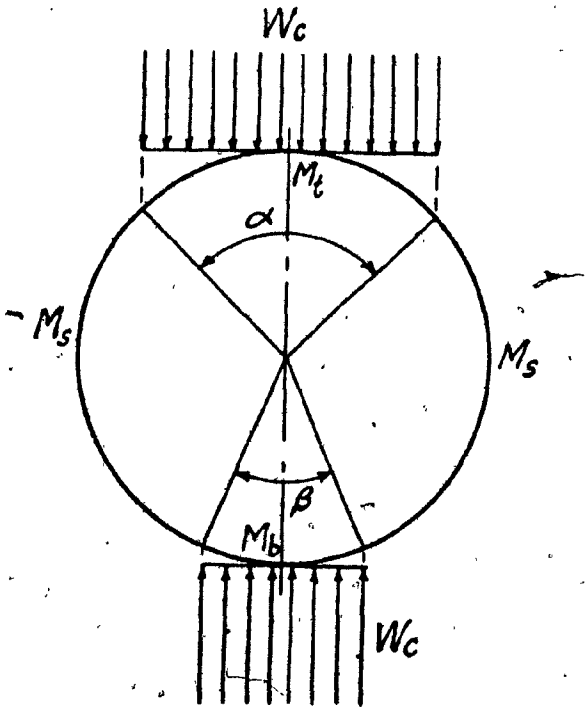

Figure 12. Definition of the angles α and β.

α Deg.	β Deg.	K_b	K_t	K_s	K_x	K_y
	0	0.318	0.318	0.182	0.149	0.137
	30	0.259	0.317	0.180	0.146	0.135
	60	0.213	0.312	0.175	0.138	0.130
0	90	0.182	0.305	0.168	0.129	0.122
	120	0.162	0.299	0.161	0.122	0.116
	150	0.153	0.295	0.156	0.117	0.111
	180	0.150	0.294	0.153	0.116	0.110
	0	0.317	0.259	0.180	0.146	0.135
	30	0.257	0.257	0.178	0.143	0.133
	60	0.211	0.252	0.173	0.135	0.127
30	90	0.180	0.246	0.166	0.127	0.120
	120	0.160	0.240	0.159	0.119	0.114
	150	0.151	0.236	0.154	0.115	0.109
	180	0.148	0.235	0.152	0.113	0.108
	0	0.312	0.213	0.175	0.138	0.129
	30	0.252	0.211	0.173	0.135	0.127
	60	0.207	0.207	0.168	0.122	0.127
60	90	0.175	0.201	0.161	0.118	0.115
	120	0.156	0.194	0.154	0.111	0.109
	150	0.146	0.190	0.149	0.107	0.104
	180	0.143	0.189	0.147	0.105	0.103
	0	0.306	0.182	0.168	0.129	0.122
	30	0.246	0.180	0.166	0.127	0.120
	60	0.201	0.175	0.161	0.118	0.115
90	90	0.169	0.169	0.154	0.110	0.108
	120	0.150	0.163	0.147	0.103	0.101
	150	0.140	0.158	0.142	0.098	0.097
	180	0.137	0.157	0.140	0.096	0.096
	0	0.299	0.162	0.161	0.122	0.116
	30	0.240	0.160	0.159	0.119	0.114
	60	0.194	0.156	0.154	0.111	0.109
120	90	0.163	0.150	0.147	0.103	0.101
	120	0.143	0.143	0.140	0.096	0.095
	150	0.134	0.139	0.135	0.091	0.091
	180	0.131	0.138	0.133	0.089	0.089
	0	0.295	0.153	0.156	0.117	0.111
	30	0.236	0.151	0.154	0.115	0.109
	60	0.190	0.146	0.149	0.107	0.104
150	90	0.158	0.140	0.142	0.098	0.097
	120	0.139	0.134	0.135	0.091	0.091
	150	0.129	0.129	0.129	0.086	0.086
	180	0.126	0.128	0.128	0.085	0.085
	0	0.294	0.150	0.153	0.116	0.110
	30	0.235	0.148	0.152	0.113	0.108
	60	0.189	0.143	0.147	0.105	0.103
180	90	0.157	0.137	0.140	0.096	0.096
	120	0.138	0.131	0.133	0.089	0.089
	150	0.128	0.126	0.127	0.085	0.085
	180	0.125	0.125	0.125	0.083	0.083

Figure 13. Coefficients for bending moments and deflections of an elastic ring under uniformly distributed vertical load and reactions.

2.3.2 Soil-Structure Interaction

Belowground pipelines may be divided into two classes on the basis of the amount of deformation which they can withstand without structural damage, rigid and flexible pipes. Rigid pipes are less flexible than the soil and consequently take a greater share of the vertical load. In the contrary flexible pipes have load shedding characteristics, i.e on account of their flexibility vertical load is taken up by the sidefill and pipe as illustrated in Figure (14). It is

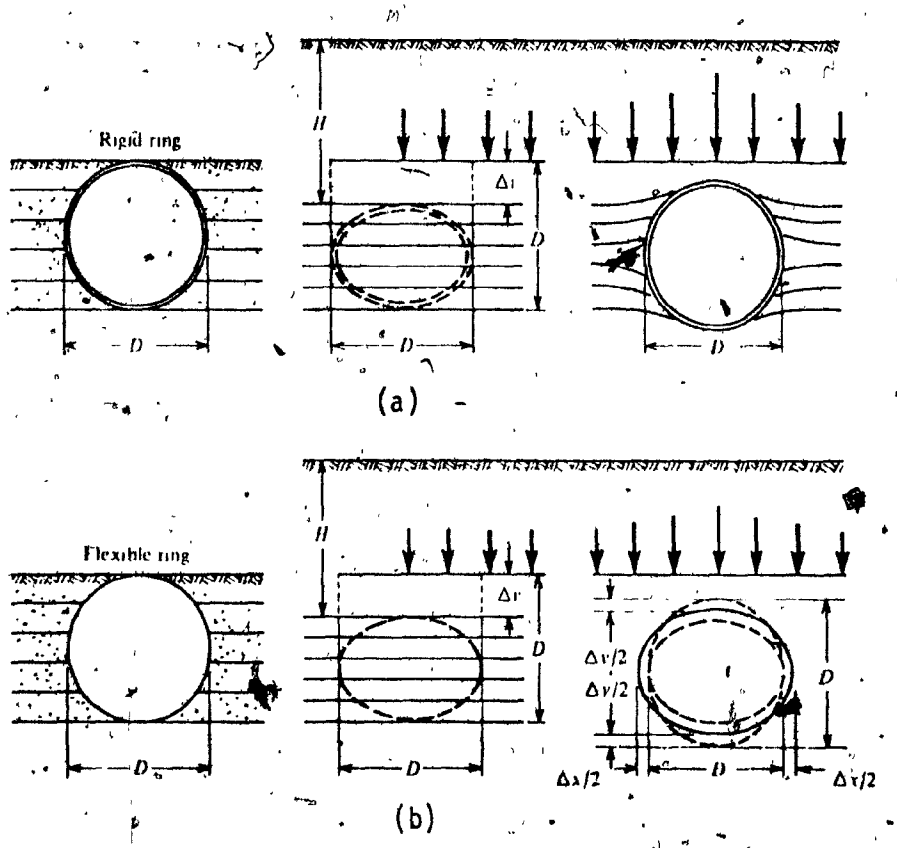

Figure 14. Conceptual sequence for ring performance in (a) rigid and (b) flexible pipe.

therefore necessary any attempt to analyse the structural behaviour of a flexible pipeline to take into account the passive resistanse pressures developed by the soil at the sides of the pipe, as a major source of supporting strength. Concrete is an example of rigid pipe, while thin-walled steel pipes are flexible. In the following only the latter case of flexible pipes is considered.

Flexible pipes are capable of withstanding relatively very large deflections without any evidence of structural damage. The manner in which such a pipe is deflected is shown in Figure (15). The first increase in the loading cause a deflection to the circular ring (curve A) and the ring tends to take an elliptical shape (curve B). With further increase of the loading this tendency continues until the top of the pipe is essentially flat (curve C). In case that the loading incre-

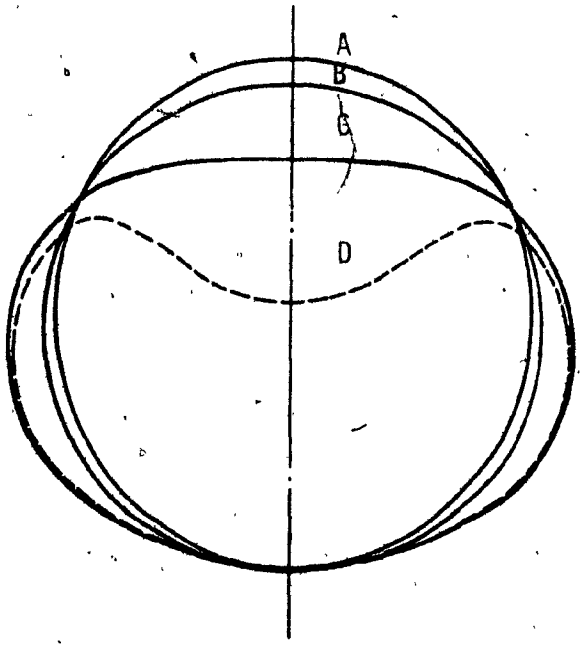

Figure 15. Stages of deflection of flexible pipes.

ases more, the top of the pipe may reverse its curvature and become concave upward, while the sides of the pipe pull inward, as the pipe procced toward complete collapse (curve D). This deformation of the pipe ring has as result, the sides to move outward against the soil a sufficient distance and to develop a substantial amount of the passive pressure of the soil. Hence, flexible pipes support the vertical loads, to which they are subjected, in two ways. From the strength of the pipe and from lateral earth pressures acting against the sides. These lateral pressures produce stresses in the pipe ring that act in the opposite direction to those caused by the vertical loads and in this way increases the load-carrying capacity of the pipe. Spangler(6) developed a method to calculate the deflection of a flexible pipe, taking into account the lateral earth pressure. The loads distribution shown in Figure (16)was asssumed.

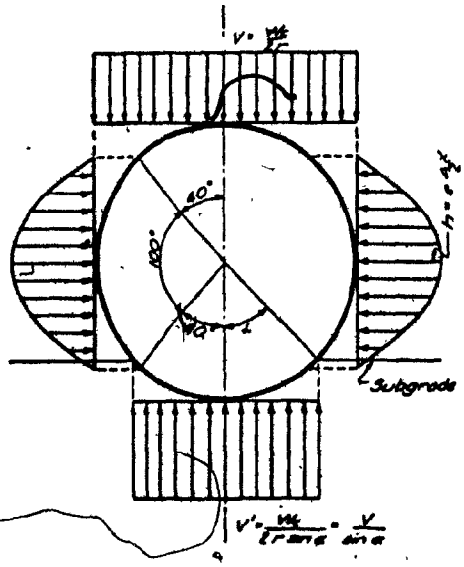

Figure 16. Assumed distribution of pressure on flexible pipe

The vertical load it is assumed to be distributed approximately uniformly over the width of the pipe. The vertical reaction in the bottom of the pipe is equal to the vertical load and is distributed approximately uniformly over the width of bedding of the pipe. The passive horizontal pressures on the sides of the pipe are assumed to be distributed parabolically over the middle hundred degrees of the pipe with maximum unit pressure equal to :

$$\text{Maximum unit pressure} : e\frac{D_x}{2}$$

Where e : the modulus of passive pressure of the side fill soil.

D_x : the horizontal deflection of the pipe.

Spangler also assumed that the deflection of a pipe continues to increase slowly over a long period of time after the vertical load on the pipe has reached its maximum value, due to a gradual yielding of the soil at the sides. With the above established load hypothesis, the mathematical expression for the horizontal deflection of a flexible pipe in terms of the load, the properties of the pipe, and the properties of the soil, is given by :

$$D_{x_1} = \frac{D_e K W_c R^3}{EI + 0.061 e R^4} \qquad (25)$$

Where

D_{x_1} : maximum horizontal deflection of pipe, inches.

W_c : vertical load on pipe, pounds per linear inch.

R : the radius of the pipe, inches.

E : modulus of elasticity of pipe material, pounds per sq. in.

I : moment of inertia of cross-section of pipe wall, in^4 per in.

K : parameter given in Figure (13).

e : modulus of passive resistance of side-fill soil, pounds per square inches per inch.

D_e : deflection lag factor, having values between 1.25 to 1.50

The deflection lag factor is intended to allow for the slow increase of deformation of the soil under sustained lateral pressure in non-pressure pipes. It is not normally applicable therefore to high pressure pipelines or to temporary pressures induced in the soil by transient wheel loads and it need only to be applied to the deflection caused by fill and permanent or long-term uniform surcharge loads.

The modulus of passive resistance of side-fill soil, e , is characteristic of the soil properties. The value of e is given by Meyerhof (10), for a particular type of soil fill as :

$$e = \frac{E_s}{2(1 - m_s^2)\, R} \quad \text{(pounds per square in. per in.)}$$

Where

m_s : Poisson's ratio for the soil.

E_s : the "modulus of deformation" of the compacted soil as determined by triaxial tests.

R : the radius of the pipe.

Poisson's ratio for the soil is usually equal to 0.5 , if we put this

value in the previous Equation we obtain : $e = E_s/1.5\ R$.

For pipelines up to 60 inches diameter, Meyerhof states that the value of K to be used in design should not be less than 20 lb. per sq. in. per inch, and that E_s should not be less than 1,000 lb. per square inch. This value of the modulus of deformation should be increased by about 200 lb/in^2 per foot of pipe diameter for $D > 5$ feet

2.3.3 Pressure Pipelines.

The stresses and deflections calculated in the preceding apply only to externally loaded pipelines. In the case of internally pressurized pipes new formulas should be developed in account of the combined stresses due to both, external load and internal pressure. Prior to being covered with fill, a steel pipeline it is nominally in a circular shape. After covering the load of the fill causes it to deflect to an eliptical shape with the major axis horizontal and the minor axis vertical. Because of this eliptical shape of the pipe, when internal pressure is introduced, the resultant of vertical components of the pressure will be greater than the resultant of the horizontal components. As a result the deflection will decrease to some equilibrium value and the shape of the pipe will be stabilized as an ellipse intermediate between the one under pressure and a circle. Figure (17) shows a typical sequence of loads on the pipe ring starting with a circle.

When a long thin-walled pipe is subjected to an internal pressure, P_i, which may be due to a fluid or gas enclosed within the pipe, tensile circumferential stresses and longitudinal stresses are intro-

duced. The circumferential or hoop stress which is the most important is given by the formula :

$$f_c = \frac{p_i D}{2t} \tag{26}$$

Where P_i the uniform internal pressure

D the diameter of the mean circumference of the pipe

t the thickness of the wall

The above formula is based on the assumption that the circumferential stress is uniformly distributed across the cylinder wall. This assumption holds only in the case of pipes having walls of infinitesimal thickness but it can be used here since the pipes under consideration are thin-walled.

When the internal pressure is introduced into a buried pipeline, and assuming that the horizontal deflection is substantially the same as the vertical deflection, the excess vertical pressure over the horizontal pressure will be $2p_iD_x$ and will cause a tendency to the pipe to return toward the circular shape. In the equilibrium position we will have :

$$W_c = \frac{D'_x}{D_x} W_c + 2p_iD_x \tag{27}$$

Where D_x the deflection of the pipe under external load only

D'_x the equilibrium deflection under combined internal pressure and external load

p_i the internal pressure

W_c the external vertical load

The width of contact between the pipe and the bottom of the ditch, is depended upon the amount which the pipe pushes into the soil bedding due to the vertical load. If it is assumed that the bottom reaction will be distributed over a width about 30 degrees, the corresponding value of the vertical deflection of a thin ring is :

$$D'_x = 0.108 \frac{W_c R^3}{EI} \tag{28}$$

From Equations (27) and (28), solving for D'_x we obtain :

$$D'_x = 0.108 \frac{W_c R^3}{EI + 0.216\, p_i R^3} \tag{29}$$

The external load bending moment is maximum at the bottom of the pipe and at the equilibrium deflection is :

$$M'_b = 2.170 \frac{D'_x EI}{R^2} \tag{30}$$

Substituting Equation (29) into Equation (30) we have

$$M'_b = 0.234 \frac{W_c R EI}{EI + 0.216\, p_i R^3} \tag{31}$$

The corresponding tensile stress at the bottom of the pipe, is :

$$f_b = \frac{M'_b}{2I} t \tag{32}$$

or

$$f_b = 0.117 \frac{W_c R EI}{E t^3 + 2.592 p_i R^3} \quad (33)$$

This stress is additive to the tensile circumferential stress due to internal pressure. The maximum combined stress, from Equation (26) and Equation (27) is :

$$f_c = f_p + f_b = \frac{p_i D}{2t} + 0.117 \frac{W_c R EI}{Et^3 + 2.592 p_i R^3} \quad (34)$$

Watkins (9) has also investigated the problem of pressurized pipes and he has concluded in the following formula to predict the final ring deflection

$$D_x'/D = \frac{C_p w}{288 \left(p_i + \frac{83.3(10^6)}{(D/t)^3}\right)} \quad (35)$$

Where

D_x' : the pressurized ring deflection

w : vertical soil pressure, pounds per square foot

t : pipe wall thickness

p_i : internal pressure, pounds per square foot

C_p : pressure transfer coefficient

The pressure transfer coefficient C_p to be used is $1 < C_p < 1.5$ for the soil wedge and crack pattern of Figure (17_c). This pattern is associated with low soil cover H , so that H/D goes from 0 to about 1 Figure (17_d) is associated with high soil cover roughly greater than D. As the cover increases, the soil compresses rather than forming wedges.

Under these conditions the coefficient C_p is $1.5 < C_p < 2$ as H / D increases from about 1 to infinity . Watkins, also presented a graph which gives the pressurized ring deflection directly. This graph is shown in Figure (18).

The following three design conditions apply to pressurized flexible pipelines.

1. The tensile circumferential stress, f_c , must be less than the strenght of the material, which is usually the yield point stress divided by an adequate factor of safety.

$$f_c = \frac{p_i R}{t} \leq \frac{f_y}{F.S} \qquad (36)$$

2. The pressurized ring deflection D'_x/D should be checked. Note that this deflection is the ring deflection still remaining in the pipe after it has been pressurized and not the installed ring deflection before the internal pressure is applied. In case that the installed ring deflection D_x is less than the predicted pressurized ring deflection D'_x it is assumed that the ring deflection will not change but will remain D_x .

3. The maximum circumferential stress, hoop tension plus flexural, should be checked with the allowable stress. This maximum combined stress is given in Equation (34) or by the following formula presented by Watkins

$$f_c = \frac{p_i R}{t} + E \left(\frac{2t}{R}\right)\left(\frac{3\, D'_x/D}{1 - 2\, D'_x/D}\right) \qquad (37)$$

If Equation (37) is to be used, the ring deflection after pressurizing, should be taken from Equation (35).

Finally it should be noted that unpressurizing the conduit after it has once pressurized is not a design condition. If the pressurized ring deflection is less than the installed ring deflection, after the conduit is unpressurized, the ring deflection may increase part way to the installed deflection. Even if it should increase all the way, stress and deflection, will not be worse than during installation. Consequently collapse of the pipe cannot occur. This has been confirmed by experimentation.

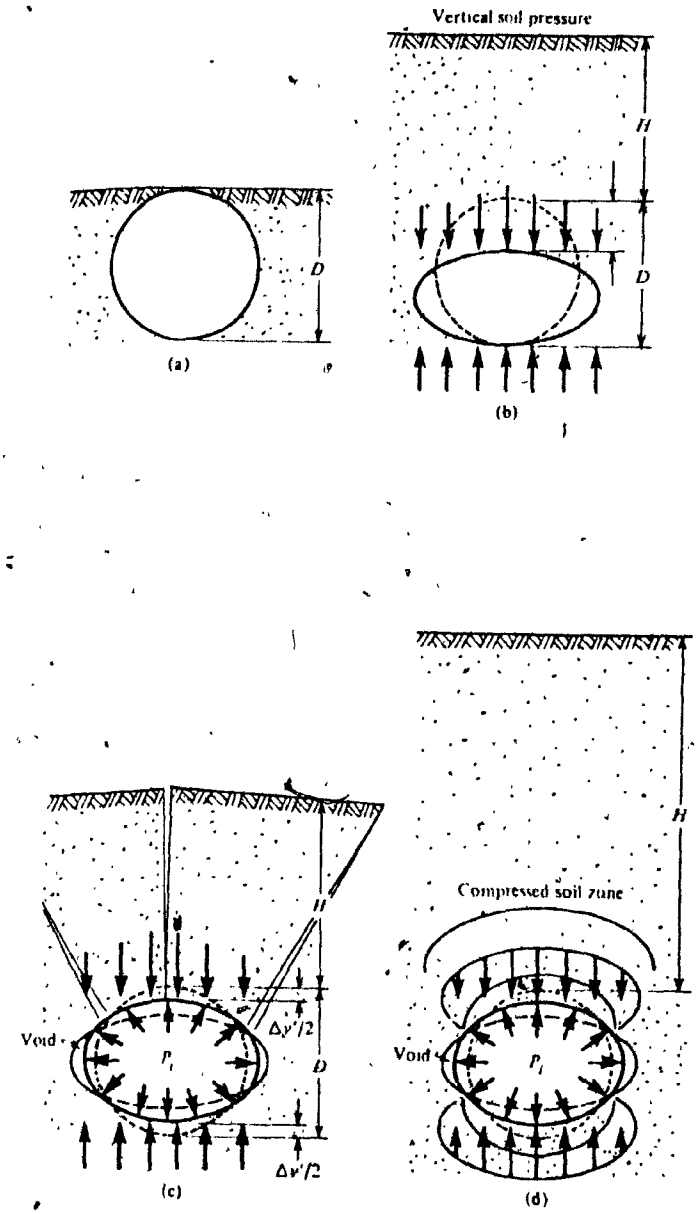

Figure 17. Conceptual sequence of loads and ring deflection of a buried flexible pipeline under internal pressure. (a) Fill to top of pipe;(b) Fill completed up to grade;(c) Internal pressure, C_p= 1.0 to 1.5;(d) P_i with : C_p = 1.5 to 2

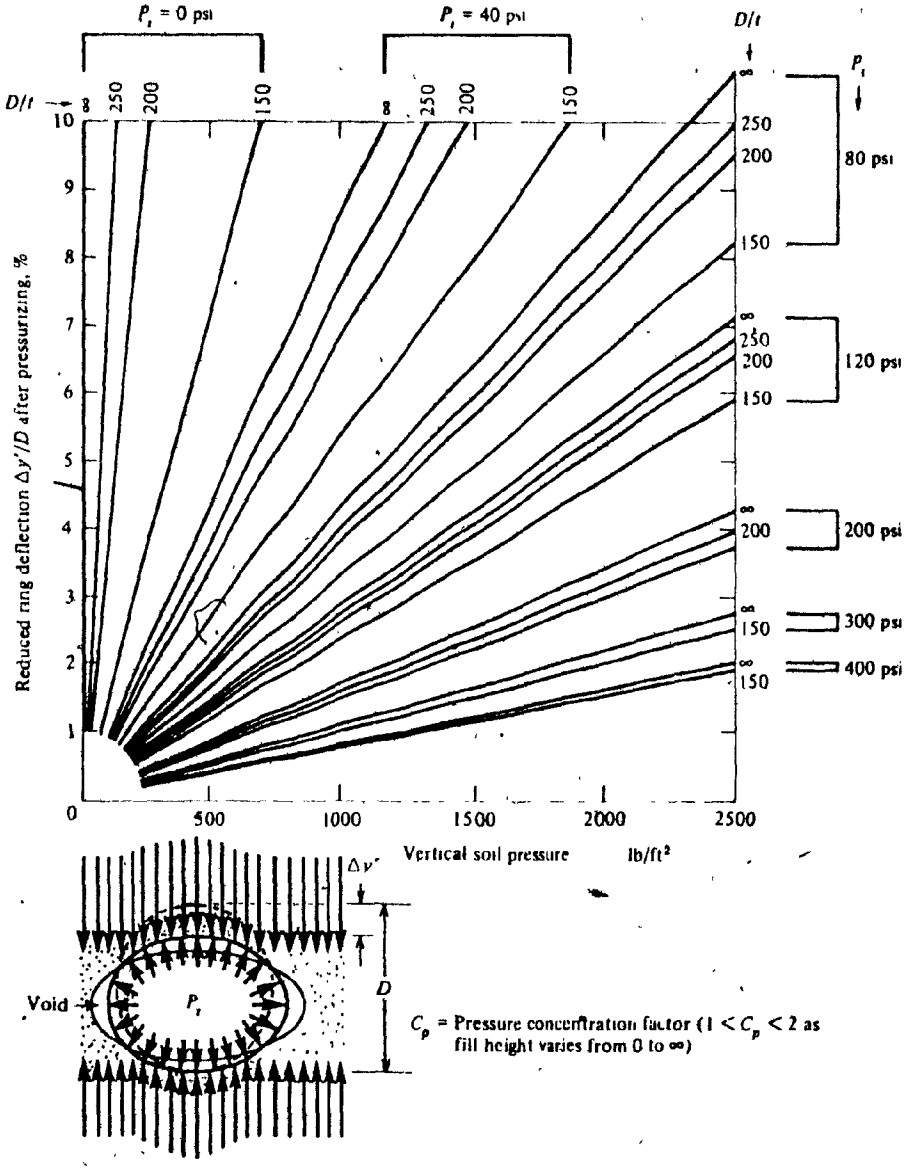

Figure 18. Diagram giving the value to which the vertical ring deflection D'_y/D will be reduced after an internal pressure is applied.

2.4 BELOWGROUND PIPELINES UNDER SEISMIC LOADING

Experience has shown that buried pipelines have been damaged heavily by earthquakes. The observed damages can be attributed to either direct or indirect effects. Direct earthquake damaging forces are taken as seismic shaking and vibration, fault displacement, and tectonic uplife subsidence. Indirect damaging forces refer to mass ground movements, such as landslides, soil liquefaction, and compaction of sediment. The pipeline failure modes due to landslide, tectonic uplife subsidence, or liquefaction are catastrophic and cover a large area. Usually such failures are accompanied by breakages of a large potion of the pipeline system in the failure area. Failure from seismic shaking may result from large dynamic tension that can cause a pull-out at joints, compression that can cause crushing or buckling, or both, shear that can cause craks or breakages of connections, and bending that can cause fracture.

Based on damages observed in earthquakes like the 1964 Alaska earthquake, the 1971 San Fernando earthquake, and earthquakes in Japan, attemps have been made to correlate similar pipeline damages to geological and other conditions. These observations conclunded that, damages occured least in bedrock, moderately in coarse-grained soil, and most frequently in fine-grained soils such as clay or silt. Pipeline damage was highest in regions of transition from one type of soil to another, also pipes parallel to the main direction of propagation of the seismic waves were more heavily damaged than pipelines normal to the main direction of propagation.

2.4.1 Seismic Design Philosophy

The seismic design criteria generally encompass two levels of earthquake hazard. The lower level is that associated with a return period for the design earthquake of approximately fifty to a hundred years and is usually designated as the "Design Probable Earthquake". The higher level is that associated with a longer return period, of the order of about two hundred to three hundred years or more, and is designated as the "Design Maximum Earthquake". The first design earthquake is generally considered as one through which the pipeline should be able to operate and continue operation after its occurence. The second design earthquake should not produce damage that has not been anticipated in the design of the pipeline. However, if the seismic data for the region may be inaccurate or insufficient and also since usually the design in such a way, involves an unreasonable degree of design effort, the relationship between the intensities of the two design earthquakes normally can been taken as a factor of two. The earthquake intensity by itself has limited significance in the seismic design, of equal importance are the structural parameters governing response, such as stress or strain and deflection, that the designer intends to use for the particular earthquake selected. Normally these criteria are selected to make the Design Maximum Earthquake govern the design.

Buried pipelines respond to earthquake motions by moving with the ground in such a way as to have nearly the same curvature and nearly the same longitudinal strain as the ground. These strains impose both

compressive and tensile forces in the pipe as well as lateral bending. These forces and moments can be computed reasonably well from the earthquake ground motions and the estimated wave propagation velocity arising from the earthquake. Of course, the assumption that the pipe moves with the ground is valid as long as the material surrounding the pipe does not liquefy or is not grossly disturbed. Under liquefaction conditions, the pipe is no longer supported directly by the material and the possibility of further large deformations must be considered. Consideration also must be given to the relative motions arising from faults crossing the pipeline. Vertical and horizontal displacements of several feet might occur where fault motions take place, but these need not necessarily cause rupture or failure, if the pipe is designed to provide for moderate amounts of such fault motion.

2.4.2 Design Criteria and Procedures

2.4.2.1 Strains In Belowground Pipelines

Buried pipelines in general will deform with the ground, and the strain in the ground will transmitted to the pipe without attenuation. Actually, because of slip between the pipe and the medium, and local deformations between the two including some slight ovaling of the pipe, the deformations of the pipe may be slightly less than that of the ground. However, it is not desirable to consider a reduction from the strain in the medium. Assuming that the relative displacement between the pipe and the soil is neglisible and also that the shape of

the seismic wave remains constant as it transverses the pipeline, the maximum axial strains and maximum curvature can be estimated.

In a pipeline oriented along a radial line from the epicenter, the radial component of the ground motion induces axial strain, ε which has a maximum value of :

$$\varepsilon_{max} = V_{max}/c \qquad (38)$$

Where

V_{max} : the maximum ground velocity in the radial direction

c : the propagation speed of the seismic wave with respect to the pipeline.

Correspondingly, the tangential component of the ground motion induces bending in the pipeline, with maximum curvature equal to :

$$\text{curvature} = A_{max}/c^2 \qquad (39)$$

Where

A_{max} : the maximum ground acceleration in the tangential direction

The problem of a pipeline at an oblique angle to the direction of the propagation of the seismic waves can also been considered, and similar formulas can be found. Here, the case of zero angle incidence, which is in general the more critical is considered. It should be noted that for reasonable values of V_{max} and A_{max}, the axtal strain would govern the design.

In applying the preceding expressions the values of wave pro-

pagation velocity, c , to be used is the effective velocity applicable to the type of motion and medium being considered. In the case of shear wave effects, the effective value should be taken as the value representative of the actual motion of the medium surrounding the point of interest and not as the value at the surface or at great depth. Representative effective velocity for shearing type propagation is 4,000 fps for rock or permafrost, 3,500 fps for massive gravel deposits and slightly lesser values for silt and clay deposits.

Considering relative settlement a strain in the pipe of the order of 0.004 is a common operating limit of deformation. A reasonable criterion for permisible deformation to avoid rupture seems to be 1% to 2% strain in the modern steel pipe at any section, computed on a nominal basis, or about twice as much at points of stress concentration. In Equation (38), V_{max} corresponds to the maximum ground velocity in the radial direction, While A_{max} in Equation (39) corresponds to the maximum ground acceleration of the tangential component. To investigate whether there is any difference between the radial and the tangential components of ground motion, ground motion time histories recorded at twenty six separate sites during the 1971 San Fernando earthquake were analysed. The result of this investigation was that the average values of the ratios $V_{radial}/V_{tangential}$ and $A_{radial}/A_{tangential}$, were all close to one.

2.4.2.2 Complex Stress System

Since the seismically induced axial strains are of greater consequence than the curvature, the stresses in the longitudinal direction are of major importance. The conventional stress analysis of belowground pipelines for non seismic loading is based on the plane strain condition which does not consider the stress or strain in the longitudinal direction of the pipe. Thus, we must first include whatever axial stress or strain which is produced under normal loading conditions. Furthermore, a failure criterion for stresses in two directions must be used.

The axial stress, f_{lp}, produced by internal pressure is given by the formula :

$$f_{lp} = \frac{p_i R}{2t} \qquad (40)$$

Where

p_i : the internal pressure

R : the nominal radius of the pipe

t : the pipe wall thickness

This stress is apeared near the end of a pipeline. The axial stress in the middle section of the pipeline may be very much smaller, since much of the axial force generated by the internal pressure will be resisted by frictional forces at the interface between the pipe and the soil.

Another source of longitudinal stress is this due to truck and

impact load. Rourke and Wang (13) presented a formula for this longitudinal bending stress, given by :

$$f_{lb} = \frac{W R}{eEI} \qquad (41)$$

In which W is the equivalent distributed load on the buried pipe due to truck and impact, EI is the flexural rigidity of the pipe and e is the lateral soil resistance constant. For the longitudinal direction of the pipe, the axial stress produced by seismic action is denoted by f_{ls} and can be obtained by multiplying the axial seismic strain by the modulus of elasticity of the pipe material. The total longitudinal stress f_l it will be the sum of the above three stresses

$$f_l = f_{lp} + f_{lb} + f_{ls} \qquad (42)$$

The pipe wall should be checked for biaxial stress state. The Von Mises failure criterion has been developed for the yielding under triaxial stress conditions for homogeneous material. For biaxial stress state this criterion can be expressed as :

$$f_c^2 + f_l^2 - f_c f_l = f_y^2 \qquad (43)$$

Where f_c and f_l are the principal stresses and f_y is the yield stress of the material from uniaxial testing. Here, as principal stresses we can take the total circumferencial and longitudinal stress

2.4.2.3 Fault Displacement

Newmark and Hall (15) presented a method that can be used to analyse belowground pipelines for large fault displacement. In the vicinity of a break in the ground surface a buried pipe will strain longitudinally and deform transversely. The pipe generally can be displaced out of the trench and in that way conform to the transverse components of motion of the fault break, although there may be distorsion of the diameter. However, the longitudinal component of fault motion can introduce compression or tension in the pipe. If the longitudinal stresses in the pipe are kept well below the ductility limit of the material of the pipe, shortening of the pipe will be accompanied by wrinkling which can absorb a great deal of strain. But extension of the pipe can produce tensile stresses that might cause failure. It is therefore advised to avoid regions where the angle of fault plane with the pipe axis is so small that nearly all of the fault displacement is transmitted to the pipe as a longitudinal deformation of the pipe.

If the average pressure exerted on the pipe is P, the resistance of the pipe to slip in the medium is determined by the angle of internal friction, between the pipe and the soil, Φ, multiplied by the pressure, P. Hence the change in stress per foot of lenght in the pipe, q, is given by the formula :

$$q = \frac{P \tan\Phi}{t} \qquad (44)$$

Where, t, is the thickness of the pipe wall.

The average strain between two points where the stresses are defined, can be computed as the average of the two strains at the ends of the region, and from this average strain multiplied by the length of the pipe that slips, the change in length of the pipe can be determined. The length of the pipe that slips can be obtained by dividing the difference in stress between the two points by the quantity, q . In the elastic range slip occurs from a point of zero stress to some maximum stress, f_1 . The length, l_e , over which slip occurs, the average strain, ε , and the displacement or change in the length of the pipe, d_e , are given by the following formulas :

$$l_e = f_1 / q \tag{45}$$

$$\varepsilon_{ave} = f_1/2E \tag{46}$$

$$d_e = f_1 l_e / 2E \tag{47}$$

If the change in the length of the pipe in each side of the fault is d_e , and the total fault motion is, F , with an angle, u , between the plane of the fault and the pipe axis, the displacement is given by:

$$d = F \cos u / 2 \tag{48}$$

Even a purely transverse fault motion will produce gross longitudinal strain in the pipe, additional to those corresponding to flexure of the pipe. For an anchor length, l , on each side, and an offset

F , the average longitudinal strain, $\bar{\varepsilon}$, is well aproximated by :

$$\bar{\varepsilon} + \tfrac{1}{2}\bar{\varepsilon}^2 = \tfrac{1}{2}(F/2l)^2 + (F/2l)\cos u \qquad (49)$$

Equation (49) can be solved to give the allowable values of, F/2l , for a particular average strain, $\bar{\varepsilon}$, over the length, 2l .Results of such calculations are given in Figure(19). This Table can be used to indicate the value of anchor length, l , required to assure survival for a combination of transverse and longitudinal components of fault motion. The approximate relation for l/F is given by :

$$l/F > \cos u / 2\bar{\varepsilon} \qquad (50)$$

The above relation indicates that the "free" length, l , on each side of the fault, relative to the fault displacement, F , for $u = 0$ should be 16.7 for $\bar{\varepsilon}$=0.03, 25 for $\bar{\varepsilon}$=0.02 and only 12.5 for $\bar{\varepsilon}$=0.04 The latter value implies a maximum strain over an appreciable length, and therefore a value of 20 is recommended for 48 in. diameter pipe. This requires a "free" length of 200 feet on each side of the fault, for a 10 feet fault motion.

Angle, Deg.	$\bar{\varepsilon}$ = 0.04	$\bar{\varepsilon}$ = 0.03	$\bar{\varepsilon}$ = 0.02
0	0.0400	0.0300	0.0200
15	0.0413	0.0310	0.0207
30	0.0459	0.0345	0.0230
45	0.0555	0.0418	0.0280
60	0.0758	0.0579	0.0389
75	0.1266	0.0988	0.0689
90	0.2857	0.2468	0.2010

Figure 19. Fault displacement divided by total free slip lenght

2.5. STABILITY OF BELOWGROUND PIPELINES

2.5.1 Buckling Under External Pressure

A ring-stiffened cylinder under external pressure may fail either by yielding or by buckling at stresses considerably below the yield point. The type of failure depends upon the properties of the material of the pipe, the thickness of the wall and the spacing of the stiffeners. If the cylinder is relatively thin or if the stiffeners are widely spaced, buckling will probably occur. If the cylinder is relatively thick or if the stiffeners are closely spaced failure will probably occur by shell yielding.

Windenburg and Trilling (8) have suggested a thinness factor, K , indicative of the type of failure to be expected. For values of the thinness factor less than 0.8 , shell yielding is likely to occur. For values of K larger than 0.8 shell buckling is probable to occur. Furthermore, for values of the factor larger than 1.2 elastic instability is likely to occur, while for values in the range of 0.8 to 1.2 plastic-shell instability should be waited. The thinness factor is given by the formula :

$$K = (D/t)^{\frac{3}{4}}(1/D)^{\frac{1}{2}}(f_y/E)^{\frac{1}{2}} \qquad (51)$$

Where

l : the lenght of the shell between the stiffeners

D : the mean diameter of the shell

t : the thickness of the shell

f_y : the yield point of the shell material

E : the modulus of Elasticity of the pipe material

A ring-stiffened shell may fail by buckling, in one or more of the three possible instability modes, shown in Figure (20), namely :

1. Axisymmetric collapse of the shell between adjacent ring stiffeners.
2. Asymmetric or lobar buckling of the shell between adjacent ring stiffeners.
3. General instability or overall collapse of the entire shell and stiffeners.

Each of the above three modes is characterized by a specific collapse shape. The first one, by accordion-shaped pleats around the circumference of the shell. The second mode, by the forming of two or more lobes around the circumference. The third mode is characterized by large dished-in portions of the stiffened shell, where the shell and stiffeners deflect together.

The ring stiffeners should not be placed too great a distance apart, otherwise the shell region between stiffeners may behave under pressure as though no stiffeners were present. The shortest length of cylinder for which the strengthening effect of the stiffeners can be ignored is called the "critical length".

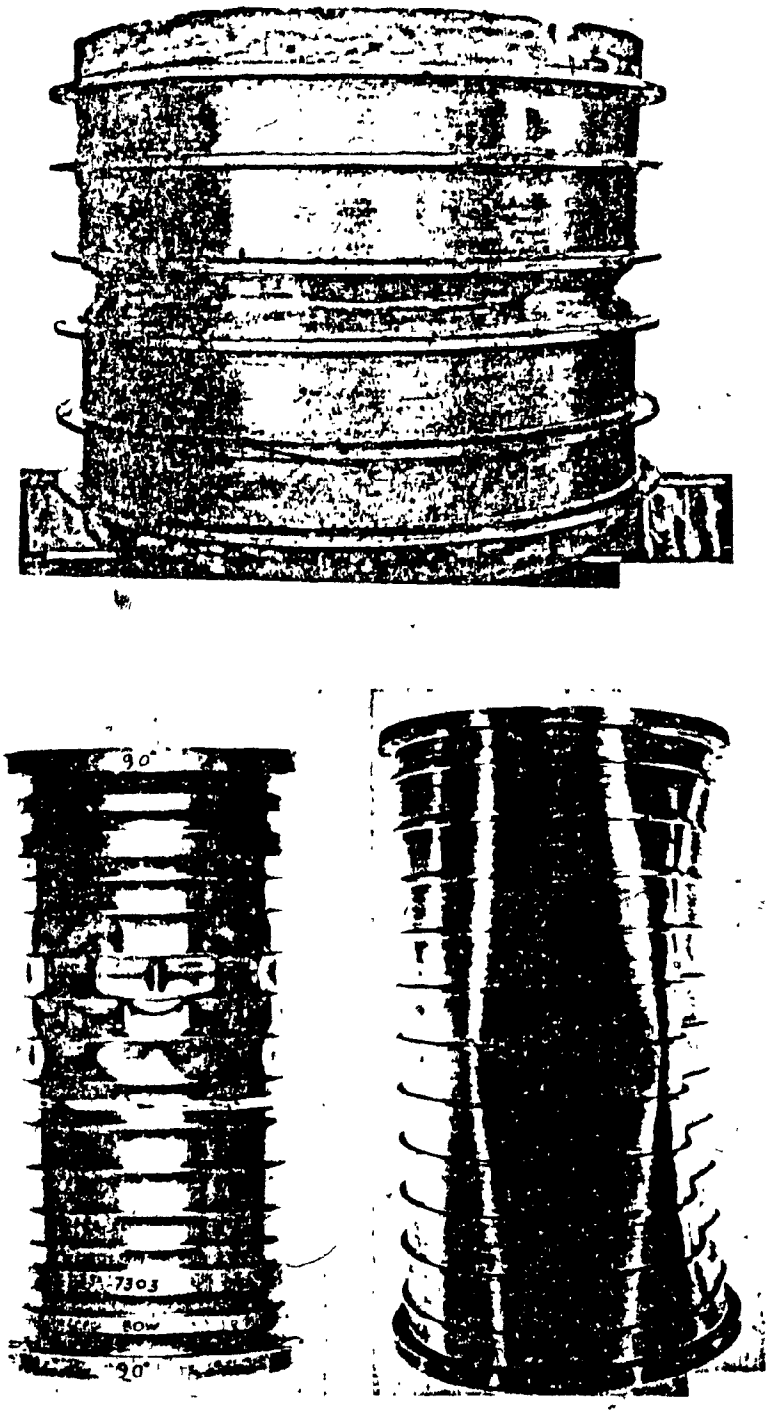

Figure 20. Buckling modes for ring-stiffened pipes. (a) Local buckling (axisymmetric); (b) Local buckling (asymmetric); (c) General instability (overall collapse).

2.5.2. Elastic Buckling of Stiffened Shells Between Ring Stiffeners

2.5.2.1 Axisymmetric or Asymmetric.

Elastic buckling between stiffeners usually occurs in a large number of circumferential lobes and the Donnell's equation can be used. The hoop compression N_y is usually assumed to be equal to $p_e R$. this would be strictly correct only if the shell deformed freely until the onset of buckling, and supports were then introduced. Actually, the rings exert some radial support from the beginning of loading, so that $N_y < p_e R$. N_y can be found from the Equation :

$$N_y = f\, p_e R \tag{52}$$

Where

$$f = 1 - (1 - \tfrac{1}{2}v)\frac{A_f}{A_f + tl}\, g_{(\theta)} \tag{53}$$

Where

A_f : the cross-sectional area of the stiffener.

t : the thickness of shell

l : the unsupported lenght of shell

v : Poisson's ratio

R : the mean radius of the shell

$g_{(\theta)}$: a function of θ which can be obtained from Fig. (21)

$$\theta : (1 - v^2)^{\frac{1}{4}} \frac{l}{(Rt)^{\frac{1}{2}}} \tag{54}$$

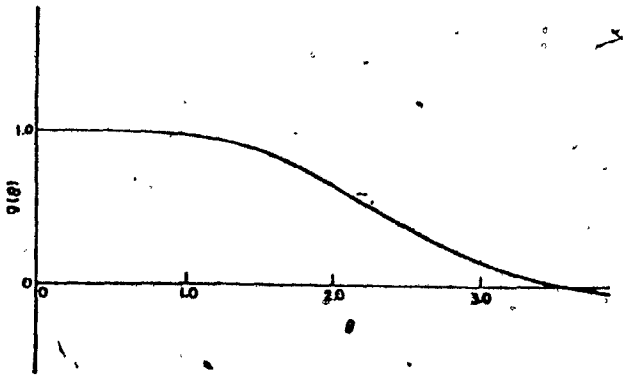

Figure 21. Hoop stress coefficient as a function of θ

Combination of the foregoing results leads to the following equation for the theoretical buckling pressure :

$$p_c = \frac{E}{n^2 + \lambda^2/2}\left(\frac{t}{R}\right)\left(\frac{1}{12(1-\nu^2)}\left(\frac{t}{R}\right)^2(n^2+\lambda^2)^2 + \frac{\lambda^4}{(n^2+\lambda^2)^2}\right). \quad (54)$$

Where

n : the number of circumferential lobes

E : elastic Modulus

If the prebuckling end restraint is neglected, $N_y = p_e R$ and the previous Equation becomes :

$$p_c = \frac{E}{n^2 + \lambda^2/2}\left(\frac{t}{R}\right)\left(\frac{1}{12(1-\nu^2)}\left(\frac{t}{R}\right)^2(n^2+\lambda^2)^2 + \frac{\lambda^4}{(n^2+\lambda^2)^2}\right) \quad (55)$$

Equation (55) was originally proposed by Von Mises. The correct value of n to be used in Equation (54) or Equation (55) is that which makes p_c a minimum. This can be found by trial and error substitu-

tion of various values of n, or by differentiation. Differentiation of Equation (54) leads to the equation :

$$p_c = 0.855 \left(\frac{t}{R}\right)^2 \frac{(1 - \nu^2)^{-\frac{1}{2}} E}{f\theta - 1.28 (f - \frac{1}{2})} \qquad (56)$$

By checking Equation (56) with results obtained by numerical minimization of Equation (54), it was found that slightly better accuracy can be obtained from the slightly different Equation (57).

$$p_c = 0.855 \left(\frac{t}{R}\right)^2 \frac{(1 - \nu^2)^{-\frac{1}{2}} E}{f\theta - 1.22 (f - \frac{1}{2})} \qquad (57)$$

If the prebuckling end restraint is neglected, the equation to be used is:

$$p_c = 0.855 \left(\frac{t}{R}\right)^2 \frac{(1 - \nu^2)^{-\frac{1}{2}} E}{\theta - 0.61} \qquad (58)$$

From experimentation it was obtained that the effect of prebuckling end restraint is important only if $\theta < 3$ and is negligible for longer cylinders. Agreement between theory and experiment is fair for cylinders with $\theta > 10$ but unsatisfactory for shorter cylinders.

The foregoing solutions are not valid for very long cylinders because of the use of the Donnell's equation which is applicable only for $n \gg 1$. For given values of R and t, n decreases as l increases. For a very long cylinder, $n = 2$. Also in this case f is approximately equal to one. The theoretical buckling pressure in such case is given by the following formula:.

$$p_c = \frac{E}{3 + \lambda^2/2}\left(\frac{t}{R}\right)\left(\frac{1}{12(1 - \nu^2)}\left(\frac{t}{R}\right)^2(3 + \lambda^2)^2 + \frac{\lambda^4}{(4 + \lambda^2)^2}\right) \qquad (59)$$

For very large values of θ this result approaches the classical formula for buckling of an infinitely long cylinder, which was presented by Bresse and Bryant :

$$p_c = \frac{E}{4(1 - \nu^2)}\left(\frac{t}{R}\right)^3 \qquad (60)$$

For $\nu = 0.3$

$$p_c = 0.275\ E\ \left(\frac{t}{R}\right)^3 \qquad (61)$$

Limits can now be assigned to the various approximations.

Equation (57) may be used if $\theta < 1.6(1 - \nu^2)^{\frac{1}{2}}(R/t)$

The simplest Equation (58), which does not require the calculation of $f_\cdot$, may be used in the range $3 < \theta < 1.6(1 - \nu^2)^{\frac{1}{2}}\left(\frac{R}{t}\right)$

Equation (60), may be used if $\theta > 4(1 - \nu^2)^{\frac{1}{2}}(R/t)$

For intermediate values of θ, Equation (59) should be used .

For a short cylinder a different solution is necessary. For $n=0$ the buckling pressure is given by :

$$p_c = 2(1 - \nu^2)^{-\frac{1}{2}}E(t/R)^2\left(\frac{\pi^2}{12\theta^2} \pm \frac{\theta^2}{\pi^2}\right) \qquad (62)$$

This is the classical equation for buckling of a short cylinder under axial compression. This type of buckling is possible as a result of the prebuckling end restraint which increases the resistance of the shell

to unsymmetrical buckling.

2.5.2.2 Elastic General Instability

To size the stiffeners, it is necessary to consider general instability. In this mode of failure, the shell and the rings buckle together. A simple solution can be obtained theoretically and is given by:

$$P_c = (n^2 + 1)\frac{E I_f}{R^3 L_f} + E\left(\frac{t}{R}\right)\frac{\lambda_b^4}{(f(n^2-1)\lambda_b^2/2)(n^2+\lambda_b^2)^2} \qquad (63)$$

Where

L_f : center to center stiffener spacing

$\lambda = \pi a/L_b$

I_f : effective moment of inertia about the centroid of a section comprising one stiffener plus an effective width of shell L_e on each side of the stiffener.

The fist term on the right side of Equation (63) represents the rigidity of the rings whereas the second term represents the membrane rigidity. Before Equation (63) can be used, f and I_f must be evaluated. Since the shell and stiffeners buckle together, it may be assumed that the hoop stress is uniform throughout the shell and stiffeners. In such case , f is given by the formula :

$$f = \frac{1}{1 + A_f/tl} \qquad (64)$$

Where

A_f : the cross-sectional area of stiffener

l : the unsupported length of the cylinder

To evaluate the moment of inertia of the stiffener, I, it is necessary to know what length of the shell, L_e, to consider that is working together with the stiffener. A satisfactory approximation is :

$$L_e = (3(1 - \nu^2))^{-\frac{1}{4}} (Rt)^{\frac{1}{2}} \qquad \text{If } l > 2(3(1 - \nu^2))^{-\frac{1}{4}}(Rt)^{-\frac{1}{2}}$$

$$L_e = l/2 \qquad \text{If } l \leq 2(3(1 - \nu^2))^{-\frac{1}{4}}(Rt)^{-\frac{1}{2}} \qquad (65)$$

The value of n which gives the minimum p_c in Equation (63) must be found by trial and error, but this requires only a few trials since n is usually a small integer.

2.5.3. Inelastic Buckling

Two basic inelastic modes of ring-stiffened cylinders can occur, namely, axisymmetric and asymmetric or lobar buckling. When the geometry and material properties are such that the computed buckling stress is in the inelastic range, the critical buckling pressure becomes a function of the secan and tangent moduli. In this case the critical pressure is given by :

$$p_c = 0.855(1 - \nu^2)^{-\frac{1}{2}} Et/\theta (E_s/E_t)^{\frac{1}{2}} (t/R)^2 \frac{\theta + 0.80(E_t/E_s)^{\frac{1}{2}}(E_s/E_t - 1)}{f\theta - 1.22(E_t/E_s)^{\frac{1}{2}}(f - \frac{1}{2})} \qquad (66)$$

Where

E_s : the secant modulus

E_t : the tangent modulus

v : the generalized Poisson's ratio, given by :

$$v = \tfrac{1}{2} - (\tfrac{1}{2} - v_e)\frac{E_s}{E}$$

v_e : the Poisson's ratio in the elastic range.

The determination of the plastic moduli E_s and E_t presents a problem because of the biaxial stress state of the pipe. A method presented by Johnston(3) can be used to overcome this difficulty. According to this method the circumferential and axial stresses are determined in the plastic range then the Hencky-von Mises distortion energy criterion is applied and the effective stress is obtained. The plastic moduli can then determined from a representative stress strain curve of the pipe material for the effective Mises stress. The applied stresses can be obtained from the following Equations :

1. Shell stresses

The circumferential shell stress can be approximated by :

$$f_c = -\frac{p_e R}{t}\left(1 - \frac{0.85\, A_f}{A_f + L_e\, t}\, F_{(\theta)}\right) \qquad (67)$$

Where

A_f : the cross-sectional area of a stiffener

L_e : the effective width

p_e : the applied hydrostatic pressure

$F_{(\theta)}$: a function which can be approximated by the following

expression :

$$F_{(\theta)} = 1 \qquad \text{for} \quad \theta \leq 1$$
$$F_{(\theta)} = 1.33 - 0.33\,\theta \qquad \text{for} \quad 1 < \theta < 4 \qquad (68)$$
$$F_{(\theta)} = 0 \qquad \text{for} \quad \theta \geq 4$$

The longitudinal shell stress may be determined from the formula :

$$f_1 = - \frac{p_e R_o}{2\,t} \qquad (69)$$

The radial shell stress is given by :

$$f_r = -p_e \qquad (70)$$

Where, p_e is the applied pressure , t is the pipe wall thickness and R_o the outside diameter of the cylinder.

2. Stiffener Stresses

The unit radial load Q acting on the stiffener ring, per unit of circumferential lenght, can be determined from the following formula applicable in steel pipes with $v = 0.3$

$$Q = -0.85\, p_e \left(b + \frac{L_e A_f}{A_f + bt + L_e t} \right) \qquad (71)$$

Where, b is the width of the stiffener web in contact with the shell and the rest of the terms are as previous. The circumferential stress is then given by the following equation .

$$f_c = \frac{Q R_o}{A_f + bt} \tag{72}$$

Equation (72) can be approximated by :

$$f_c = -0.85 \frac{p_e R_o L_e}{A_f + L_e t} \tag{73}$$

The longitudinal and radial stresses can be determined by Equation (69) and Equation (70) respectively. All terms encounter in these Equations are as previous.

Assuming that the Hencky-von Mises criterion apply in the plastic range, the stress intensity f_i for a biaxial stress state is defined as :

$$f_i = (f_c^2 + f_l^2 - f_c f_l)^{\frac{1}{2}} \tag{74}$$

Having obtain the stress intensity, from a representative stress-strain curve of the material of the pipe, the values of the desired moduli, E_s and E_t , which correspond to this stress are determined.

Equation (66) requires a trial and error solution, but the procedure is straight forward. A stress intensity f_i is assumed, E_s and E_t are found from the stress strain curve, p can then be found from Equation (66) after which the circumferential and axial stresses f_c and f_l are evaluated and finally, f_i is found. The calculated value of the stress intensity f_i is compared with the assumed value, the pro-

cess is repeated until the assumed and calculated values of f_i match to the desired degree of accuracy. The corresponding value of p is the buckling pressure.

2.5.4. Effect Of Imperfections

All of the above theoretical approaches assume a perfectly cylindrical shape, but in the reality it is impossible to built such a cylinder. These imperfections should be taken in account, since they can reduce significantly the load carrying capacity of a cylinder.

Most analyses of the effect of initial imperfections are based on the assumption that the initial out-of-roundness is similar in form to one of the assumed buckling modes. Timoshenko (1) has developed a formula to determine the elastic critical pressure for a cylinder of infinite length having some eccentricity. The hydrostatic pressure at which yielding occurs is given by :

$$p_y^2 - \left(2f_y t / D + \left(1 + \frac{1.5De_o}{t}\right)p_c \right) p_y + \frac{2f_y t}{D} p_c = 0 \qquad (75)$$

Where

e_o : out of roundness, given by : $(D_{max} - D_{min})/D = 4e/D$

e : radial eccentricity

p_c : critical pressure

This Equation is applicable for buckling modes with $n = 2$. The American Petroleum Institute recommends a value of $e = 0.01$ for fabricated tubes.

A method to determine the initial eccentricity is the one proposed by Holt (30) in which e is the maximum radial deviation from a perfect circle when measured over an arc length, A , corresponding to one half lobe length. The arc length can be determined by :

$$A = \frac{\pi D}{2n} \tag{76}$$

Where n is the lobar number. Windenburg (31) developed an empirical formula for the maximum value of the ratio of the initial eccentricity over the thickness of the pipe wall, which is permitted in the arc length of one half lobe length. It was assumed that an imperfect shell with the maximum permisible out-of-roundness would have a collapse pressure not less than 80 % of that of a corresponding perfect shell. The allowable value for e/t is given by :

$$e/t = \frac{1.8}{n\ (\ 100\ t/D\ )} + 0.015\ n \tag{77}$$

The values of n were obtained from Von-Mises's Equation (55).

The initial out-of-roundness of the stiffening rings is equally important. Analytical studies of the effects of stiffener out-of-roundness were considered by Hom. He developed the following approximate formula for the maximum bending stress f_b introduced in the stiffener by stiffener eccentricity. This formula is applicable in the elastic range only and is given by :

$$f_b = \pm \frac{16}{\pi} \left(\frac{E\, e_f\, e}{D^2} (n^2 - 1) \left(\frac{p_e}{p_c - p_e} \right) \right) \qquad (78)$$

Where

n : the number of circumferential buckling lobes

e_f : the distance from midthickness of the shell to the extreme fiber of the stiffener, positive or negative for internal or external stiffeners, respectively.

p_e : the applied pressure

p_c : the critical pressure for perfect ring-stiffened cylinder

e : the radial eccentricity from a true circle

2.6 DESIGN PROCEDURE

A design procedure which may allow for the direct inclusion of the effects of plasticity and imperfections on stiffened shells is presented below. The results of this method are conservative, because it is assumed that the circumferential bending strengh of the shell provides the resistance to ovalization of the shell, and in this way the appreciable contribution of the stiffening rings and the membrane action are neglected. The method involves the following steps.

1. The imposed compressive circumferential stress due to external pressure is determined.
2. A suitable factor of safety against yielding is assumed.
3. The deflection of the pipe are checked against the allowable.
4. The longitudinal stresses included those due to earthquake are evaluated.
5. The Hencky Von-Mises distortion energy criterion is applied and the stress intensity is defined and checked against the allowable one.
6. If the cylinder is not overstressed, the critical buckling stress for a perfectly round cylinder is determined, assuming that the cylinder fails by elastic general instability.
7. The critical buckling stress of the stiffened cylinder is checked against local buckling.
8. The critical circumferential stress for an imperfect cylinder is determined.

9. The ratio of the circumferential stress determined in step eight to the applied circumferential stress is evaluated.

10. The ratio established in the previous step is compared to the assumed factor of safety.

11. The above procedure is repeated until an acceptable safety factor is achieved.

CHAPTER III

ABOVEGROUND PIPELINES

3.1. Loads

Loading conditions vary in different projects, but the following general loads and forces should be considered in the design of aboveground pipelines. The necessary combination of these loads can be obtained from the appropriate design codes for each specific case.

(a)	Dead Load	(DL)
(b)	Live Load	(LL)
(c)	Wind Pressure	(W)
(d)	Earthquake Force	(E)
(e)	Icing	(I)
(f)	Temperature Effects	(T)

3.1.1 Dead Load

Dead load computation is based on the unit weight of the materials. Dead load is permanent and it consists of the weight of the pipe and reinforcing rings. In thin-walled pipelines the dead load is insignificant and usually it is not considered in the design, but if a detailed analysis is required, the following formula can be used to obtain the dead load per linear foot.

$$DL = \pi D\, t\, \gamma_s + \frac{N}{l}\, b\pi\, D_f\, t_f\, \gamma_s \qquad (79)$$

Where

D : mean diameter of the pipe, in.

t : thickness of the pipe wall, in.

γ_s : unit weight of the material of the pipe, pound per $in.^3$

l : span between two adjacent supports

N : number of stiffening rings at the span

D_f : mean diameter of the stiffening ring, in.

t_f : thickness of the stiffening ring, in.

3.1.2 Live Load

Live load is defined as the weight superimposed on the structure by the use of it. It is a transient type of loading and it is not climatologically dependent. Live load consists of the weight of the fluid or the maximum gas pressure, p_i, in gas pipelines. Internal pressure may also occur where a pipeline is hydraulically surcharged. The weight of the liquid is given by :

(a) Precisely full pipe.

$$LL = \frac{\pi D_i}{4} \gamma_L \qquad (80)$$

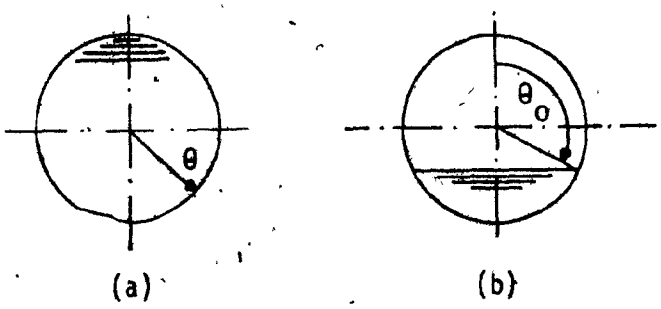

Figure 22. (a) Precisely full pipe; (b) Partially full pipe.

(b) Partially full pipe

$$LL = \left(\frac{\pi \theta_o}{90} - \sin 2\theta_o\right)\frac{D_i^2}{8}\gamma_L \qquad (81)$$

Where

D_i : Inside diameter of the pipe, in.

γ_L : density of the fluid , pounds per in^3

θ_o : central angle, defining the level of the fluid in the pipe in rads.

3.1.3 Wind Pressure

Wind pressures are defined as those forces originating from the natural movement of the air. These pressures may produce forces on a pipeline of significant magnitude. The design wind pressure, W (lb/ft) is specified by the National Building Code of Canada, subsection 4.1.8. The total force per linear foot on the pipe is given by :

$$W = q\, C_e\, C_g\, C_p\, D_o \qquad (82)$$

Where

q : velocity pressure

C_e : exposure factor

C_g : gust factor

C_p : shape factor, (0.7 for circle)

3.1.4 Earthquake Forces

Earthquake forces should be considered according to seismic zones and following the provisions of the National Building Code of Canada, subsection 4.1.9.

3.1.5 Icing

Pipelines must be checked assuming an ice covering in accordance with the National Building Code of Canada subsection 4.1.7.

3.1.6 Temperature Effects

Temperature loads are originated from dimensional changes induced by variations in ambient temperature. If extreme temperature variations are likely to occur, the magnitude of movements and stresses that may be induced by expansion and contraction, must be estimated in order to determine the required controlling joints or the necessary reinforcement.

3.2. STRESS ANALYSIS OF ABOVEGROUND PIPELINES

To evaluate the introduced forces and the corresponding stresses in the pipe wall, due to the external loading, a small element of the pipe shell is considered and the equations of equilibrium are determined. In the case of pipelines some simplifications can be done from the very beginning regarding the introduced internal forces and moments. This is due to the cylindrical shape of the shell, and to the fact that in the most loading cases, pipelines are under the action of forces distributed symmetrically with respect to the axis of the pipeline. The twisting moments are usually equal to zero and they will not be considered here. Also the shearing force, Q_x , and the bending moment, M_x , are very small quantities and will be herein considered equal to zero. For loading cases such as, dead load or live load in pipes precisely full, it has been proved by Skytte (26), that the shearing force, Q_u , becomes zero. With these simplifications, lets assume that the generator of the cylinder is horizontal and paralel to the x-axis. An infinitesimal element is cut from the shell by two adjacent generators and two cross sections perpendicular to the x-axis. Its position is defined by the coordinates x and u . The external load acting on the element is represented by the external force components X , Y , and Z . The element is held in equilibrium by the internal forces and moment shown in Figure (23). Namely, the normal forces N_x and N_u , the shearing forces $N_{xu} = N_{ux}$, and the bending moment M_u . Considering the equations of equilibrium obtained by projecting the forces on the x , y , and z axes and by taking the moments about

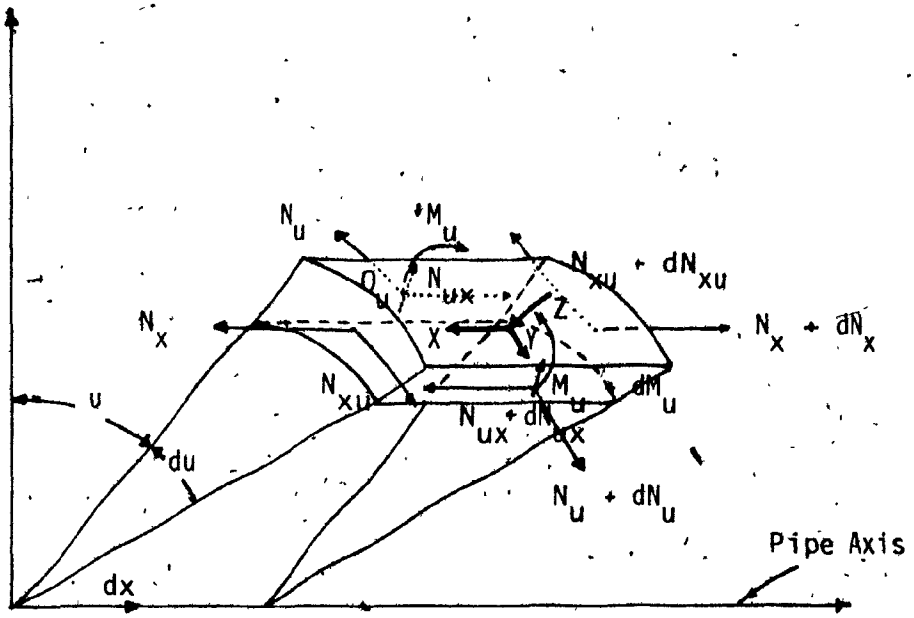

Figure 23. Free body diagram of the pipe wall.

the x-axis , we will have.

Projection on the z-axis :

$$ZR\,du\,dx + (N_u + dN_u)\,dx\,\tfrac{1}{2}du + N_u\,dx\,\tfrac{1}{2}du + dQ_u\,dx = 0 . \qquad (85)$$

eliminating the differential of higher order $dN_u\,dx\,\frac{1}{2}du$, we obtain :

$$N_u = -R\left(Z + \frac{dQ_u}{R\,du}\right) \qquad (84)$$

Projection on the y-axis, gives :

$$YR\,du\,dx + (N_u + dN_u)dx - N_u dx - 2Q_u \tfrac{1}{2} du\,dx + (N_{xu} + dN_{xu})R\,du - N_{xu}R\,du = 0$$

or (85)

$$dN_{xu} = -\frac{dN_u\,dx}{R\,d_u} + \frac{Q_u}{R}dx - Y\,dx \qquad (86)$$

by intergrating :

$$N_{xu} = -\int \frac{dN_u}{R\,d_u}dx + \int \frac{Q_u}{R}dx - \int Y\,dx + f_1(u) \qquad (87)$$

Projection on the x-axis provides :

$$N_x = -\int \frac{dN_{xu}}{R\,d_u}dx - \int X\,dx + f_2(u) \qquad (88)$$

By taking the moments around the x-axis we obtain :

$$dM_u + R\,du\,Q_u = 0 \qquad (89)$$

or

$$M_u = -R\int Q_u\,du + f_3(u) \qquad (90)$$

The functions $f_1(u)$ and $f_2(u)$ depend on the origin of the coordinate system and the conditions at the supports. With the origin of the coordinate system at the center of the span, $f_1(u) = 0$.

3.2.1 Dead Load

In calculating the applying forces on the pipe wall, it has been proved by Larson (26) that under dead load and under liquid load in a pipe precisellly full, the shearing forces act tangentially and consequently there are no circumferential bending stresses in the pipe shell under such loading. Therefore, the Equations of equilibrium became :

$$N_u = - R Z \tag{91}$$

$$N_{xu} = - \int \frac{dN_u}{Rdu} dx - \int Y dx + f_1(u) \tag{92}$$

$$N_x = - \int \frac{dN_{xu}}{Rdu} dx - \int X dx + f_2(u) \tag{93}$$

Considering a pipe supported by two stiff disks, which prevent large deformations of the rim and designating the dead weight of the pipe per unit area by g the load components are :

$$Z = g \cos u$$

$$Y = g \sin u$$

$$X = 0$$

From Equation (91) we obtain :

$$N_u = - R\, g\, \cos u \qquad (94)$$

From Equation (92), for $\frac{dN_u}{du} = Rg\sin u$ we have :

$$N_{xu} = - 2g\, x \sin u \qquad (95)$$

Equation (93), with $\frac{dN_{xu}}{du} = -2gx\cos u$, becomes :

$$N_x = \frac{g\, x^2}{R} \cos u + f_2(u) \qquad (96)$$

The function $f_2(u)$ can be calculated assuming that any inside pressure on the end disks is resisted by corresponding forces in the opposite direction, the stress component N_x must be equal to zero at the supports, or :

$$f_2(u) = - \frac{g\, l^2}{4\, R} \cos u \qquad (97)$$

and Equation (96) becomes :

$$N_x = \frac{g}{R} \left(x^2 - \frac{l^2}{4} \right) \cos u \qquad (98)$$

Equation (98) shows that the longitudinal stress component has a straight line variation with maximum for $x = 0$, equal to :

$$\max N_x = g l^2 / 4R$$

The corresponding unit stresses are obtained by dividing the stress components by the shell thickness, t , hence :

$$\max f_1 = g\, l^2 / 4\, R\, t \qquad (99)$$

From Equation (94) becomes that the ring stress is independent of the span, and that it has a maximum of :

$$\max N_u = \mp\, g\, R\, / \, t \qquad (100)$$

This stress is compressive at the top and tensile at the bottom of the pipe cross-section.

The shearing stresses reach their maximum at the end disks, and they are distributed over the cross-section as in a hollow cylindrical beam subjected to bending.

It should be noted that the stresses obtained with the preceding analysis, are identical with those obtained by the ordinary theory of flexure. But the addition of the ring stress, N_u , changes the principal stress system.

For multispan ring stiffened pipelines a stress analysis has been presented by Troitsky (5), which was based on Russian references. This analysis is based on the Vlassov's Theory for cylindrical shells. In Vlassov's theory it is assumed that the longitudinal bending moment and twisting moments are too small and can be neglected. It is also assumed that the shear deformations can be neglected and that in the cross-section the shell is able to take without deformation the axial forces, both normal and tangential and the transverse bending moment. According to this analysis a parameter, B , is introduced which

depends on the support conditions and it has the following values:

If the pipe may freely rotate at the support, then $B = 1$

If the pipe cannot rotate freely, then $B = -2/3$ at the supports and $B = 1/3$ at the midspan.

The results of this analysis will be presented in the following for each loading case separately. For the case of dead load the internal forces are given by :

$$N_x = B\, K_{Nx}\, \frac{g\, l^2}{R} \cos \frac{\pi\, x}{l} \qquad (101)$$

$$N_u = K_{Nu}\, g\, R \cos \frac{\pi\, x}{l} \qquad (102)$$

$$N_{xu} = K_{Nxu}\, g\, l \sin \frac{\pi\, x}{l} \qquad (103)$$

Where

$K_{Nx} = -0.258 \cos \theta$

$K_{Nu} = 1.273 \cos \theta$

$K_{Nxu} = - \sin \theta$

l : the span between supports.

R : the radius of the pipe.

θ : central angle with the vertical, defining a specific point on the pipe shell.

3.2.2. Live Load

3.2.2.1. Pipe Precisely Full

When the pipe is precisely full with a liquid of unit weight per unit area of, q ,the load components are equal to zero except in the z-direction, where :

$$Z = -qR(1 - \cos u)$$

Substituting this value into Equations (91), (92), and (93) we obtain :

From Equation (91) :

$$N_u = q R^2 (1 - \cos u) \qquad (104)$$

From Equation (92) :

$$N_{xu} = q R x \sin u \qquad (105)$$

From Equation (93) :

$$N_x = - \frac{q}{8} (l^2 - 4x^2) \cos u \qquad (106)$$

The ring stress is tensile, it increases from zero at the top of the cross section of the pipe, to a maximum value at the bottom equal to :

$$N_u = 2qR^2 \qquad (107)$$

The shearing stresses and the longitudinal stress are identical to those obtained by the ordinary beam theory. For a multispan pipeline reinforced with stiffening rings the stress components can be found with more accuracy from the formulas of a partially full pipe for $\theta_o = 0$

3.2.2.2. Pipe Partially Full

The previously mentioned analysis based on Vlassov's Theory provides the following formulas for the introduced forces in a partially full pipe. The angle θ_0 defines the level of the liquid in the pipe. The forces at any point defined by the central angle θ are :

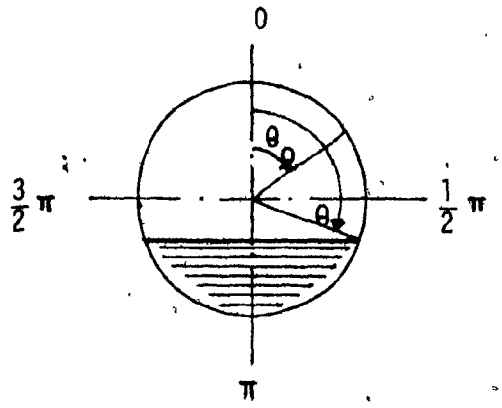

Figure 25. Pipe partially full. Definitions.

$$M_u = K_{Mu}\, \gamma_L\, R^3 \cos\frac{\pi x}{l}$$

$$N_x = B\, K_{Nx}\, \gamma_L\, l^2 \cos\frac{\pi x}{l} \qquad (108)$$

$$N_u = K_{Nu}\, \frac{\gamma_L\, t\, l^2}{R} \cos\frac{\pi x}{l} \qquad (109)$$

$$N_{xu} = K_{Nxu}\, \frac{\gamma_L\, R^4}{t\, l} \sin\frac{\pi x}{l} \qquad (110)$$

The coefficients K_{Nx} , K_{Nu}, K_{Nxu}, are given from the expressions:

$$K_{Nx} = -0.041\, A_1 \cos\theta + \frac{128\,\varepsilon^2\, A_2 \cos 2\theta}{1168.92\,\varepsilon^2 + 256\, c^3}$$

$$K_{Nu} = -0.811\,\varepsilon\left(-\frac{(\pi - \theta_o)\cos\theta_o + \sin\theta_o}{2} + \frac{A_1 \cos\theta}{2} - \frac{A_2 \cos 2\theta}{3} + A_3 \cos 3\theta + A_4 \cos 4\theta\right)$$

$$K_{Nxu} = -0.159\, A_1 \sin\theta/\varepsilon$$

$$K_{Mu} = 0.81\, c^3\left(-\frac{21.33\, A_2 \cos 2\theta}{1168.92\,\varepsilon^2 + 256\, c^3} + \frac{729\, A_3 \cos 3\theta}{1168.92\,\varepsilon^2 + 6561\, c^3} + \frac{4096\, A_4 \cos 4\theta}{1168.92\,\varepsilon^2 + 65536\, c^3} + \frac{.15625\, A_5 \cos 5\theta}{1168.92\,\varepsilon^2 + 390625\, c^3}\right)$$

Where

$\varepsilon = R^3/tl^3$ defines the geometric characteristics of the pipe

A_1, A_2, A_3, A_4, A_5 : constants which can be obtained from Fig(26)

I : the moment of inertia of the stiffening ring including the wall of the pipe in width equal to the spacing of the rings

c : defines the equivalent thickness of the shell in the transverse direction, so that :

$$I = l\,(ct)^3/\,12$$

l : the span between two adjacent supports of the pipe.

It should be pointed out that experimentaly it was proved that the case of a partially full pipe is more critical than the one of a full pipe and therefore the preceding solution althought lenghtly

is of great importance, wherever the provided accuracy is needed.

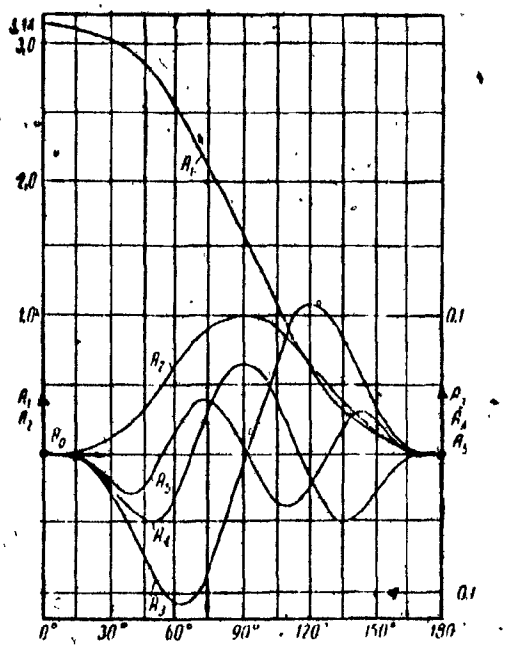

Figure 26. Diagram for the constants A_1, A_2, A_3, A_4, A_5.

3.2.3 Wind Load

In the case of a wind force w and assuming the wind pressure distribution shown in Figure (27), the forces acting on each point of the pipe wall can be obtained, according to the previous method, from the folowing Equations .

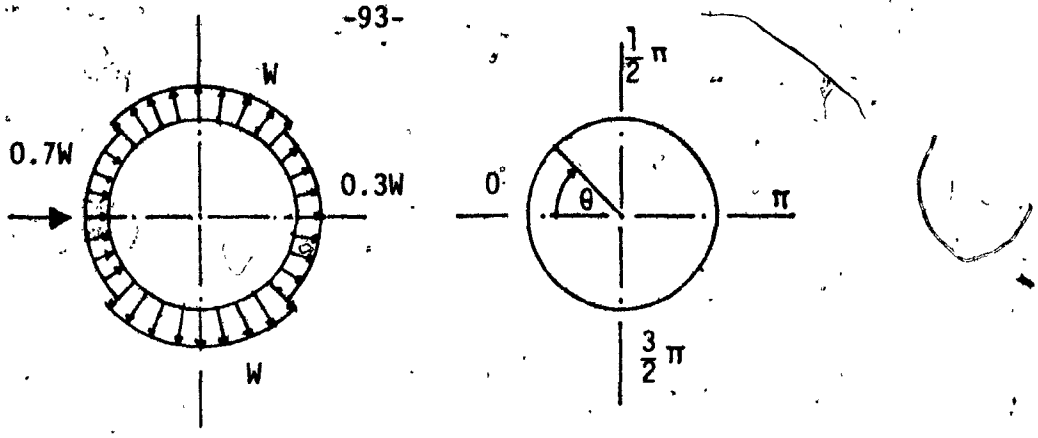

Figure 27. Wind pressure on a pipeline.

Longitudinal force N_x :

$$N_x = B\, K_{Nx} \frac{W R^2}{t} \cos \frac{\pi x}{l} \qquad (112)$$

Circumferential force N_u :

$$N_u = K_{Nu} \frac{W t l^2}{R^2} \cos \frac{\pi x}{l} \qquad (113)$$

Shearing force N_{xu} :

$$N_{xu} = K_{Nxu} \frac{W R^3}{t l} \sin \frac{\pi x}{l} \qquad (114)$$

Circumferential moment M_u :

$$M_u = K_{mu}\ W R^2 \cos \frac{\pi x}{l} \qquad (115)$$

Where

$$K_{Nx} = -0.0581 \frac{1}{\varepsilon} \cos\theta \lambda \frac{460.8\, \varepsilon \cos 2\theta}{1168.92\, \varepsilon^2 + 256\, c^3}$$

$$K_{Nu} = 0.101\,(-5.026 + 5.66\cos\theta + 9.6\cos 2\theta + 1.886\cos 3\theta - 1.131\cos 5\theta)\,\varepsilon$$

$$K_{Nxu} = -0.225 \frac{1}{\varepsilon} \sin\theta$$

$$K_{Mu} = 0.1\, c^3 \left(\frac{614.4\cos 2\theta}{1168.92\, \varepsilon^2 + 256\, c^3} + \frac{1374.6\cos 3\theta}{1168.92\, \varepsilon^2 + 6561\, c^3} + \frac{17677.5\cos 5\theta}{1168.92\, \varepsilon^2 + 390625\, c^3} \right)$$

3.2.4 Icing

If the specific weight of the ice is γ_i, and the maximum ice cover is denoted by h as in Figure (28), the forces acting on the wall of the pipe can be obtained from the following formulas.

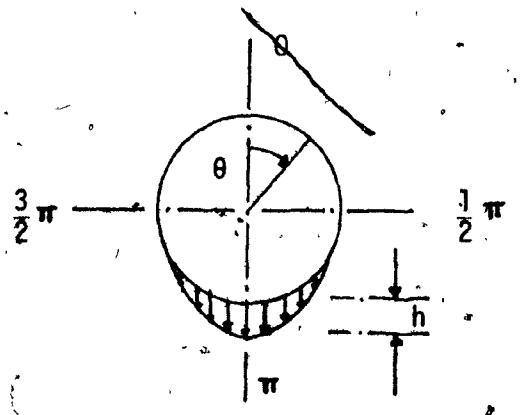

Figure 28. Loading due to icing on a pipeline.

Longitudinal force N_x :

$$N_x = B\, K_{Nx} \frac{\gamma_i\, h\, R^3}{t} \cos\frac{\pi x}{l} \tag{116}$$

Circumferential force N_u :

$$N_u = K_{Nu} \frac{\gamma_i\, h\, t\, l^2}{R^2} \cos\frac{\pi x}{l} \tag{117}$$

Shearing force N_{xu} :

$$N_{xu} = K_{Nxu} \frac{\gamma_i\, h\, R^3}{t\, l} \sin\frac{\pi x}{l} \tag{118}$$

Circumferential moment M_u :

$$M_u = K_{Mu}\, \gamma_i\, h\, R^2 \cos\frac{\pi x}{l} \tag{119}$$

Where

$$K_{Nx} = -0.129 \frac{1}{\varepsilon} \cos\theta + \frac{226.2\, \varepsilon \cos 2\theta}{1168.92\, \varepsilon^2 + 256\, c^3}$$

$$K_{Nu} = 0.318\, \varepsilon\, (-1 + 2\cos\theta + \cos 2\theta)$$

$$K_{Nxu} = -0.5 \frac{1}{\varepsilon} \sin\theta$$

$$K_{M_u} = -30.56\, c^3 \frac{\cos 2\theta}{1168.92\, \varepsilon^2 + 256\, c^3}$$

3.2.5 Internal Pressure

Timoshenko and Krieger (2) presented a method to evaluate the stresses acting on a pipeline subjected to internal pressure and reinforced with rings at equispacing. This internal pressure p_i may be due to a fluid or gas enclosed within the pipe. According to this method the applied stresses are given by the following equations :

Circumferential pipe wall stress midway between the rings :

$$f_c = \frac{p_i D}{2 t} \left(1 + 2\left(f_r \frac{2 t}{p_i D} - 1\right) X_4 \right) \qquad (120)$$

The ring stress

$$f_r = \frac{p_i D}{2 t} \Big/ \left(1 + \frac{b A_f}{t} \left(X_1 - \frac{X_2^2}{2 X_3}\right)\right) \qquad (121)$$

The longitudinal bending stress in the pipe under the ring is :

$$f_l = \frac{p_i D}{2 t} \left(\frac{3}{1 - \nu^2} \right)^{\frac{1}{2}} \left(1 - f_r \frac{2 t}{p_i D}\right) X_2 \qquad (122)$$

The parameters X_1, X_2, X_3, X_4, are given by the expressions :

$$X_1 = \frac{\cosh a + \cos a}{\sinh a + \sin a}$$

$$X_2 = \frac{\sinh a - \sin a}{\sinh a + \sin a}$$

$$X_3 = \frac{\cosh a - \cos a}{\sinh a + \sin a}$$

$$X_4 = \frac{\sin (a/2) \cosh (a/2) + \cos(a/2) \sinh (a/2)}{\sinh a + \sin a}$$

Where

b : parameter given by :

$b^4 = 12(1 - v^2) / D^2 t^2$

a : parameter given by :

$a = b\, l$

v : Poisson's ratio

D : mean diameter of the pipe

t : pipe wall thickness

L : spacing of the rings

A_f : cross-sectional area of stiffening ring

Stephenson (7) observed that the above Equations are very much simplified when the spacing of the rings increases. He recommends that for spacing of the rings greater than $2(t\,D)^{\frac{1}{2}}$, the following equations may be used :

$$f_r = \frac{\frac{1}{2}\, p_i\, D}{t + 0.91\, A_f / (t\, D)^{\frac{1}{2}}} \qquad (123)$$

$$f_c = p_i\, D / 2\, t \qquad (124)$$

$$f_l = \frac{0.827\, Pi\, D\, A_f}{t^2\, (t\, D)^{\frac{1}{2}} + 0.91\, A_f\, t} \qquad (125)$$

3.2.6. Temperature Effects

If a cylindrical shell with free edges undergoes a uniform temperature change, no thermal stresses will be introduced. But if the edges are supported or champed, free expansion of the shell is prevented and bending stresses are introduced. For a pipe of lenght, l, having a uniform thermal strain, the linear deformation Δl due to a change in temperature of ΔT is

Longitudinal

$$\Delta l = a\,(\Delta T)\,l \qquad (126)$$

Radial

$$\Delta D = a\,(\Delta T)\,D \qquad (127)$$

Where

a : the coefficient of thermal expansion

D : the diameter of the pipe

l : the considered lenght of the pipe

In the above deformations, the deformations produced by the liquid flow should be added. If p_i is the uniform pressure of the pipe or the average of the pressures at the edges of the lenght l, the free longitudinal increase in lenght owing to this pressure is given by the

formula :

$$\Delta l = \frac{p_i D l}{4 E t} (1 - 2v) \qquad (128)$$

If these strains are prevented by restrains an additional longitudinal stress is introduced, which produce a longitudinal strain equal to :

$$f_l / E \qquad (129)$$

with a deformation over the lenght l equal to :

$$f_l l / E \qquad (130)$$

The sum of all the longitudinal deformations should be equal to zero due to the end restrains, or :

$$\frac{p_i D l}{4 E t}(1 - 2v) + a (\Delta T) l + \frac{f_l l}{E} = 0 \qquad (131)$$

or

$$f_l = - \frac{p_i D}{4 t}(1 - 2v) - a E (\Delta T) \qquad (132)$$

In the above stress, the stress produced because of the internal pressure should be added. Depending on the value of the temperature change the above stress can be either negative or positive, and it will occur at the point with the minimum or maximum liquid pressure respectively. In cases in which the pipe is empty the pressure term should be eliminated.

3.3 Stiffener Stresses

The determination of the nature and forces acting on ring stiffeners in thin-walled cylinders subjected to bending, is as essential as the rigidity of the stiffener in the selection of the appropriate ring properties. The stresses in the stiffeners are caused by the beam bending moments in the structure and also by the direct effect of the transverse loading on the shell. The stresses on the stiffener due to an applied pure bending moment on the cylinder are caused by two types of action, the flattening and the bulging of the cylinder. Flattening of the cylinder is an increase in the horizontal diameter and a decrease in the vertical diameter, caused by the curvature of the cylinder under bending. Due to this curvature the longitudinal stresses at the top and the bottom halves of the cylinder have resultant forces acting towards the center of the cylinder, and in this way cause the flattening of the cylinder. Bulging of the cylinder is the increase of the radii of the cylinder on the compression side and their decrease on the tensile side due to Poisson's ratio. The types of stress due to these two types of action is shown in Figure (29). Both of these two actions have the same sign of the stress at point 9 and opposite signs at point 1. At point 5 flattening will be the main contributing factor to the stress, whereas bulging will be the main contributing factor to the stress at points 3 and 7.

In Figure (30) the stresses on the outside face of the stiffener due to applied pure applied bending moment, is shown. A comparison between Figures (29) and (30) points out that the stresses due to flattening vary at a faster rate than the stresses due to bulging.

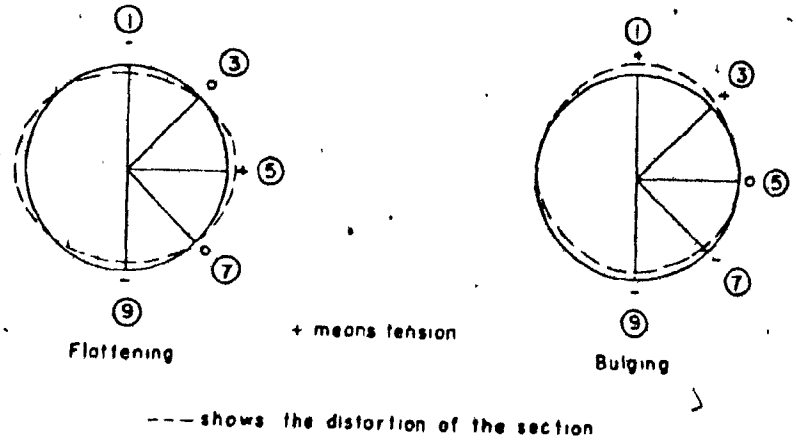

Figure 29. Types of stress on the outside face of the stiffeners.

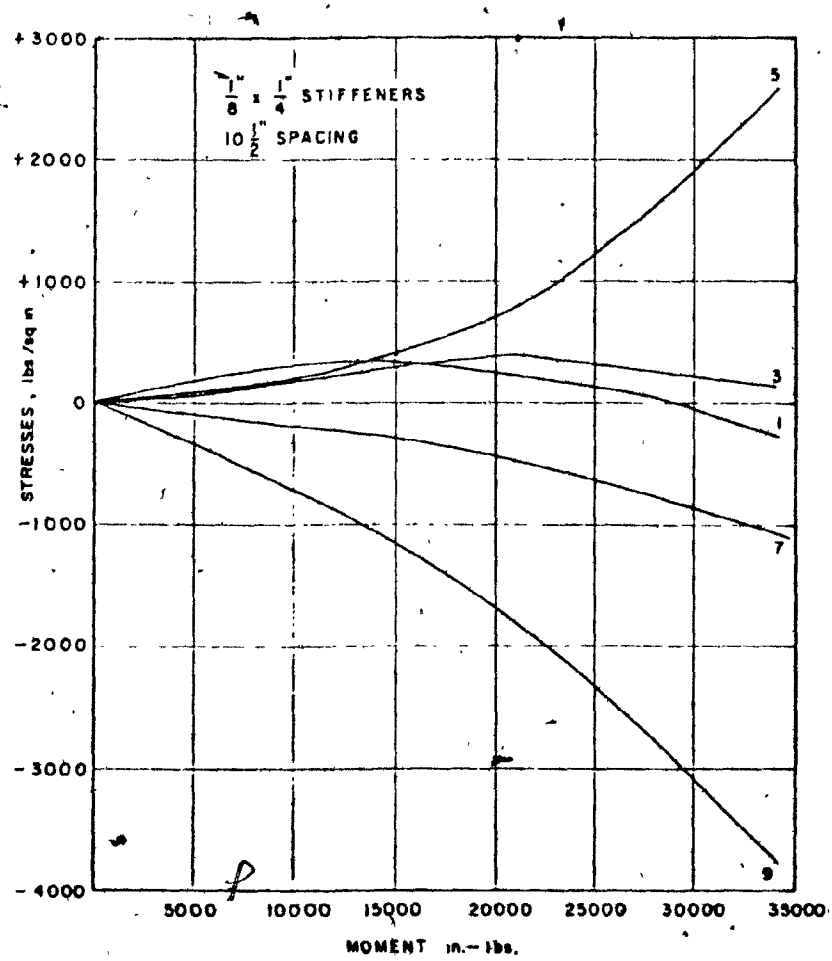

Figure 30. Stresses on the outside face of the stiffeners.

3.3.1 Flattening Of The Cylinder

If we consider a cylinder under the action of a bending moment M , the resultant forces of both the compressive and tensile longitudinal stresses at the top and the bottom of the cylinder, are vertical and acting toward the inside of the cylinder, as is shown in Figure (31). The longitudinal stress at a point on the cylinder is equal to :

$$f_1 = - \frac{E R}{\rho} \cos\theta \qquad (133)$$

Where

ρ : the radius of the curvature of the cylinder

θ : angle measured from the vertical, defining the point on the pipe shell in which the stresses are considered.

E : the modulus of Elasticity

R : the mean radius of the cylinder

The resultant force acting toward the inside of the cylinder, per unit of surface, will be given by :

$$F = \frac{E R t}{\rho^2} \cos\theta \qquad (134)$$

Where t is the wall thickness of the pipe. Therefore the cylinder is like being subjecting to the action of vertical pressure with magnitude equal to F . The distribution of the forces on any stiffener as

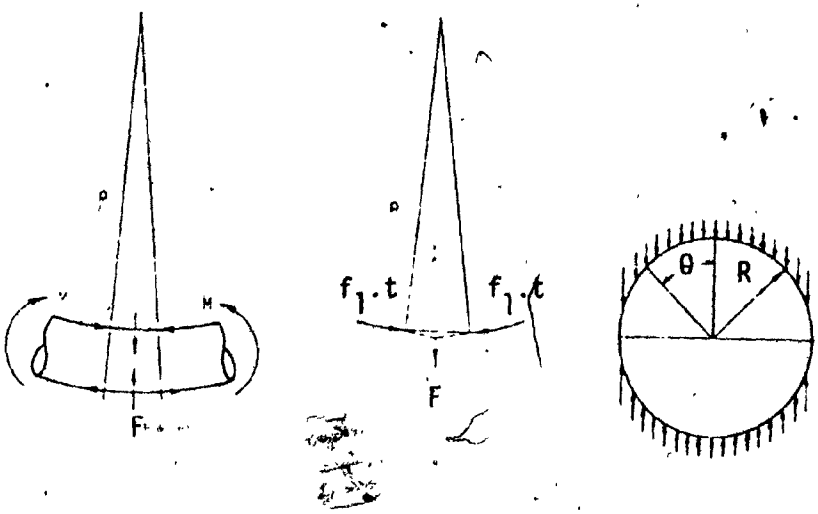

Figure 31. Flattening of cylinder.

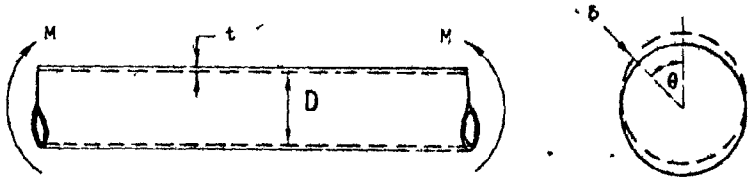

Figure 32. Bulging of cylinder.

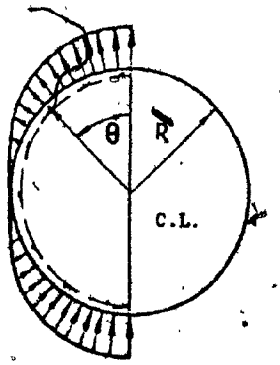

Figure 33. Distribution of forces due to bulging of cylinder.

a result of flattening of the cylinder is assumed to vary according to the variation of the pressure on the cylinder, and they are taken as :

$$K \frac{E R t}{\rho^2} \cos\theta \qquad (135)$$

The term K, is a function of the ring spacing and also of other parameters and has the unit of length. The corresponding bending moment M_r, and normal force, N_r, in the stiffener are given by :

$$M_r = - K \frac{E R^3 t}{4 \rho^2} \cos(2\theta) \qquad (136)$$

and

$$N_r = - K \frac{E R^2 t}{\rho^2} \sin^2\theta \qquad (137)$$

For closely spaced rings, it can be assumed that the flattening forces are resisted by the stiffener only. In such cases the term K, may be taken as equal to the spacing of the rings L_f. From Equation (136) we have :

$$M_r = - L_f \frac{E R^3 t}{4 \rho^2} \cos(2\theta) \qquad (138)$$

For $\rho = EI/M$ Equation (138) becomes

$$M_r = - \frac{1}{4 \rho^2 R^3 t} \frac{M^2}{E} L_f \cos(2\theta) \qquad (139)$$

Where

I : the moment of inertia of the cylinder

M : the applied on the cylinder bending moment

If more accuracy is needed, a better approximation can be achieved by considering the term K equal to :

$$K = \frac{1}{\frac{C_2}{2R}\left(\Psi_{(\lambda_s)}\right) + C_1\frac{t^3}{I_f}} \qquad (140)$$

Where

I_f : the moment of inertia of the stiffener

C_1 , C_2 , constants.

Experimentaly it was found that the average values of the constants C_1 and C_2 to be used are $C_1 = 1.0$, and $C_2 = 1.1$. Values of the function $\Psi(x)$ are given in Fig. (34) . The moment of inertia of the stiffener I_f can be calculated assuming that the effective width of the shell acting together with the stiffener is equal to twenty four times the thickness of the shell.

x	ψ(x)	x	ψ(x)	x	ψ(x)
0 10	20.002	1.40	1.459	3.40	0.921
0.20	10.001	1.50	1 370	3.60	0.929
0.30	6.667	1.60	1.295	3.80	0.938
0.40	5.001	1.70	1 230	4.00	0.949
0.50	4.002	1.80	1 174	4.50	0.973
0.60	3.336	1.90	1.127	5 00	0.991
0.70	2.861	2.00	1.086	5 50	1.000
0.80	2.506	2.20	1.021	6.00	1.003
0.90	2.230	2.40	0.976	6.50	1.004
1.00	2.011	2.60	0.945	7.00	1.003
1 10	1.833	2.80	0.927	7.50	1.001
1.20	1.686	3.00	0.919	8.00	1.001
1.30	1.563	3 20	0.917		

Figure 34. Values of function $\Psi(x)$

3.3.2 Bulging Of the Cylinder

The longitudinal stresses in the cylinder due to pure bending moment will be equal to :

$$f_1 = - \frac{M}{\pi R^2 t} \cos\theta \qquad (141)$$

The distortion of the cross-section d is given by the formula :

$$d = \frac{v M}{\pi R t E} \cos\theta \qquad (142)$$

Where

M : the applied pure bending moment

v : Poisson's ratio

R : mean radius of the cylinder

t : wall thickness of the cylinder

E : modulus of Elasticity

θ : angle measured as in Figure (32)

The radial forces are assumed to be proportional to the distortion and equal to $Z \cos\theta$, and the tangential forces equal to $Z \sin\theta$. This type of loading is shown in Figure (33). If the shear and normal deformations are ignored, no bending moments are produced in the ring. The normal force acting in the ring is in this case given by :

$$N_r = Z R \cos\theta \qquad (143)$$

Where, Z is a parameter for which the value was given by Rumman (18) in the following form

$$Z = \frac{\nu M / \pi R^3}{\frac{b_1}{2}\left(\Psi_{(b_1 L_f)}\right) - \frac{t}{A_f}} \qquad (144)$$

Where

M : the applied bending moment

A_f : the cross-sectional area of the stiffener

$b_1 = 0.35/(R\ t)^{\frac{1}{2}}$

ν : Poisson's ratio

Substituting the value of Z , given by Equation (144) into Equation (143) the normal forces can be obtained in the following form

$$N_r = \frac{(\nu M / \pi R^2)\cos\theta}{\frac{b_1}{2}\left(\Psi_{(b_1 L_f)}\right) + t/A_f} \qquad (145)$$

The stresses in the stiffener, will vary linearly with the applied bending moment on the cylinder. The variations of the stresses around the ring stiffener due to bulging should be proportional to $\cos\theta$.

The forces produced by flattening and bulging, as well as, those produced by any local loading, are considered to be the major forces acting on ring stiffeners in long thin-walled cylinders subjected to bending. Experimentaly it was confirmed a good agreement between the calculated and measured stresses in a ring stiffener.

3.4 Strenght Requirements

The maximum stress at a point of a cross-section, selected so that the moments and forces due to one loading case or a combination of loading cases are maximum, must be smaller than the allowable stresses provided by the appropriate design code. In the preceeding the resulting forces for each loading case were evaluated. Due to these stress components the following stresses are introduced in the pipe wall of thickness t.

Longitudinal stress due to the longitudinal normal force N_x.

$$f_1 = N_x / t \tag{146}$$

Circumferential stress due to the tangential normal force N_u

$$f_c = N_u / t \tag{147}$$

Circumferential stress due to the tangential bending moment M_u

$$f_c = 6 M_u / t^2 \tag{148}$$

Shearing stress produced by the shearing force N_{xu}

$$s = N_{xu} / t \tag{149}$$

Some of the loading cases, such as the own weight of the pipe, are permanent, while others, like the icing, are temporary. It is up to the designer to decide which loading cases combination is necessary to consider for each specific project. After the loading combination has been established, the corresponding stresses for each loading must be added, and the total stresses are obtained. From these stresses the principal stresses and the maximum shearing stress can be evaluated according to the formulas, for $f_1 > f_c$.

$$f_{1,2} = \frac{f_1 + f_c}{2} \pm \left(\left(\frac{f_1 - f_c}{2} \right)^2 - s^2 \right)^{\frac{1}{2}} \qquad (150)$$

and

$$s_{max} = \frac{f_1 - f_c}{2} \qquad (151)$$

These stresses should be smaller than the allowable stresses. The complex stress system of the principal stresses should be checked by the appropriate yield criterio. The Von Mises-Hencky criterio is defined as :

$$(f_1 - f_2)^2 + (f_2 - f_3)^2 + (f_3 - f_1)^2 = 2 f_y^2 \qquad (152)$$

For two principal stresses the Equation (152) is reduced to :

$$f_1^2 - f_2^2 - f_1 f_2 = f_y^2 \qquad (153)$$

Where f_y is the yield point of the material in uniaxial testing.

3.5 Stability Requirements

From the stress analysis of aboveground pipelines it was concluded that the pipe shell is subjected to compression, in the direction of its longitudinal axis. The stability of the compressed zone of the pipe in the longitudinal direction should be checked against buckling according to the formula :

$$f_1 \leq \frac{f_{cr}}{F.S} \qquad (154)$$

Where, f_{cr} is the critical buckling stress of the pipe and FS is the appropriate factor of safety. The evaluation of the critical buckling stress is discussed in the following.

Pipes subject to axial compression, bending or internal pressure may fail in buckling. Depending on the dimensions of the pipe, either local or overall buckling failures may occur. The ring stiffeners provide additional strenght to pipes of relatively large diameter to wall thickness ratios. Buckling failure on ring stiffened pipelines may occur in several different modes, similar to those of unstiffened pipes. The prediction of the appropriate buckling mode and the calculation of the corresponding buckling stress in a pipeline reinforced with rings, is a very complicated problem. Because stiffeners, in addition to the nature of the applied load and the supporting conditions, introduce even more parameters such as stiffeners size, spacing and position with respect to the pipe wall. Furthermore, the buckling strenght of thin-walled pipes is very sensitive to geometric imperfe-

ctions. All these parameters and the multiple mechanisms of failure possible, make the stability analysis of stiffened pipes very complicated, so that a universal set of design formulas substantiated by tests is virtually impossible to be provided. Therefore the designer is forced to choose the applicable formulas from a very scattered literature wherever references are available, and to make approximations and assumptions based on the behaviour of unstiffened pipes in many cases. In the following a review of the buckling of circular pipes under various loading conditions, as well as several forms of structural interactions which can influense the buckling strenght of pipelines are discussed.

3.5.1 Axial Compression

The buckling behaviour of axially compressed circular cylinders is usually classified into four ranges, depending on the ratio of length to radius and the buckling pattern. The four ranges are "very long", "long", "transition" and "short" cylinders, as shown in Figure (35). Very long, are cylinders in which the ratio of lenght to radius is very large and primary instability or Euler buckling occurs. In short cylinders buckling occurs with sinusoidal buckles, whereas long cylinders buckle in a characteristic diamond pattern. Transition range covers those cylinders with lenghts between short and long cylinders. The buckling in transition range seems to be an interaction between the plate sine-wave bucle pattern and the diamond pattern.

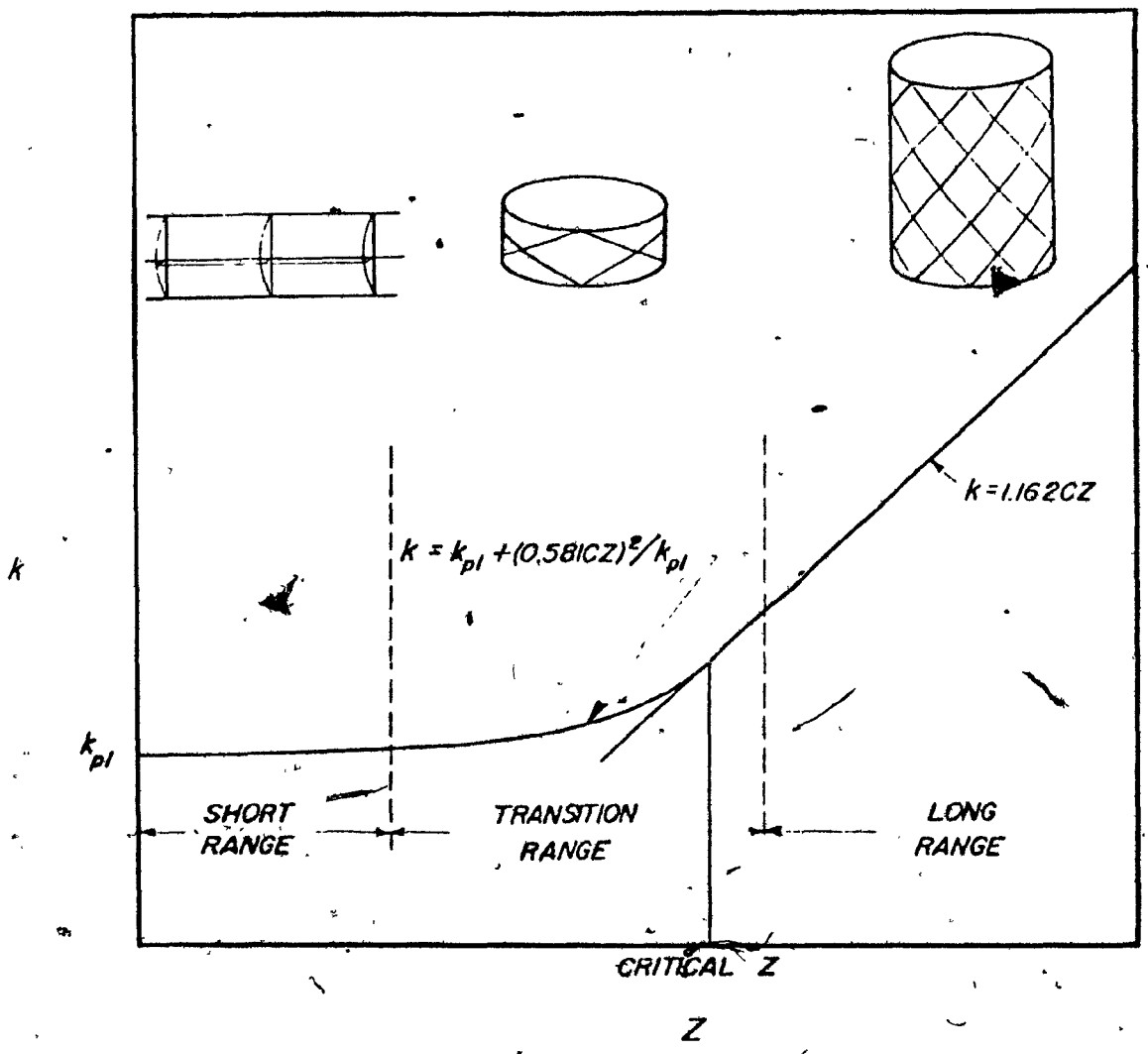

Figure 35. Diagram of k as a function of the parameter Z. Typical buckle patterns for cylinders in each range of Z.

3.5.1.1 Short Cylinders

The elastic buckling strenght of short cylinders depends on both the lenght to radius ratio, and the diameter to thickness ratio while the buckling strenght of long cylinders depends on only the diameter to thickness ratio. The dimensionless parameter Z was introduced by Bardorf (31) and it is used to define the four ranges. This parameter is given by :

$$Z = 2(l/D)^2(D/t)(1 - v^2)^{\frac{1}{2}} \qquad (155)$$

Where

D : the diameter of the cylinder

l : the lenght of the cylinder

t : the thickness of the cylinder's wall

v : Poisson's ratio

For values of parameter Z less than 2.85 the surface of the cylinder buckles like an infinitely wide plate. The theoretical buckling stress in this case is given by :

$$f_{cr} = k_c \frac{\pi^2 E}{12(1 - v^2)(l/t)^2} \qquad (156)$$

for v = 0.3

$$f_{cr} = 0.904\ E\ (t/l)^2 \qquad (157)$$

Where the coefficient k_c has the following values depending on the supporting conditions

Simply supported edges

$$k_c = \frac{1 + 12\ Z^2}{\pi^4}$$

Fully champed edges

$$k_c = \frac{4 + 3\ Z^2}{\pi^4}$$

As the ratio of lenght to radius decreases, k_c approaches the buckling stress coefficient of a flat plate, and the corresponding critical buckling stress becomes identical to that of a plate strip of unit width.

3.5.1.2. Very long cylinders

Purely column type buckling of tubular members may occur with no local buckling as long as the ratio of diameter to wall thickness does not exceed $3300/f_y$, where f_y is the yield strenght of the material in kips per square inch. The critical buckling stress of a very long cylinder is a function of a parameter called the slenderness ratio of the cylinder. The nondimensional slenderness ratio λ for a cylinder with mean diameter D and lenght l may be expressed as :

$$\lambda = \frac{Kl}{R} \frac{1}{\pi} (f_y/E)^{\frac{1}{2}} \qquad (158)$$

Where Kl is the effective lenght of circular cylinder.

In terms of λ the critical axial buckling stress is given by the CRC Column Strenght Curve, in the following form.

for $\lambda \leq \sqrt{2}$

$$f_{cr} = (1 - 0.25\lambda^2) f_y \quad \text{(a)}$$

for $\lambda > \sqrt{2}$ (159)

$$f_{cr} = f_y / \lambda^2 \quad \text{(b)}$$

With the above Equation it is recommended to use a factor of safety given by :

for $\lambda \leq \sqrt{2}$

$$F.S = 1.67 + 0.265\lambda - 0.044\lambda^3$$

for $\lambda > \sqrt{2}$

$$F.S = 1.92$$

Woldord and Rebholz (31) proposed a more conservative column curve, given by :

for $\lambda \leq \sqrt{3}$

$$f_{cr} = (1 - 2\lambda/3\sqrt{3}) f_y \quad \text{(a)}$$

for $\lambda > \sqrt{3}$ (160)

$$f_{cr} = f_y / \lambda^2 \quad \text{(b)}$$

With a factor of safety of :

for $\lambda \leq \sqrt{3}$

$$F.S = 1.67 + 0.145\lambda$$

for $\lambda > \sqrt{3}$

$$F.S = 1.92$$

The corresponding curves to these two proposals, as well as experimental data are shown in Figure (36).

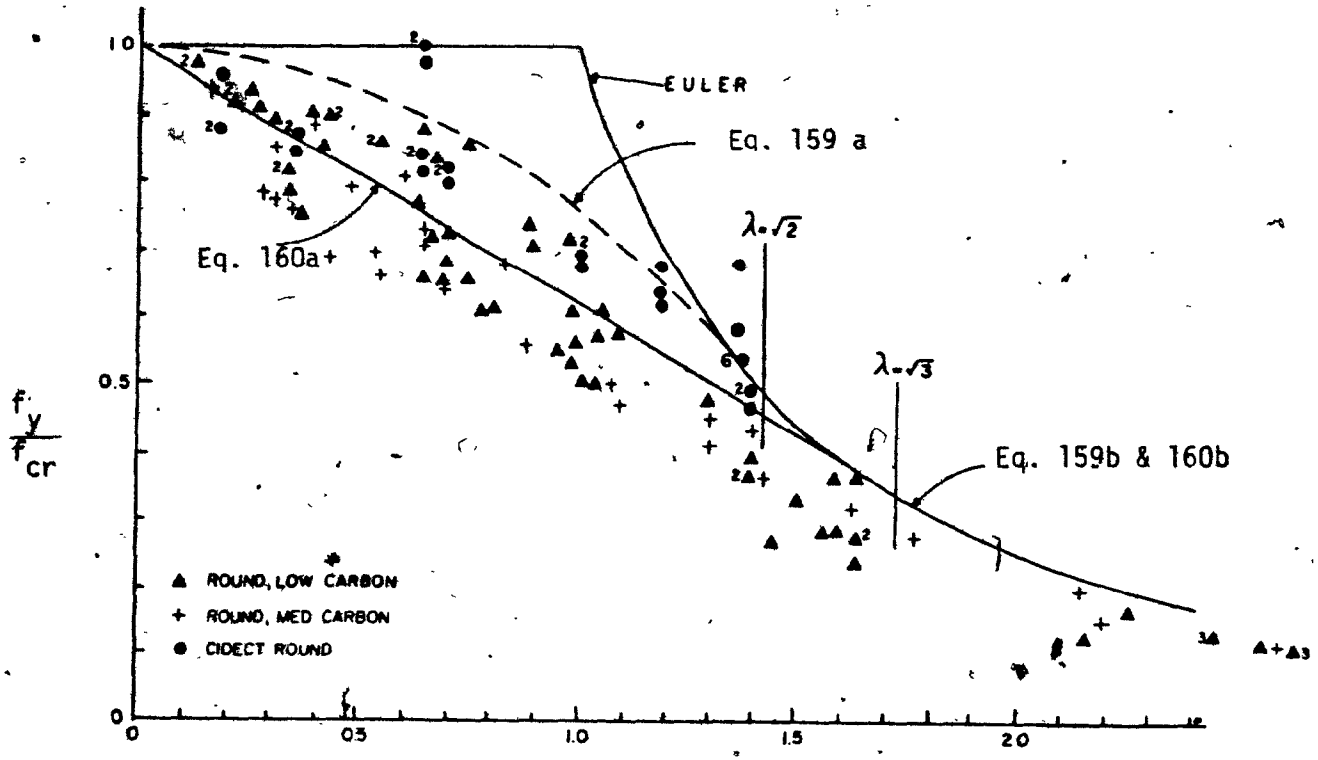

$$\lambda = \frac{2\sqrt{2}\,K1}{D}\,(f_y/E\,\pi^2)$$

Figure 36. Test data for axially loaded cylinders.

3.5.1.3. Transition Range

In the transition range where the number of integer forms changes as in Figure (35), the buckling stress depends upon the lenght to thickness ratio, the radius to thickness ratio, and also upon the parameter, Z_L ,which is given by the expression :

$$Z_L = \frac{l^2(1 - \nu^2)^{\frac{1}{2}}}{Rt} \qquad (161)$$

Since Z_L is a function of length, and since linear theory predicts changes of wave number with lenght, there is a basis for expecting cusps in the empirical data as the wave number changes by integral values in the transition region. Since there appears to be little possibility of establishing a completely theoretical variation, a semi-empirical approach has been presented by Gerard and Becker (27). In this approach two basic data were selected; the flat plate buckling coefficient at $Z_L = 0$ and the straight line drawn through the logarithmic plot of k_c as a function of Z_L for large values of Z_L . Transition curves were then fitted to these data using linear theory as a guide. The simplest transition, which matches the linear theory in the special case of $C = 0.6$ is obtained from Bardorf (30), with the k_c expressed as :

$$k_c = k_{pl} + (12\, Z_L^2 / \pi^4\, k_{pl}) \qquad (162)$$

This expression was then modified to account for the effect of R/t

$$k_c = k_{pl} + ((0.581\ C\ Z_L)^2 / k_{pl}) \qquad (163)$$

The complete buckling coefficient curve is shown in Figure (35). For each value of R/t complete curves can be drawn, utilizing the values of C obtained from Figure (37). C is a coefficient which depends primarily on the degree of initial imperfections associated with the cylinder and on the R/t ratio. For cylinders of intermediate lenght in which the coefficient Z is greater than 2.85, the theoretical buckling stress is :

$$f_{cr} = C\ E\ t/R \qquad (164)$$

The magnification ratio k_{exp}/k_{emp}, of the test value of k_c to the theoretical value from the curve for the corresponding value of Z_L were plotted in Figure (38). The highest peak occurs at $Z_L = 35$ approximately, with a second peak at about $Z_L = 650$. These peaks presumably due to the interaction between the sine-curve deflection shape of the short plate and the diamond buckle pattern of the intermediate lenght cylinder. Because the cylinder is long enough to permit diamond buckles to form and yet is short enough for the end boundary conditions to influence the details of this pattern.

3.5.1.4. Long Cylinder Range

Axial compression, which generates compressive membrane stresses in a cylinder after buckling, has been shown by Gerard and Becker

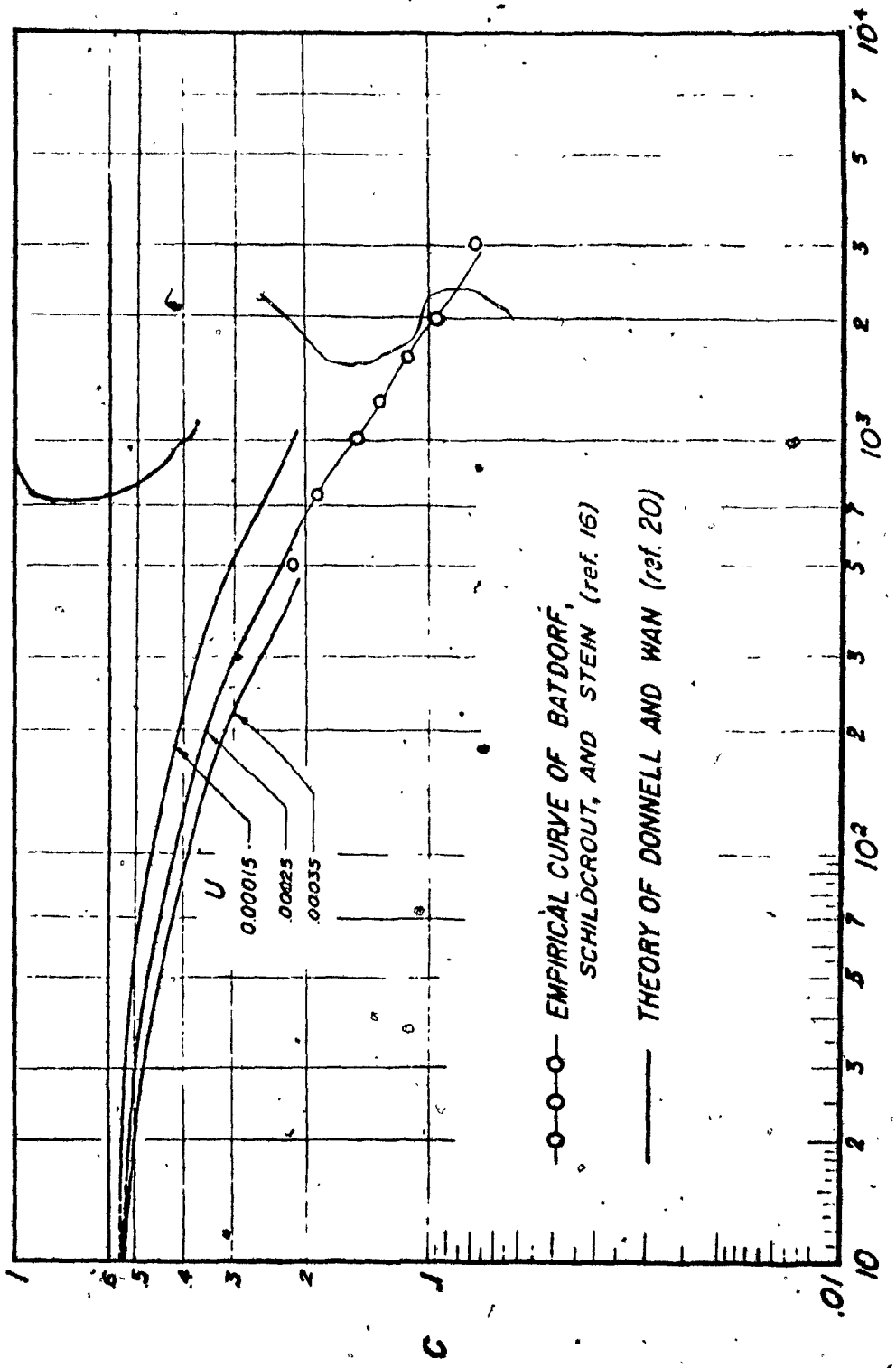

Figure 37. Buckling coefficient C as a function of the ratio R/t .

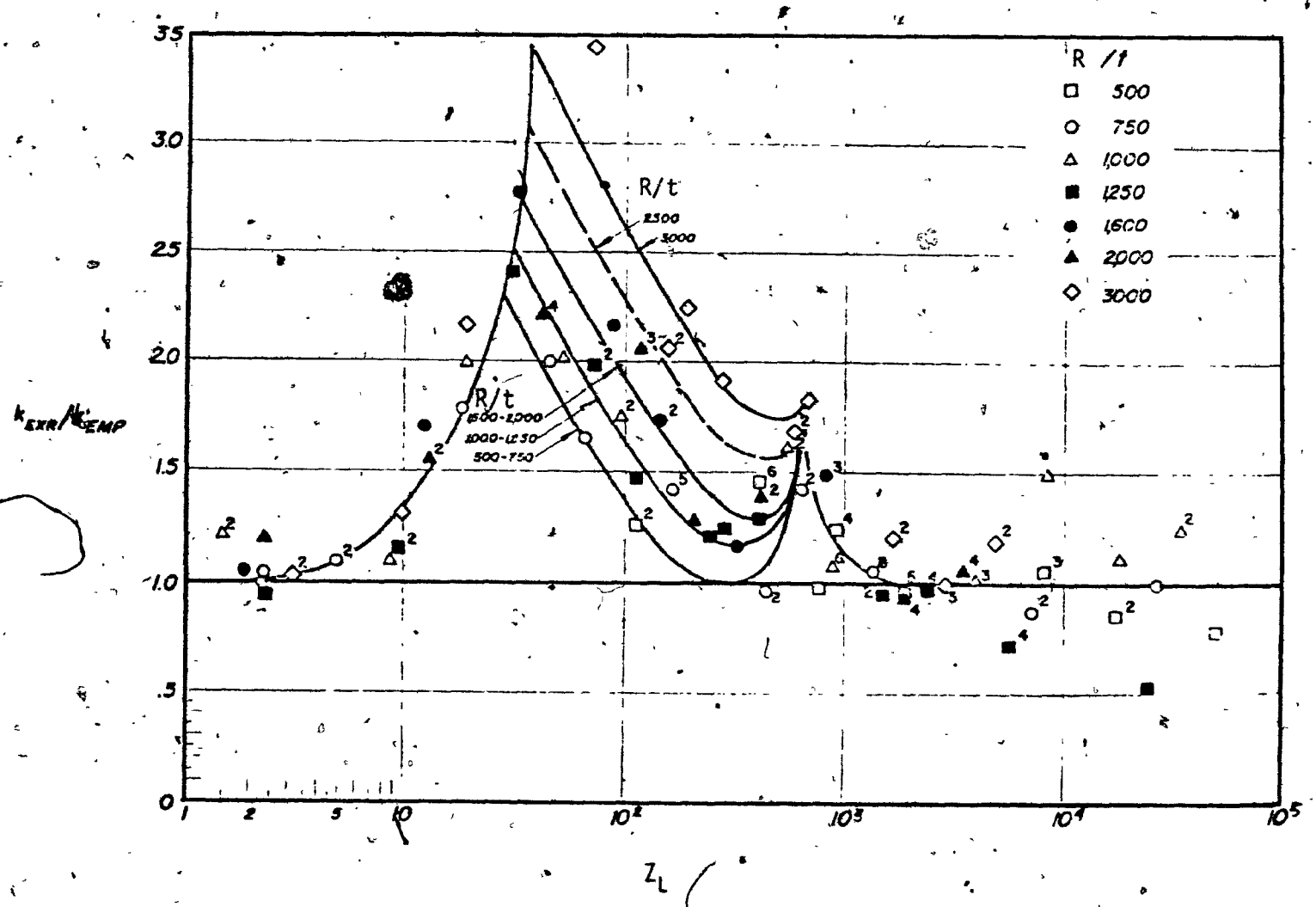

Figure 38. Composite chart of magnification factors for axially compressed cylinders.

to require consideration of large deflection behaviour. Because the diamond buckle pattern deflection functions which are assumed in the energy equations do not satisfy the end boundary conditions. Furthermore, experiments show that for long cylinders the buckling stress is independent of the boundary conditions. Bardorf et al (31), have performed an empirical correlation for long cylinders, in which k_c is plotted as a function of Z_L for various values of the ratio R/t and which clearly depicts the dependence of the parameter C upon the ratio R/t in the transition and long ranges. They defined an expression for the buckling stress equivalent to the classical equation

$$f_{cr} = C\ E\ R/t \qquad (165)$$

In the new expression the parameter C instead of a constant value (usually equal to 0.6) is now depended on the ratio R/t , as shown in the Figure (37). In Figure (37) there are also shown the theoretical curves of Donnell and Wan (33) for several values of the unevenness factor U , which is related to the initial imperfections of the cylinder. It can be seen that all curves converge at a very low value of R/t to a value approaching the classical value of $C = 0.6$ as an upper limit.

3.5.1.5 Plasticity-Reduction Factor

The inelastic buckling stress of cylindrical shells is usually obtained using the elastic formula with an effective modulus in place

of the elastic modulus. A plasticity reduction factor, n, is introduced so that when the computed buckling stress is in the plastic range the elastic modulus E is replaced by nE, where :

$$n = (E_t/E_s)^{\frac{1}{2}} \left(E_s/E \right) \left[(1-v_e^2) / (1-v_p^2) \right]^{\frac{1}{2}} \qquad (166)$$

Where

E_s : the secant modulus

E_t : the tangent modulus

v_e : elastic value of Poisson's ratio

v_p : plastic value of the ratio of Poisson

For the analysis of long cylinders the plastic-buckling curves shown in Figure (39) can be used, with $\varepsilon_{cr} = C\ t/R$. The plasticity correction factor is applicable to homogeneous materials such as aluminum alloys and stainless steels. But, the inelastic buckling of cylinders made from structural steel, which is generally nonhomogeneous due to the presence of residual stresses is more conviniently handled with an empirical formula. Such formulas have been presented by various authors and a very detailed review has been prepared by Johnston (3). For manufactured tubes, the most commonly used is the Plantema equation which is given by :

$$\begin{aligned} f_{cr}/f_y &= 1.0 && \text{For} \quad a > 8 \\ f_{cr}/f_y &= 0.75 + 0.031\ a && \text{For} \quad 2.5 < a < 8 \\ f_{cr}/f_y &= 0.33\ a && \text{For} \quad a < 2.5 \end{aligned} \qquad (167)$$

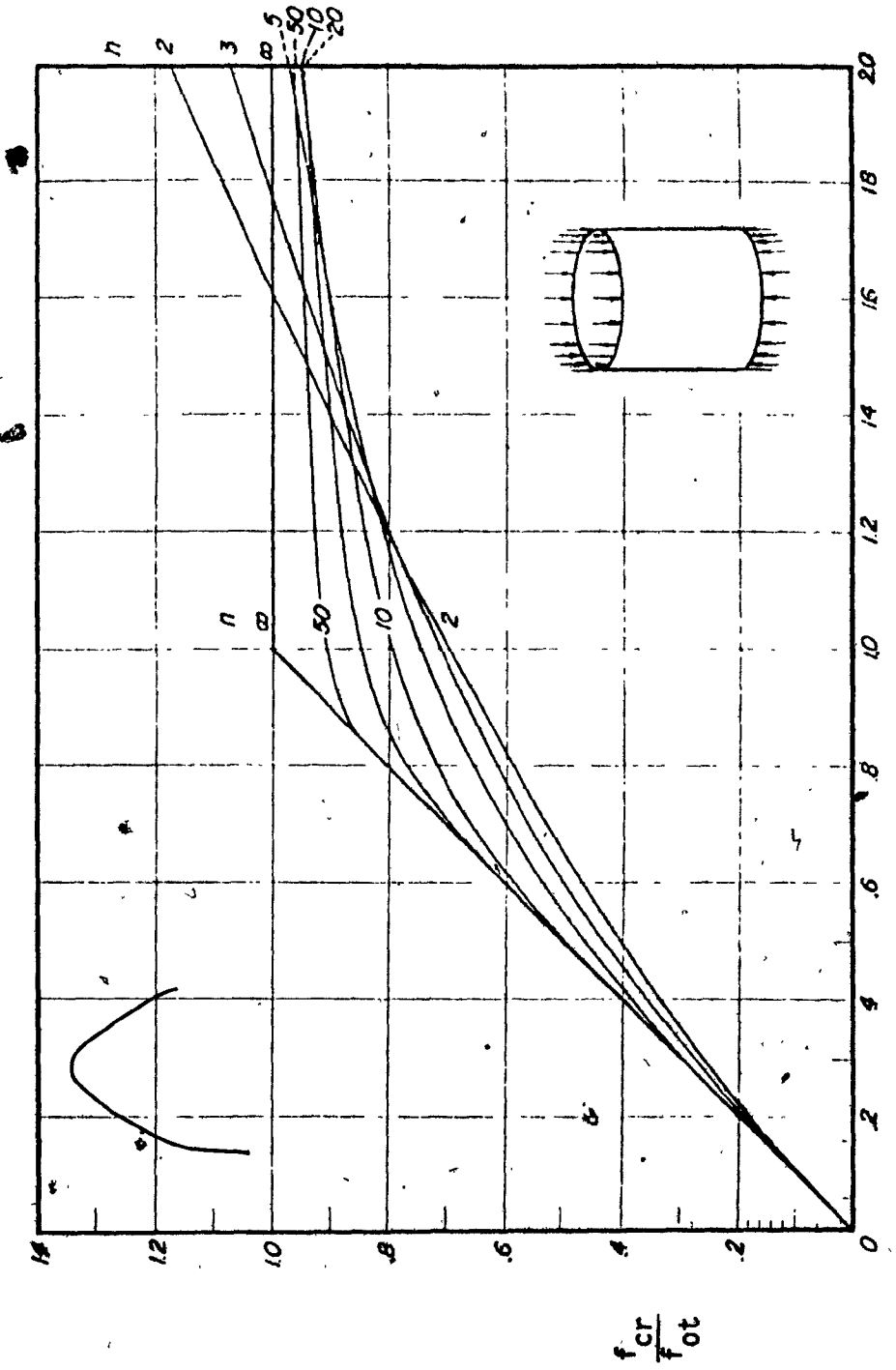

Figure 39. Nondimentional chart for axially compressed long circular cylinders.

Where the function a can be expressed as :

$$\bar{a} = (E/f_y)(t/D)$$

3.5.1.6 Effect Of Internal Pressure

Many tests conducted by several investigators have shown that internal pressure increases the axial buckling stress as long as the failure stress remains elastic. This increase in buckling stress can be evaluated by a graphical method which is presented in Figure (40). The effective stress f_i is given by :

$$f_i = f_{cr} + \overline{\Delta C} (Et/R) \qquad (168)$$

Where, f_{cr} is the critical buckling stress in axial compression and $\overline{\Delta C}$ can be obtained from Figure (40).

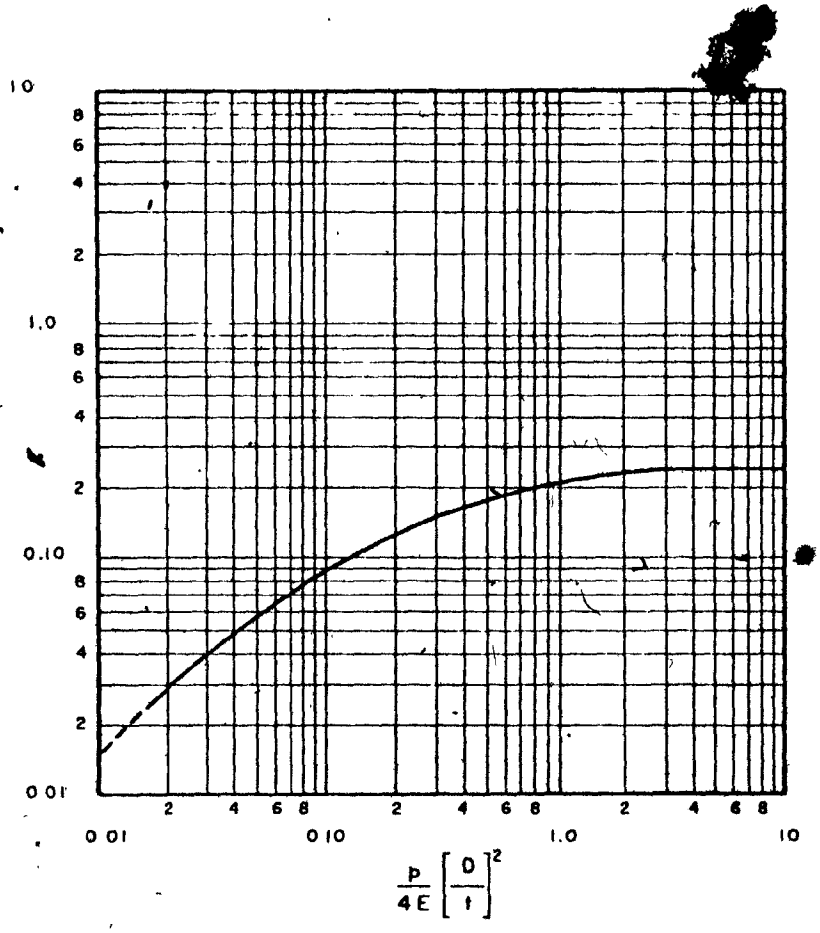

Figure 40. Diagram for the increase in axial compressive buckling stress due to internal pressure.

3.5.2. Cylindrical Shells Subjected To Bending

The buckling behaviour of cylinders under bending loads is similar to that of axially compressed cylinders, except that the bent cylinders are influenced by several considerations beyond those encountered in the buckling of axially compressed cylinders. So, the linear variation of bending strain across the section results in a strain gradient and hence a stress gradient at any location on the cylinder surface. A "gradient factor" is used to calculate the bending-buckling stress from the axial-compressive buckling stress of a corresponding cylinder. Furthermore, in the inelastic range two additional effects occur. First, the nonlinear distribution of bending stress across the section leads to the modulus of rupture. Second, the reduction of local wall stiffness due to plasticity leads to the plasticity-reduction factor.

The local-buckling behaviour of circular cylinders in pure bending may be divided into ranges similar to those observed in cylinders under axial compression. In the short-cylinder range , the buckling coefficient k_b approaches that of a wide compressed plate as a lower limit. The buckling stress is given by :

$$f_{cr}=\frac{k_b E \pi^2}{12(1-\nu_e^2)} \left(t/l \right)^2 \qquad (169)$$

and

$$Z_L=\frac{l^2}{Rt} (1-\nu_e^2)^{\frac{1}{2}} \qquad (170)$$

In the long-cylinder range the buckling stress is of the form :

$$f_{cr} = C\ E\ R/t \qquad (171)$$

Between these two limits is the transition region, and throughout this entire region buckling occurs in the diamohd pattern. When the cylinder is very long, the flattening of the cross-section leads to a large reduction of the effective section modulus of the cylinder, and instability occurs as a single transverse wave on the compression side of the shell. This type of buckling caused by the radial components of the axial deformation in the bent cylinder has been investigated by Brazier (20) for the first time. In Figure (41) test data obtained from Lundquist and Donnell are shown, and also a theoretical curve account for a 30 percent increase over the classical axial value which was recommended by Flugge and Timoshenko. This increase is attributed to the strain gradient associated with the linear cross-sectional strain distribution and is noted as the gradient factor γ . A comparison of axial-compression and bending data obtained by Lundquist on Duralumin cylinders apears in Figure (42). Lunquist reported an average value of 1.4 for the gradient factor and this is in good agreement with Donnell's tests on steel cylinders.

Since stress and strain are linearly related in the elastic range the gradient factor pertains to both. The ratio of the f/E intercepts at any value of the ratio R/t leads to the gradient factor γ since the slopes of the curves are virtually the same. For example, at R/t = 1,000 , the gradient factor is equal to

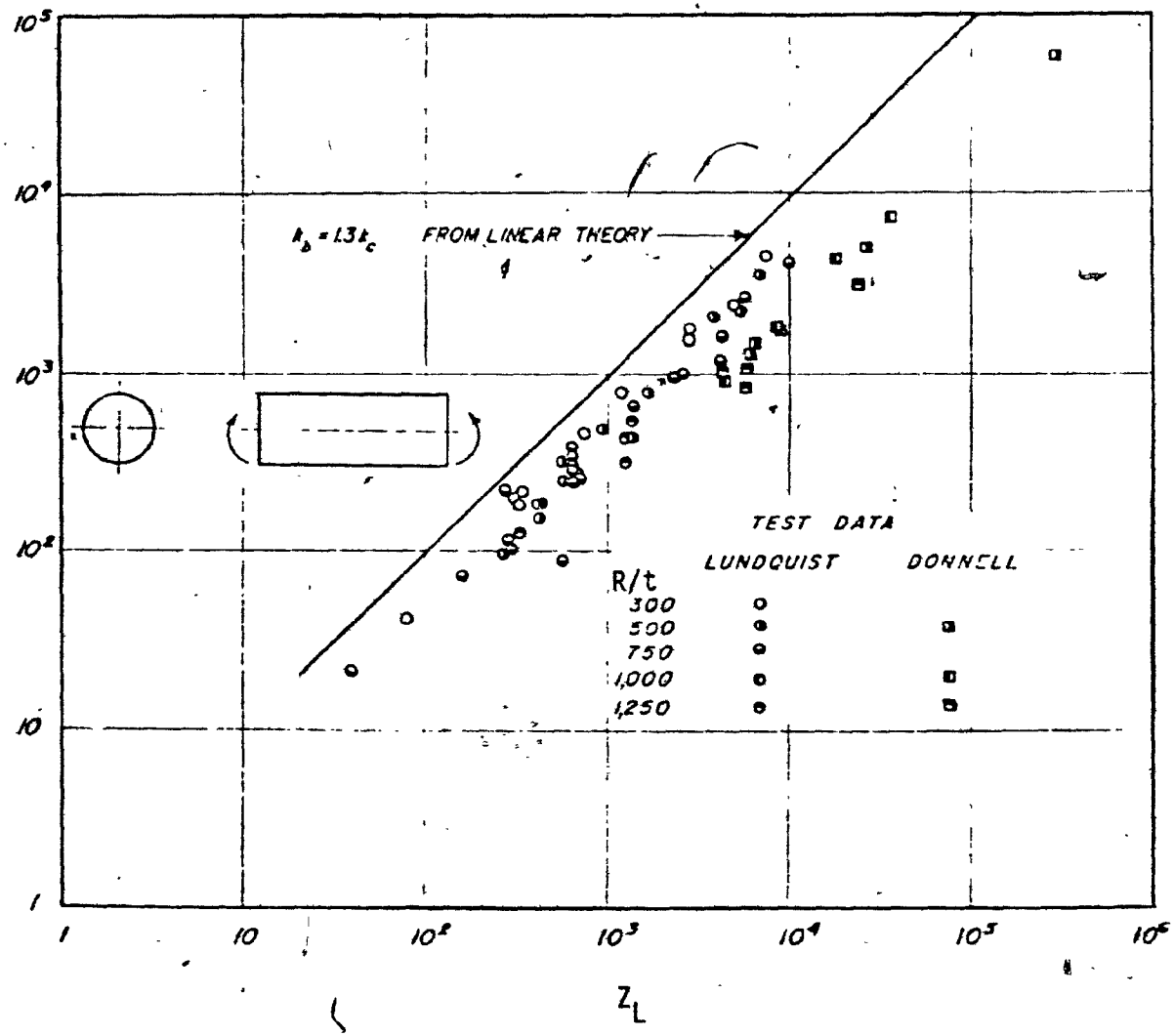

Figure 41. Comparison of linear theory with experimental data for cylinders in bending.

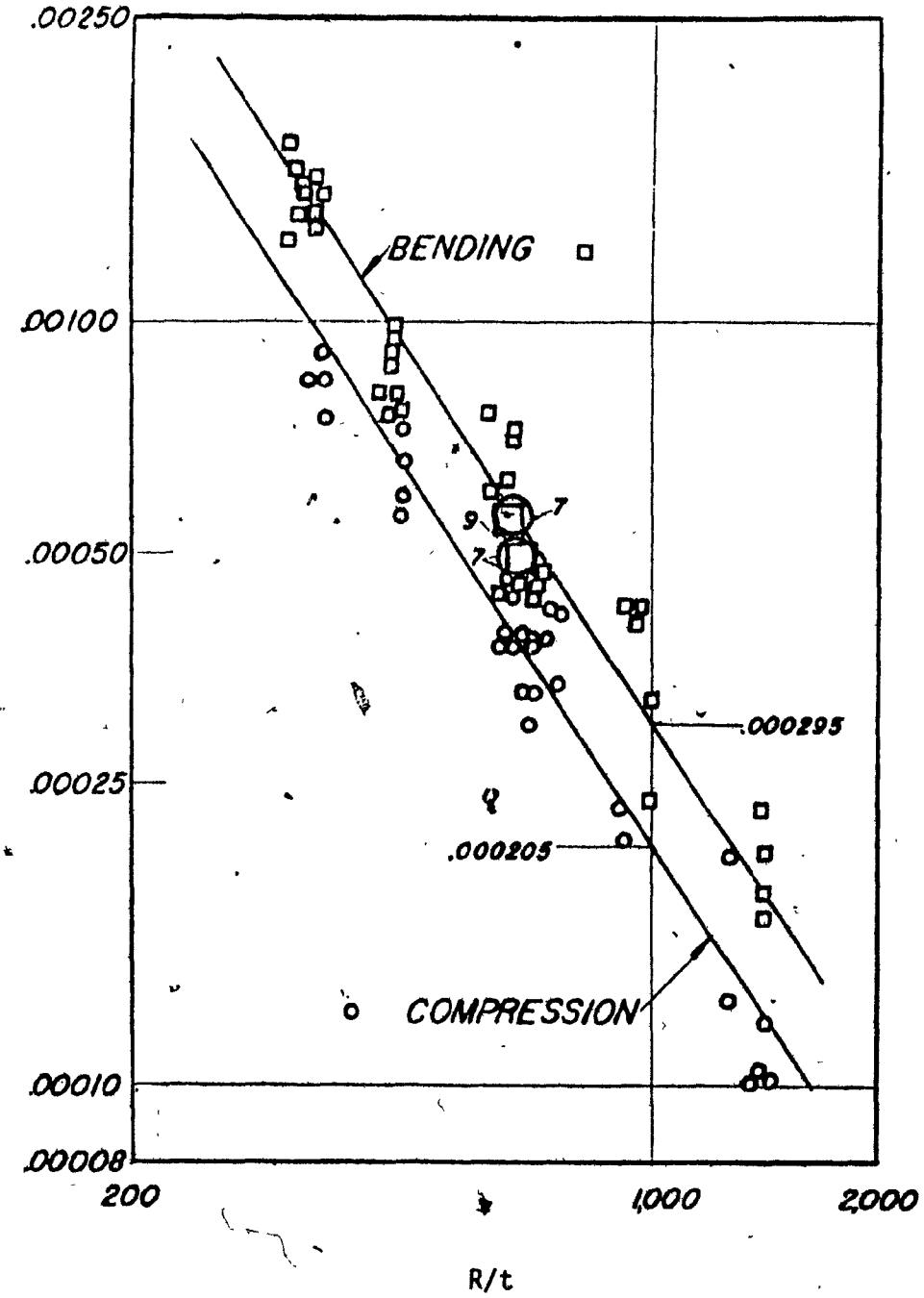

Figure 42. Test data for long cylinders in axial compression and bending.

$\gamma = 0.000295 / 0.000205$ or $\gamma = 1.44$.

To determine the buckling stress of long cylinders the following Equation may be used :

$$f_{cr} = C_b E\, t/R \qquad (172)$$

It is recommended that $C_b = 1.3C$, where C is the coefficient determined for axially compressed cylinders. The gradient factor of 1.3 represents a conservative average value to be used with the curve of C as a function of the ratio R/t obtainable from Figure (37). For short and transition-range cylinders no data are available to permit recommendation of a gradient factor.

3.5.3. Ring-Stiffened Circular Cylinders Under Bending

Design curves have been presented by Peterson (28) which are applicable to cylinders with heavy rings that fail as a result of local buckling. Values of the buckling stresses for the cylinders are given in Figure (43) on a plot which has as ordinate and abscissa the parameters obtained by small-deflection theory. Also shown in Figure (43), is a curve for the buckling stress of cylinders in compression as given by small-deflection theory. This curve has a slope of unity for values of the abscissa greater than 10 and is given by the equation :

$$f_{cr} = \frac{E}{\left[3(1-\nu)^2\right]^{\frac{1}{2}}} \frac{t}{R} \qquad (173)$$

When data for a given radius to thickness ratio are parallel to this

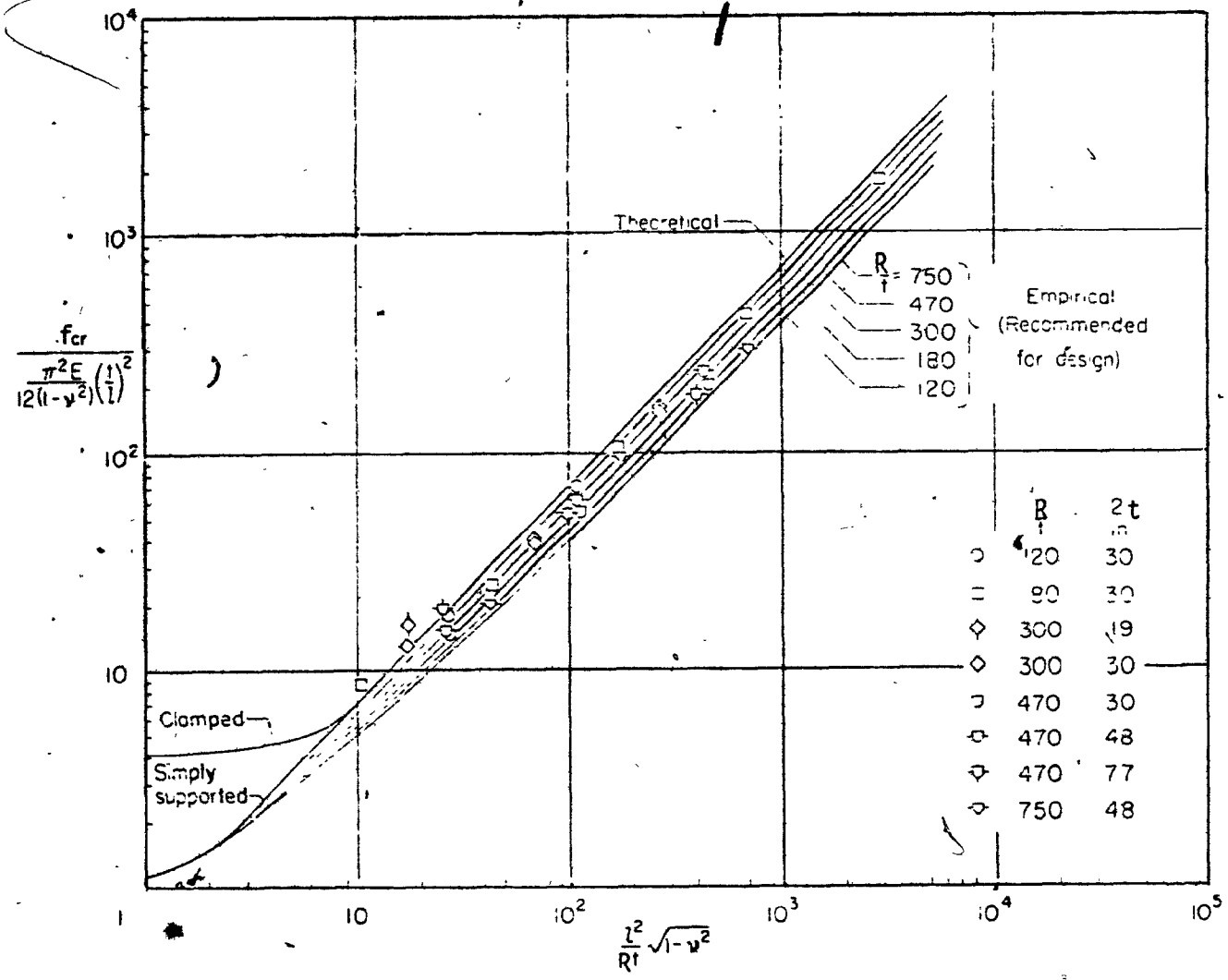

Figure 43. Plot of test data for cylinders in bending. The theoretical curve is for axially compressed cylinders.

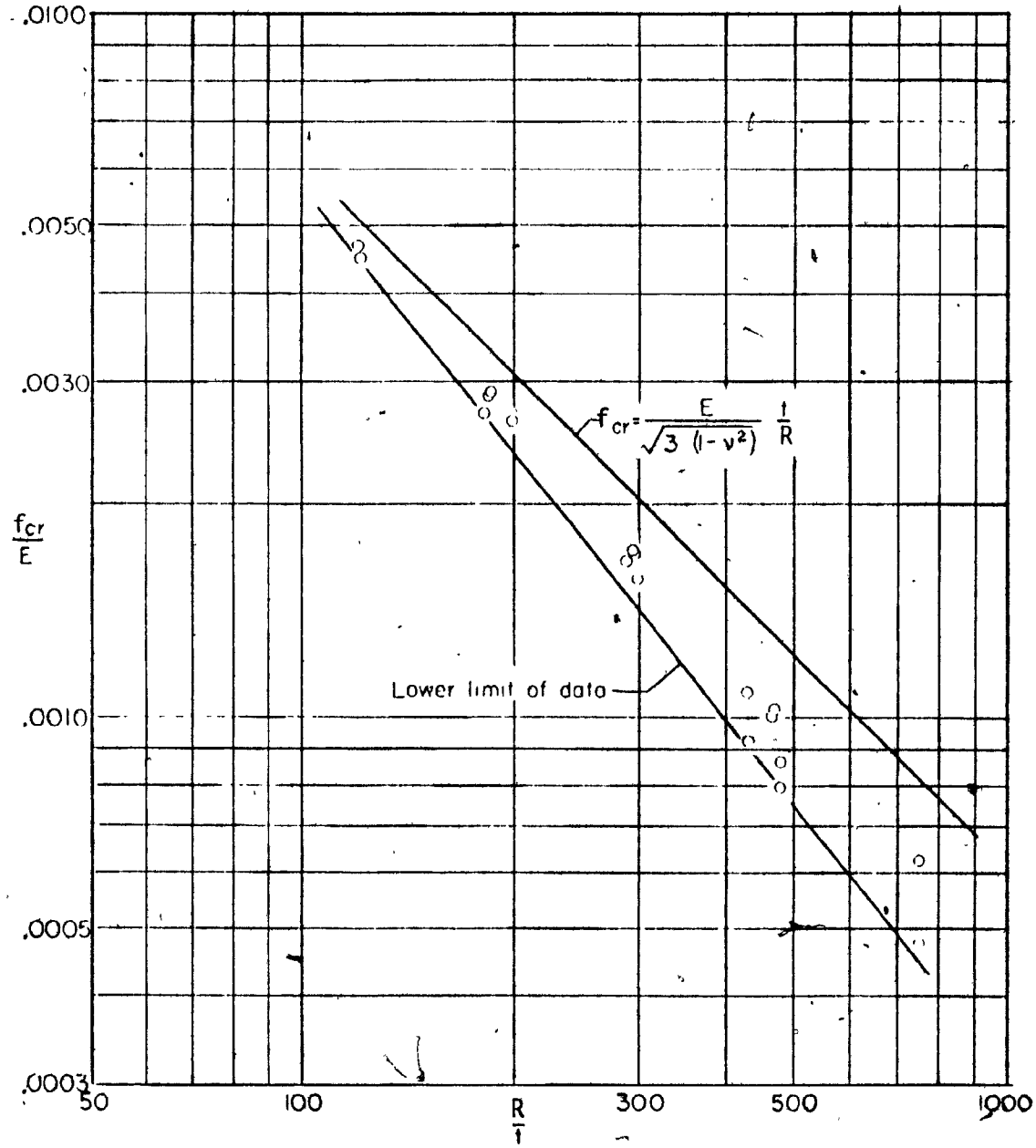

Figure 44. Plot of test data from those cylinders with a ring spacing over radius ratio greater than about 0.5

theoretical curve, the effect of ring spacing on the buckling stress is negligible. There is some gain in strenght as the ring spacing is decreased but the gain is negligible until a value of 1/R of 1/2 has been reached. The curves of Figure (43) give buckling stresses as much as two times the buckling stresses given by the corresponding curves for cylinders tested in axial compression. But they were obtained from data on a different type of structure as well as for different loading conditions, and of course the specimens were ring-stiffened cylinders. Peterson recommends that the curves of Figure (43) are suitable for the prediction of the bending strenght of ring-stiffened circular cylinders in which the rings are heavy enough so that general instability types do not occur and failure is expected by local instability between the stiffening rings.

3.5.4 Inelastic Behaviour of Long Circular Cylinders In Bending

When the extreme-fiber stresses are in the inelastic range, the redistribution of the cross-sectional stresses leads to a significant reduction in the stress gradient, which would be expected to reduce the gradient factor. As a countermeasure to the diminished stress-gradient effect, the nonlinearity of the stress distribution permits the cylinder to sustain a plastic bending moment greater than the fictitious elastic moment calculated according to $f_{cr}\, S_c$. This is the well known modulus of rupture effect. A further plasticity effect is the decrease in the local rigidity of the cylinder wall, which is re-

presented by the plasticity-reduction factor n.

In a beam with the extreme fiber stress in the inelastic range a fictitious elastic stress f_r is defined as the bending modulus of rupture, where :

$$f_r = \frac{M}{S_c} \tag{174}$$

Since the actual stress distribution is nonlinear, a "shape factor" is used to determine the actual plastic stress at the extreme fiber f_b.

$$\rho = \frac{f_r}{f_b} \tag{175}$$

Therefore, the actual stress f_b is :

$$f_b = \frac{M}{\rho S_c} \tag{176}$$

and

$$\frac{M / S_c}{f_{c_{cr}}} = \rho \frac{f_{bcr}}{f_{c_{cr}}} = \rho \gamma_\sigma \tag{177}$$

where

$$f_{b_{cr}} = \gamma_\varepsilon C n_b E (t/R)$$

$$f_{c_{cr}} = C n_c E (t/R)$$

γ_ε : the strain gradient factor

γ_σ : the stress gradient factor

It is assumed that

$$\gamma_\varepsilon = 1.3 = \varepsilon_{b_{cr}} / \varepsilon_{c_{cr}} = (f_{b_{cr}} / n_b)/(f_{c_{cr}} / n_c)$$

3.5.5. Effect of Internal Pressure

Internal pressure increases the bending buckling stress as long as the failure stress remains elastic. The increased buckling stress is given by :

$$f_i = f_{cr} + \Delta C_b(Et/R) \qquad (178)$$

Where, f_{cr} is the buckling stress due to pure bending and ΔC_b can be obtained from Figure (45).

3.5.6 Axial Compression and Bending

Since the nature of the buckle pattern is the same for axial compression and bending of a circular cylinder, a linear interaction equation might be expected. Bruhn (34) has shown this to be a good approximation to the experimental data, as can be seen in Figure (46). The stress ratios R_b and R_c represent the ratio of the allowable value of the stress caused by a particular kind of load in a combined loading condition, to the allowable stress for the same kind of load

when it is acting alone. The subscripts b and c are used to denote the stress due to bending and axial compression respectively.

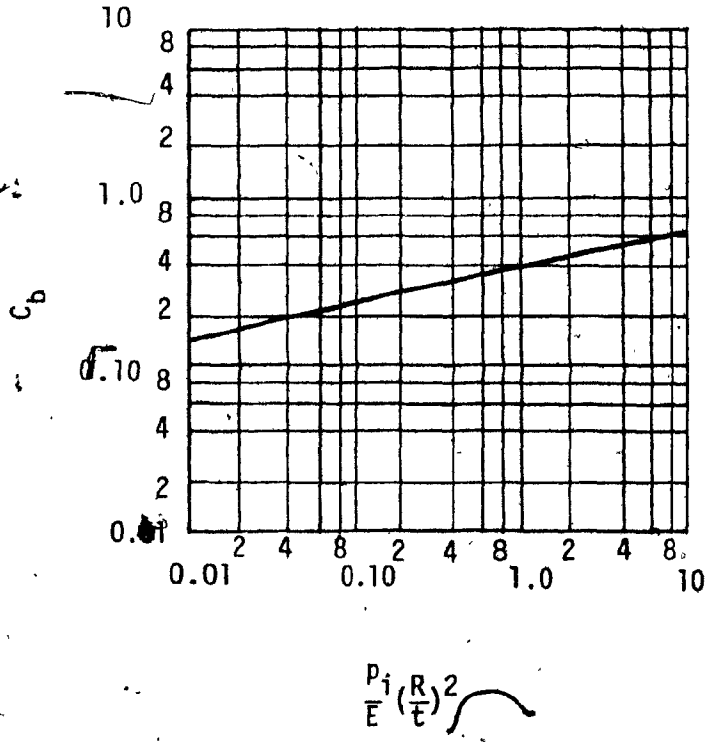

Figure (45). Increase in bending buckling stress due to internal pressure for a circular cylinder.

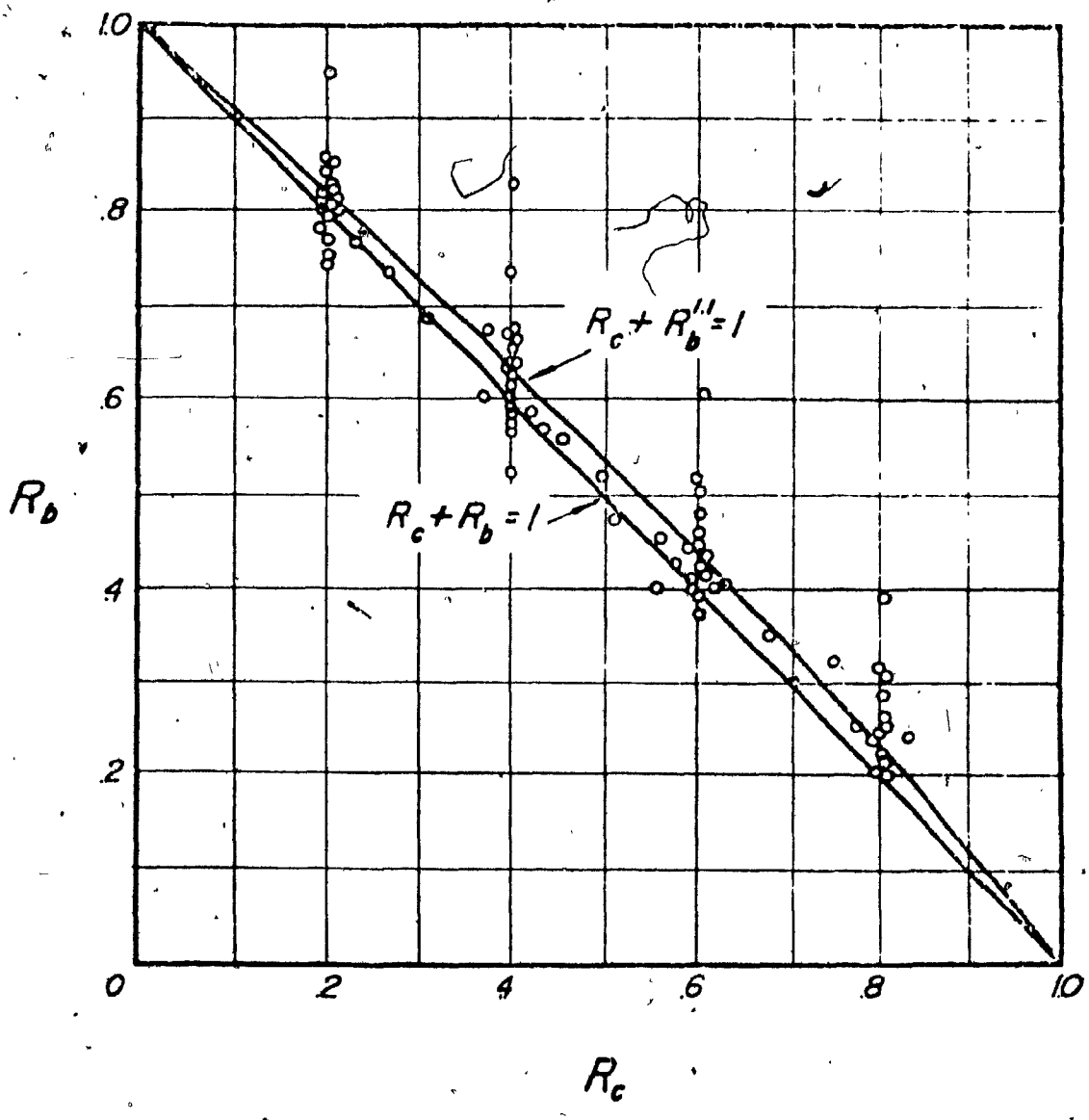

Figure 46. Interaction curves and test data for combined stresses due to axial compression and bending.

REFERENCES

REFERENCES

(1) Timoshenko, P.S., & Gere, M.J., " Theory of Elastic Stability" Mc Graw-Hill, 2nd Edition, 1961.

(2) Timoshenko, P.S., & Krieger, S., " Theory Of Plates and Shells" Mc Graw Hill, 2nd Edition , 1959.

(3) Johnston, G. B., et al. " Guide to Stability Design Criteria For Metal Structures". John Wiley & Sons, 3rd Edition, 1976.

(4) National Research Council of Canada , Supplement No. 4 to the National Building Code of Canada, 1975.

(5) Troitsky, M.S., " Design Guidelines for Steel Tubular Thin-Walled Structures. " 4th Progress Report, Canadian Steel Industries Construction Council, Project No. 724, Jan. 1974.

(6) Spangler, M.G., "Stresses In Pressure Pipelines and Protective Casing PIpes." American Society Of Civil Engineers, Structural Division, September 1956.

(7) Stephenson, D. " Stiffening Rings For Pipes. " Pipes and Pipelines International, April 1973.

(8) Winderburg, D.F & Trilling, C. "Collapse By Instability of Thin Cylindrical Shells Under External Pressure". Trans. ASME, Vol. 56, 1934.

(9) Watkins, R.K., "Buried Structures", Foundation Engineering Handbook, " Edited by Winterkorn, H. F. & Fang, H., Van Nostrand Reinhold Co., New York, 1975.

(10) Meyerhof, G.G. & Fisher, C.L., "Composite Design Of Under-Ground Steel Structures." The Engineering Journal, Sept. 1963.

(11) White, H. L., & Layer J.P., " The Corrugated Metal Conduit As A Compression Ring." Proc. Highw. Res. Board, Vol. 39, 1960

(12) Clarke, N.W.B., "Buried Pipelines." Maclaren and Sons, London, 1968.

(13) Wang, L.R., & O'Rourke, M. J., "Overview Of Buried Pipelines Under Seismic Loading". Journ. of Technical Councils of ASCE, TC_1, November 1978.

(14) Hall, W.J., & Newmark, N.M., " Seismic Design Criteria For Pipelines And Facilities". Jour. Of Techn. Councils of ASCE, TC_1, November 1978.

(15) Newmark, N.M., & Hall, W.J., "Pipeline Design To Resist Large Fault Displacement." Proceedings of The United States National Conference on Earthquake Engineering, Earthquake Research Institute, 1975.

(16) Meck, H.R., "A Survey of Methods of Stability Analysis Of Ring Stiffened Cylinders Under Hydrostatic Pressure". ASME, Jour. Eng. Ind., Vol. 87, Series B, No. 3, August 1965.

(17) Gallerly G., et al. "General Instability of Ring-Stiffened Cylindrical Shells Subjected to External Hydrostatic Pressure a Comparison of Theory and Experiment". Trans. ASME, Jour. of Appl.Mech., Vol. 25,1958.

(18) Rumman, W.S., "Stresses in Ring Stiffeners in Cylinders". ASCE, Str. Division, ST8, December 1961.

(19) Troitsy, M.S., "On the Local and Overall Stability of Thin-Walled Large Diameter Tubular Structures". Canadian Structural Engineering Conference, 1976.

(20) Brazier, L.G., "On the Flexure of Thin Cylindrical Shells and Other Thin Sections". Philos. Trans. Royal Soc., London, Vol. CXVI, November 1927.

(21) Donnell, L.H., "A New Theory for the Buckling of Thin Cylinders Under Axial Compression and Bending". Trans. ASME, Vol. 56, 1934.

(22) Seide, P. & Weingarten, V.I., "On the Buckling of Circular Cylindrical Shells Under Pure Bending". Trans. ASME, March 1961.

(23) Calcit. "Some Investigations of the General INstability of Stiffened Metal Cylinders". National Advisor Comitee for Aeronautics, Tech. Note 905, 1943.

(24) Southwell, R.V., "On the General Theory of Elastic Stability". Philos. Trans. Royal Soc., London, Series A, Vol. 213, 1913.

(25) Schilling, C.G., "Buckling Strenght of Circular Tubes". ASCE, Jour. Struct. Div., Vol. 91, No. ST5, October 1965.

(26) Schorer, H., "Design of Large Pipelines". Trans. ASCE, Vol. 98:101, 1933.

(27) Gerard, G. & Becker, H., "Handbook of Structural Stability Part III- Buckling of Curved Plates and Shells". NACA, Techn. Note 3783. August 1957.

(28) Peterson, J.P., " Bending Tests of Ring-Stiffened Circular Cylinders". NACA, Techn. Note 3735, July 1956.

(29) Windenburg, D.F., "Vessels Under External Pressure", Pressure Vessels Piping Des., ASME. 1960.

(30) Holt, M., "A Procedure for Determining the Allowable Out-Of-Roundness for Vessels Under External Pressure", ASME Trans., Vol.74, 1952.

(31) Bardorf,S.B., "A Simplified Method of Elastic Stability Analysis for Thin Cylindrical Shells," NACA Rep., 874. 1947.

(32) Wolford, D.S., and Rebholz, M.J., "Beam and Column Tests of Welded Steel Tubing with Design Recommendations," ASTM Bull., No. 233, 1958.

(33) Donnell, L.H., and Wan, C.C., "Effect of Imperfections on Buckling of Thin Cylinders and Columns Under Axial Compression," Jour. Appl. Mech., Vol. 17, No. 1. 1950.

(34) Bruhn, E.F., "Tests on Thin-Walled Celluloid Cylinders to Determine the Interaction Curves Under Combined Bending, Torsion, and Compression or Tension Loads," NACA, TN 951, 1945.